Analysis of the Buoyant Plume Above a Heated Horizontal Cylinder in a Free Convection Flow

Frank Andrew Tessier, Jr

Introduction

General Overview

Years of experimentation have confirmed that the buoyant plume above a heated horizontal source sways [1-15]. The plume generally begins as a plane near the cylinder and forms a sinusoidal, oscillating wave as it rises towards the surface. Several experiments have confirmed the sinusoidal nature of the plume's structure [7, 8]. However, this thesis will present new data on the formation and specific characteristics of this structure and formulate a hypothesis for how the features in the flow affect the structure.

Literature Review

Noto wrote an extremely informative historical review of the research conducted on buoyant plumes above heat sources in his paper "Swaying Motion in Thermal Plume Above a Horizontal Line Heat Source" [13]. Since the writing of Noto's paper, several other authors have published new data on the subject. In 1993, Desrayaud and Lauriat published a numerical study on buoyant plumes above heated horizontal line sources [15]. Cesini et al. wrote a study including both numerical and experimental data on convection from buoyant plumes from heated horizontal cylinders [16]. Kitamura, Kami-iwa, and Misumi investigated the formation of buoyant plumes at the surface of large cylinders [17]. Gorman et al. [18] studied the heat transfer interaction between a pair of cylinders aligned vertically, and Atmane et al. [19] studied the effects of vertical confinement (by the water free surface) on the heat transfer of a heated horizontal cylinder.

Specific Overview

In Eichhorn and Vedhanayagam [7], the major characteristics of the buoyant plume above a heated line source were analyzed. They observed that the number of horizontal nodes of the plume depended strongly on depth but only weakly on source strength [7]. Furthermore, the schematics of the flow presented in the article match the general descriptions of the plume as presented in this thesis.[1] In Urakawa, Morioka, Kiyota [8], they noted that the plume would form a standing wave only when the length of the tank in the direction of the axis of the heat source was an integer of ½ the wavelength of the plume; otherwise, the plume formed an oscillating wave which appeared to move along the heat source.

Present Experimental Setup

The experiment setup consisted of a tank of dimensions 2' by 2' by 4' with two walls which were made of ¾ inch thick glass, two walls which were made of aluminum, a heated stainless steel cylinder with an outer diameter of 1 inch, water seeded with neutrally buoyant 10 micron diameter glass microspheres, a DaVis high frequency digital camera, and a Spectra-Physics Nd:YAG laser. Using optics, the laser was focused into a thin sheet which measured less than one mm in thickness. This sheet laser was directed at the tank through a glass wall. By keeping the camera's view perpendicular to this sheet laser, the computer was able to see the reflections of the laser light off from the microspheres. By moving both the laser plane and the camera so that they were always perpendicular, three orthogonal planes could be observed using Particle Image Velocimetry, or PIV (refer to figure 1).

[1] As do the schematics in Urakawa, Morioka, and Kiyota [8]. The data in this thesis also compares to the schematics in Noto, Matsui, and Matsumoto [12].

This thesis focuses mainly on the structure of the buoyant plume in three orthogonal planes and how this structure changes with varying vertical confinement (by the water free surface). The height of the water is presented in H/D, or height per diameter of the cylinder as measured from the top of the cylinder. Velocimetry data were taken at various H/D in each plane.

While the sheet laser was in the X-Y plane, data were taken at laser level heights of 3 H/D and 3.75 H/D and water level heights of 4 H/D, 6 H/D, 8 H/D, and 12 H/D. While the sheet laser was in the X-Z and Y-Z planes, data was recorded with water levels at 4 H/D, 6 H/D, 8 H/D, and 12 H/D.

In each experiment, the temperature of the cylinder was maintained at 82 degrees Fahrenheit while the water temperature in the nominally quiescent region was 74.5 degrees Fahrenheit. The Rayleigh number for these experiments was $1.4*10^6$.

To produce the vector fields, images of the suspended microspheres were taken in sets of two 80 milliseconds apart. After calibrating the images, the DaVis software would then compare the two images, note the movement of the microspheres, and produce a vector field. Ten of these sets would be taken, each 200 milliseconds apart, constituting a group of vector fields. The ten vector fields in each group would then be averaged, creating the images seen in this thesis. The software was programmed to take one hundred and seventy-one groups, each 5 seconds apart, constituting a data set. Two data sets were taken for each H/D and laser setup.

Data Description

To clarify the description of the flow, various features in the flow are named. The main flow of water upwards away from the cylinder will be referred to as the plume. Vortices near the plume which are close to the surface of the water will be referred to as A vortices. Vortices which are created next to the plume but which are not near the surface of the water will be referred to as B vortices. B vortices move mostly in the positive Z direction while A vortices tend to move mostly in either Y direction while near the surface. Also to note, B vortices lie tangent to the sinusoidal plume structure but meander up and along it. This orientation means that B vortices are not truly in only one plane, though they are easiest to see in the Y-Z plane. As described in the general overview, the plume tends to sway in a regular, repeated motion. Viewed in the Y-Z plane, the plume appears to lean from one side to another. The side of the plume to which the plume leans will be referred to as the "strong" side, and the opposite side will be referred to as the "weak" side, with the plume as the divider between the two. The section of the plume which turns sharply in the Y direction after reaching the surface of the water will be referred to as the "lip" of the plume (see figure 2).[2]

When viewed in the X-Y plane, the plume appears as a sinusoid. The length of this sinusoid will be referred to as the wavelength of the plume. When the sinusoid does move along the axis of the cylinder (the X axis), this movement will be referred to as meandering.[3] As many of the larger elements of the flow occur at regular intervals (including the swaying of the plume), the time between these intervals will be referred to as a period. Other terms and references will be introduced later as necessary.

[2] In this figure, various features are labeled. However, in an effort to reduce clutter in the velocimetry fields, the mm scaling will be referenced to focus the readers' attention to specific structures. The bottom axis scaling will be listed first, followed by the scaling along the right side of the figure.

[3] N.B.: Not all buoyant plumes meander. Indeed, it is unclear in some of the cases in this thesis whether the plume meanders or acts as a standing wave. The swaying motion of the plume in the Y direction as viewed in the X-Y plane will be referred to as oscillations.

Major structural elements in each plane will be discussed, at various water levels (H/D = 4, 6, 8, and 12). After each plane is discussed separately, various features from each plane will be related to each other to form a general view of the whole structure.

H/D = 4

Y-Z Plane

As the plume sways back and forth, it sheds vortices (A vortices). The plume sheds these vortices when it is at its most extreme “strong” position, i.e., when its Y direction is greatest. The period of the swaying motion of the plume averages to approximately 135 seconds. As the plume leans more to its strong side, the lip of the plume tilts somewhat in the negative Z direction (see (75, -60) in figure 3). In this position, the lip tends to have A vortices both above it and below it (see (90, -50) and (80, -80) in figure 3), though the vortex above this lip is usually fainter and sometimes not present. These two A vortices always counter-rotate. On the weak side of the plume, the lip of the plume starts out mostly horizontal. There is a vortex (referred to as the shearing vortex) which begins between the weak side lip and the plume, and this vortex begins moving towards the strong side of the plume. The plume slows its movement as it reaches its limit in the Y direction (i.e., leans as far as it can to the strong side), but the shearing vortex continues to moves at the same speed to the strong side. The shearing vortex pulls the weak side lip down as it continues to travel towards the strong side, and continues straight through the plume. The top of the plume buckles around this vortex while the rest of the plume quickly moves back to the center (see figures 4-10). As the plume continues its motion towards the weak side (now the new strong side), the top of the plume which had buckled around the vortex shears away from the main plume, continuing to move away from the main plume and spawning several A vortices (see (100, -70) and (60, -70) in figure 10). It should be noted that most of the vortices described in the H/D = 4 case are relatively weak compared to other cases, especially the bottom half of the vortices. Indeed, some of the features seem to be almost muted. A possible cause for this is that the water in the plume has comparatively less time to gain speed because the heated water near the cylinder has a relatively short distance to travel before reaching the surface of the water. Furthermore, when the water reaches the surface, it has had little time and distance to dissipate heat, and therefore is relatively more buoyant than the water at the surface in any of the other cases studied. This increased buoyancy tends to limit vortices as the buoyant water resists travelling downward, apparently weakening the bottom half of most vortices.

X-Y Plane

The oscillating nature of the plume is clear in this plane. For the H/D = 4 case, the plume does not exhibit standing wave behavior. The imaging of the plume is in a plane at H/D = 3, while the water height is at H/D = 4. Interestingly enough, while the wave seems to be moving along the X axis, the velocity vectors in the wave has little to no component of velocity in the X direction. The plume wave has a wavelength of approximately 7 to 7.5 H/D, and a period of 125 to 130 seconds and an amplitude of roughly H/D = 2, which varied in time as the wave often bulged out (see (15, -50) in figure 11). The main wave is quite clear, but there are also fainter but significant features in the flow. There seems to be an oblong source, weaker than the main plume, on the outer edge of the wave (see (5, 20) figure 12).

X-Z Plane

In the X-Z plane, the main flow feature is a moving U-shape. This U-shape corresponds to the sinusoidal shape envisioned by meshing the images of the X-Y and Y-Z planes (see figure 13). There are several other important features to note as well. The lip of the plume is clearly visible on the edge of the U-shape (at (-15, 30) and at (95, 30) in figure 14). Below the lip is a vortex. It is important to note that a vortex or a down-leaning lip is present between the edges and on both outside edges of the U profile (see (-30, 10) and (35, 30) in figure 14 and (50, 25) and (125, 25) in figure 15). These flow features weaken, strengthen, and sometimes disappear into the motion near the surface.

General Structure

The plume starts at the surface of the cylinder as a nearly flat plane emerging from the highest point on the cylinder. This plane curves as it approaches the surface, creating a sinusoidal profile (see figure 13). This sinusoid, as viewed from above, meanders along the X axis. The cause of this meandering (as opposed to the sinusoid acting as a standing wave) is unclear.

Water from the plume spills over on both sides of the plume once it reaches the boundary between the water and the air, forming a lip to the plume (see figure 2). On the weak side of the anti-nodes of the sinusoid (point A in figure 16), the lip is folded on itself. A vortex forms between the lip and the plume. With so much flow from the lip in such a confined area, a large amount of water is forced relatively far downward (see (0, -70) to (10, -110) in figure 17). This water interferes with both the plume at around 2 to 2.5 H/D and with the A vortex (at (50, -60) in figure 5), forcing it to both become smaller and move closer to the surface of the water. Eventually, the water moving downward from the lip of the plume interacts strongly enough with the lower part of the plume that the lower part of the plume moves relatively quickly back to center and then continues this motion until it leans in the other direction. The top of the plume is essentially sheared off as the flow from the lip of the plume creates too large of an obstacle (see figure 7-9 at roughly (75, -60)). It appears that a combination of the downward flow of the water and the upward flow from the plume creates an area of low pressure which draws the plume back to the center. Indeed, very faint vortices can be seen at these lower parts of the plume. Interestingly, these faint vortices tear away from the plume well before reaching the surface and move horizontally away from the plume (see (15, -90), (20, -85), (40, -85), and (55, -85) in figures 18-21, respectively). These regions of vorticity are the proposed cause of the swaying motion of the plume. Furthermore, it is important to note that the height of the water will substantially change the formation of these areas of vorticity because the height will substantially change where and how the surge of water from the lip of the plume interacts with the lower parts of the plume.

The structure as presented compares well with data previously observed, in which Carlomagno et al. [14] noted that the plume was laminar at its lower sections, laminar but oscillatory (i.e., swaying) in its middle sections, and turbulent at the top (which corresponds to the A vortices seen in this experiment).

H/D = 6

Y-Z Plane

The H/D = 6 case has several differences from the H/D = 4 case. The period of the swaying motion is approximately 80 seconds, considerably less than the approximately 130 - 135 seconds of the H/D = 4 case. In the H/D = 6 case, noticeable vortices form on the lower edges of the plume. These vortices (B vortices), which are often quite elongated while at the lower sections of the plume, usually form at around H/D = 2.5. They move in the vertical direction alongside of the plume and become much more circular near the top of the plume. As they round out and reach the top of the plume, they develop into A vortices, shed, and roll away from the plume in the Y direction. A single B vortex usually forms on the weak side of the plume, and as it moves up the plume, the plume moves towards the side which it formed. In fact, B vortices seem to control the movements of the upper section of the plume, as the top of the vortex corresponds to an inflection point in the plume. As the vortex moves up the plume, the inflection point also moves up the plume (see (35, -85), (40, -70), (45, -50), (50, -40), and (65, -30) in figures 22-27, respectively). Once the B vortex has reached the surface of the water, the top of the vortex becomes enveloped by the lip of the plume and it turns into an A vortex, which sheds from the main plume and moves away from the plume.

By the time that this vortex is shed, another B vortex on the other side of the plume has already formed, and the same phenomenon occurs, only mirrored on the other side of the plume. This process seems to be rather repeatable; however, other A vortices can and often are created and shed off without any apparent B vortex origin. Some of these A vortices possibly form because the plume cannot remain intact when a B vortex forces the bottom of the plume to move too quickly away from the location of the top of the plume (see (10, -20), (5, -15), (15, -15), and (25, -20) in figures 24-27).

Another phenomenon is also present: occasionally, flow seems to come from the surface of the water (see (75, -5) in figures 27). Since no water can come through the surface, this flow must be coming into the plane from another point in the plume. Often, the plume will buckle around these flow sources, as in the H/D = 4 case. And, just like the H/D = 4 case, this flow most likely comes from the lip of the concave sections of the plume (see point A in figure 16).

X-Y Plane

The H/D = 6 case (the velocity plane was still imaged at H/D = 3) is significantly different from the H/D = 4 case. The plume still oscillates, but the whole plume moves more uniformly, either because of a much greater wavelength or because of a longer wavelength and that the plume forms a standing wave. There is an interesting bend in the plume which reoccurs at the same X coordinate somewhat consistently (see (30, -35) in figure 28 and (30, -30) in figure 29).[4] This may suggest that the plume is exhibiting standing wave behavior because these bends may correlate to an anti-node of a standing wave, but the data are not conclusive. The period of the wave was measured at approximately 80 seconds. Another important feature is an apparently large sink which occurs directly in front of the plume just before the plume moves in that direction (see (0, -20) in figure 30). These sinks always appear before the plume sways; but their size and shape drastically differ, sometimes appearing as large line sinks, other times appearing as smaller point sinks.

[4] In figures in the X-Y plane, there is a line of interference at roughly -10 in the horizontal direction as seen in the figure. This interference is due to laser light scattered from the surface of the cylinder.

X-Z Plane

The H/D = 6 case is rather different at first glance from the H/D = 4 case (see figures 14 and 31). Instead of a clear U-shaped profile, the H/D = 6 case has a much broader and somewhat less defined swath of (relatively) high upward velocity. However, this is mainly due to the larger wavelength and the more uniform lean of the H/D = 6 plume. In figure 31, note the main U-shaped feature (at (15, 20) to (60, 20) note the change in water velocity; tracing these changes forms a U-shape similar to the inner section of the U shape in the H/D = 4 case). The outside of the U-shape has substantial upward velocity, while the inside of the U-shape has downward velocity. As the flow progresses, the downward moving flow turns mostly uniformly in the positive X direction (see figure 32). A few frames later, all of the water in the flow is uniformly moving upwards (see figure 33). The period of the plume is also approximately 80 seconds.

General Structure

The H/D = 6 case is quite similar in general structure to the H/D = 4 case. The most general feature, the sinusoidal nature (as seen in the X-Y plane) and the swaying motion (as seen in the Y-Z plane) of the buoyant plume, remains the same. However, the wavelength of the H/D = 6 case is significantly longer than in the H/D = 4 case. Unfortunately, the scope of the images is not large enough to reliably measure the wavelength. The period of the swaying motion of the plume, on the other hand, is quite smaller than the H/D = 4 case at around 80 seconds (compared to approximately 130 seconds). If the plume is not a standing wave in the X-Y plane, then this wave is moving much faster in the X direction than the wave in the H/D = 4 case; however, no conclusions can be draw on whether the plume (as seen in the X-Y plane) meanders in the X direction or oscillates as a standing wave.

The biggest difference between the two cases is the formation of B vortices, which in the H/D = 6 case remain next to the plume until they reach the surface. These B vortices are incredibly important to the rest of the plume as they affect the swaying motion and the vortex shedding at the top of the plume.

These B vortices appear to stretch the length of a quarter of a wavelength of a plume, starting nearly halfway up the plume in the Z direction and near the midline of the sinusoid and extending to the edge of the plume (in both the Y and Z directions), where the vortex is shed (see figure 13 for a 3-D rendition). It is unknown whether these B vortices rise up as small (in the X direction), discrete vortices or if they are larger vortex tubes. If these B vortices are vortex tubes, it is also unclear whether the vortex remains fully connected and whole after it is shed though the lack of quick or breaking movements of the vortex after it is shed could signal that the vortex tube remains intact.

Most B vortices are formed due to downward flows of water which are caused by the interaction of the combined flows of the lip of the concave section of the sinusoid (see point A in figure 16). Just as this downward flow causes vortices to form in the H/D of 4 case, here the increase in speed allows much stronger vortices to form. With greater speed, it allows stronger B vortices to form—there is faster flow in both the plume and the downward water flow from the lip, making stronger vortex formation possible. Also, because the water in the plume has a longer distance in the Z direction to dissipate heat before reaching the surface, the water in the plume has a lower temperature difference with the nominally quiescent regions surrounding it (as compared to the H/D = 4 case); and therefore the upper sections of the plume in the H/D = 6 case are less buoyant than those of the H/D = 4 case. This reduction in buoyancy allows water from the lip to be moved farther down after exiting the lip—and it allows the plume to be moved much more easily away from the ideal vertical case.

Because these strong vortices create areas of low pressure, they can alter the position of the plume as they move in the Z direction. They typically move mostly in the Z direction but also travel in the Y direction, pulling the plume with them. These B vortices seem to create a feedback loop for the system because they tend to pull the plume relatively far in the positive Y direction. Because the plume is pulled in one direction by the B vortex, on the opposite side of the plume a larger concave section is created (see point A in figure 16), allowing a larger flow of water from the lip of the plume on the weak side of the plume to interact with lower sections of the weak side of the plume (see the downward flow of water at (50, -50) in figures 39 and 40). This interaction causes a new B vortex to form on the weak side (see (40, -70) in figure 40), pulling the plume in the other (negative) Y direction. As this new B vortex pulls the plume in the negative Y direction, a concave section forms on the positive Y side of the plume which soon creates another B vortex, continuing the cycle (for the whole cycle, see figures 34-51).

It is possible that these B vortices may be the reason behind the larger wavelength of the H/D = 6 case, as they dictate how far and when the plume sways. Thus the speed with which these B vortices rise up the plume and the rate at which they are created could potentially set the wavelength of the plume. It is unlikely that the wavelength sets the formation of the B vortices because the wavelength does not significantly interfere with the speed with which the B vortices rise (though that speed can affect the plume wavelength). If the wavelength were small, the flow from the lip of the plume would be more concentrated (because the opposite side of the sinusoid would be sharply concave) and would be pushed farther down in the negative Z direction. This more concentrated water flow would then cause a B vortex to form farther down (in the negative

Z direction) on the plume than it would otherwise; since it would take longer for this B vortex to rise up the plume (as it has a longer Z distance to travel), the next wavelength of the plume would be longer. In this process, this longer wavelength would produce a small wavelength (though larger than the first, and smallest, wavelength). Eventually, in this process, the wavelengths would even out (see figure 52). It is possible that such a feedback mechanism regulates the wavelength of the plume; however, the data are inconclusive at this time.

In Urakawa, Morioka, and Kiyota, it was observed that standing waves only appeared when the length of the water tank (in this experiment, the X direction) was an integer of ½ of a wavelength of the plume [8]. Even though their experiment dealt with line sources, this observation seems to fit with the hypothesis that B vortices could set the wavelength as B vortices would not be able to fully form at the walls of the tank.

There are other ways that B vortices can form. In the H/D = 6 case, the other prominent process is caused by a flow fracture in the flow originating from the nominally quiescent regions (see (25, -110), (25, -105), (25, -100), (25, -95), and (35, -85) in figures 53-62). Usually, these nominally quiescent regions of colder water surrounding the plume move quite slowly towards the plume and eventually turn upwards to join and expand the plume. However, sometimes the water from these regions diverges, with some water moving in the positive Z direction and some moving in the negative Z direction. The area where the flow diverges often interferes with the plume, eventually creating a B vortex. These B vortices tend to form lower on the plume, become larger, and move the plume farther in the Y direction than those formed from interactions with water from the lip of the plume. The exact cause of these regions of divergence is unclear, though they occur frequently enough to warrant further data collection.

Relation to H/D = 4 Case

The largest difference between the two cases is the formation of the B vortices and the wavelength. However, it is unclear why the B vortices form strongly in the H/D = 6 case, though it is possible that it is due to differences in buoyancy of the water which interacts with the plume after leaving the lip of the concave section of the plume (see point A in figure 16). It is also unclear how the differences in vertical confinement (from the water free surface) affect the wavelength. In the X direction, even though the wavelength is significantly longer in the H/D = 6 than in the H/D = 4 case, the period is significantly lower, indicating much faster movement if the plume is indeed meandering in the X direction rather than oscillating as a standing wave.

H/D = 8

Y-Z Plane

The H/D = 8 case is similar to the H/D = 6 case. The transition of the B vortices to A vortices is somewhat stronger, and the B vortices usually form higher up on the plume, around H/D = 4. The B vortices are also more visible and much stronger than in the other two cases. The most noticeable difference, however, is another process for creating B vortices. In this case, B vortices can be created by other B vortices. When B vortices become too large (most often due to an unusually low starting point for the first B vortex), they can cause disturbances in the plume that can trigger the formation of secondary B vortices (see figures 63-72).[5] These secondary B vortices can be on the same side or on the opposite side as the original B vortex. Because of the unknown cause of the formation of these strong B vortices, the plume moves in the Y direction much less predictably, and the period of the plume is much less consistent than in the previous two cases.

X-Y Plane

The H/D = 8 case (again with the image plane at H/D = 3) is different from both the H/D = 4 and H/D = 6 cases. At times, it exhibits the same consistent nature of the H/D = 6 case, but at other times seems to oscillate without a standing wave pattern. Like the H/D = 6 case, some local features, such as bends in the plume, seem to reoccur near the same area.

X-Z Plane

[5] The original vortex forms at (50, -40) in figure 63. The secondary vortices are most noticeable during their formation at (0, 35) and at (50, -40) in figure 69.

The H/D = 8 case is both less clear and less consistent than the H/D = 6 case. The period of the appearance of the major features varies between 70 seconds and 100 seconds. Besides large flow features, such as the strong vertical flow of the plume and the weaker, less organized flow of the area between the curves of the plume, very little information can be gleaned from the data.

General Structure

The general structure of the H/D = 8 case is similar to the H/D = 6 case but with less consistency. Due to the greater height of the water, the water in the plume is able to dissipate more heat and thus is more susceptible to disturbances as it has lost more of its buoyancy. In this case, the top of the plume is therefore more heavily influenced by the formation of vortices, especially B vortices, compared to the other previous cases. The greater impact and the less consistently repeatable formation of B vortices (either due to regions of divergence or due to disturbances from other B vortices) cause the motion of the top of the plume to become less regular. Furthermore, the feedback of the plume to create B vortices at regular intervals (due to the downward water flow from the lip of the concave sections of the plume) is decreased somewhat because the lip of the plume is relatively much farther away from the bottom of the plume where the strongest B vortices are produced. The combination of these two phenomena causes the plume's swaying motions to become less consistent.

H/D = 12

Y-Z Plane

Due to the scale of the camera used, data was not able to be taken near the surface of the water. However, new, interesting features still arose. Near the bottom of the plume, but in the nominally quiescent region, a vortex appeared. This vortex came from the nominally quiescent water and rotated counter to the plume (e.g., it would rotate clockwise if it was on the left side). As the vortex approaches the plume, it slowly dies out. It is unclear what the origins of these vortices are, or how they affect the plume (see (-40, -100) in figure 73).

Another interesting feature is that B vortices still formed at about the same height away from the cylinder as they form in the H/D = 8 case, roughly at H/D = 4. Furthermore, they also seem to shed from the plume as A vortices significantly before reaching the surface of the water, usually around H/D = 5, but sometimes as low as H/D = 4.2 (see (65, -30), (45, -20), (50, -5), (55, 0), and (60, 10) in figures 74-78, respectively).

X-Y Plane

This case has significantly more movement than either the H/D = 6 or the H/D = 8 case. Part of the plume sways back and forth while other parts of the plume bulge far away from the centerline (see figure 79). The plume bulges out far enough in some areas to go beyond the image of the camera, and thus much informative data is lost. However, these bulges do occur at roughly the same location, leading the author to believe that the plume is exhibiting standing wave behavior, though there is not enough data to fully substantiate this claim. Also, when the plume bulges out, it sometimes causes vortices in the X-Y plane to form (see (-40, -50) in figure 79). Very few of these vortices are available in the data, often only portions of the vortex due to the magnification used in the experiment. Therefore, not much can be theorized about these vortices.

X-Z Plane[6]

The data presented in this case is only slightly different from the data of the H/D of 8 case. The main difference is the further lack of consistency and regular period of the features. Some features, such as weak vortices and point or oblong sources and sinks, exist in between the plume's sinusoid, though they are not consistent in form and do not repeat (see (30, 110) in figure 80; (60, 80) and (135, 110) in figure 81; and (75, 95), (125, 80), and (170, 75) in figure 82).

General Structure

The H/D = 12 case is similar to the H/D = 8 case with some features being exaggerated. B vortices formed by the downward flow of water from the concave lip of the top of the plume (in the regular feedback mechanism) are weak compared to those formed through other processes (due to disturbances from regions of divergence or from other B vortices). The less repeatable nature of these processes allow for a much less regular plume structure with little to no obviously predictable pattern.

It appears that the B vortices sometimes shed from the plume before reaching the surface because the abundance of B vortices does not allow the plume to remain tangent to all of them simultaneously. However, the data do not fully confirm this hypothesis.

[6] Data from Jock Pflug

To fully understand the structure of this case, more research must be conducted on the formation and development of the B vortices, especially those not caused by feedback from the top of the plume.

Conclusion

The PIV velocimetry data confirms other data recorded on buoyant plumes in free convection flow. The data present in this thesis also shows several new phenomena, including the formation of multiple vortices and their impacts on the plume's overall structure.

The conjoining of the downward water flow from the concave section of the plume causes disturbances which create B vortices which in turn maintain the regular swaying motion of the plume. As the height of the vertical confinement of the water increases (i.e., the water level), this downward flow at first has a stronger impact on the overall structure of the plume due to increased speeds (caused by less buoyant downward flowing water and longer acceleration distances inside the plume). The increase in speed of this water causes greater disturbances and stronger B vortices, which have lower pressure and subsequently can have a greater impact on the plume. However, as the height further increases, this downward flow does not cause as large of disturbances due to its greater distance to the lower sections of the plume. Furthermore, other processes, which are less regular, begin to form new B vortices and therefore impact the structure of the plume. Eventually, the plume's motion becomes less repeatable as minor changes in the flow at the bottom of the plume build and strongly impact the structure of the top of the plume.

More data, especially of the area where B vortices form, are necessary to predict or manipulate the buoyant plume's complete structure. Furthermore, more data are necessary to show whether the B vortices are long tubes stretching half of a wavelength of the plume or more numerous discrete vortices moving up independently. It is proposed that the B vortices are tubular in shape due to the seemingly smooth transition of the plume; however, the data do not confirm nor reject this hypothesis. Hopefully, the data presented in this thesis might spur new research into these vortices and eventually into various techniques to manipulate the structure of the plume to increase heat transfer.

Figure 1

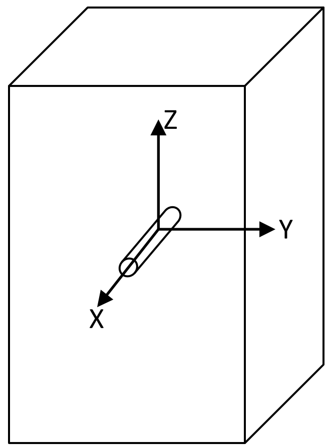

Figure 1. The experiment and coordinate system

Figure 2

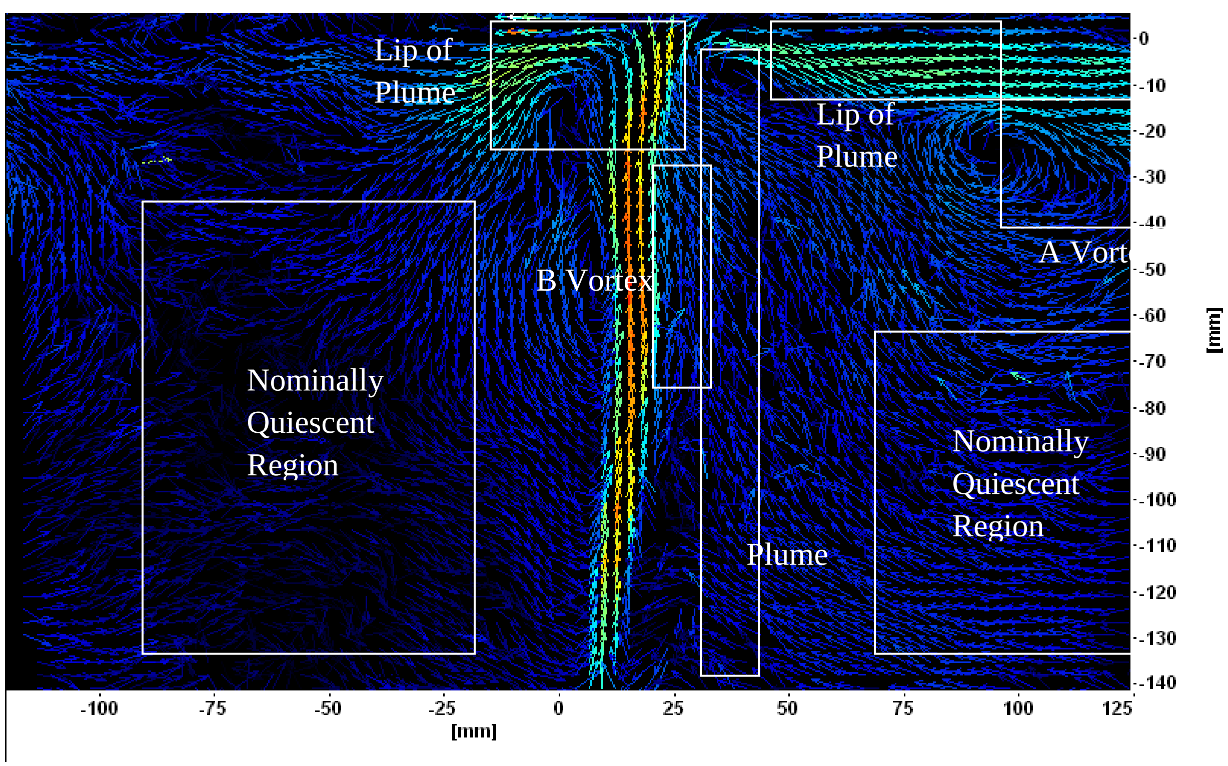

Figure 3

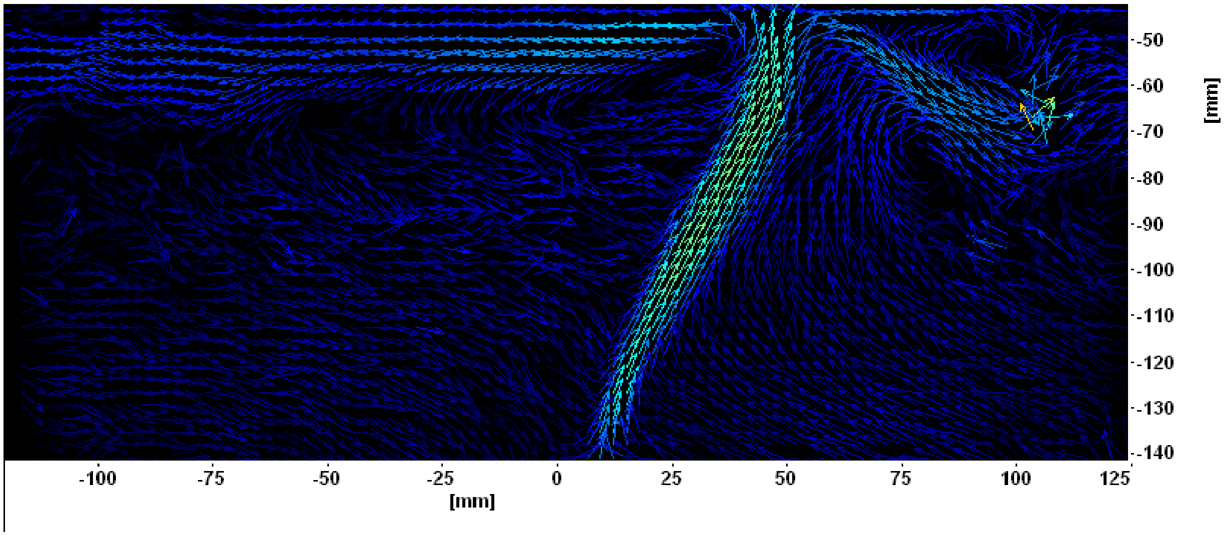

Figure 4

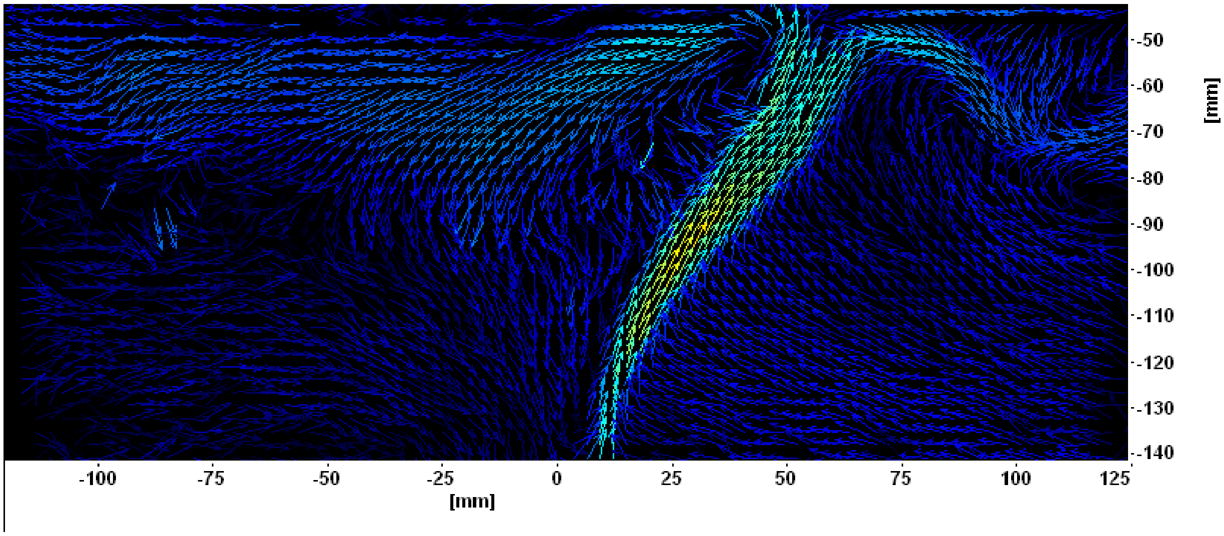

Figure 5

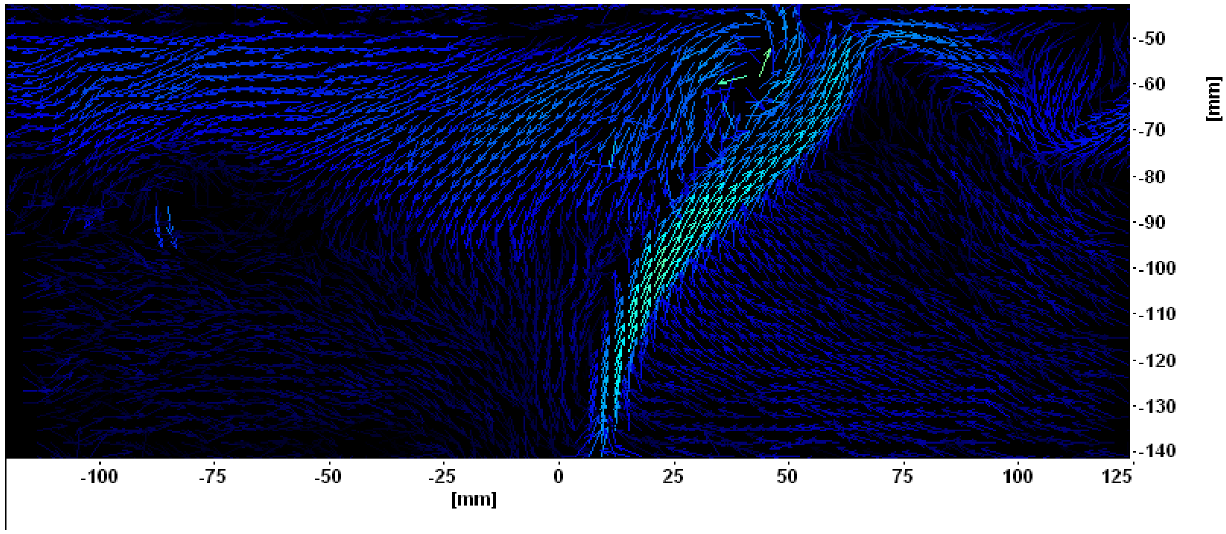

Figure 6

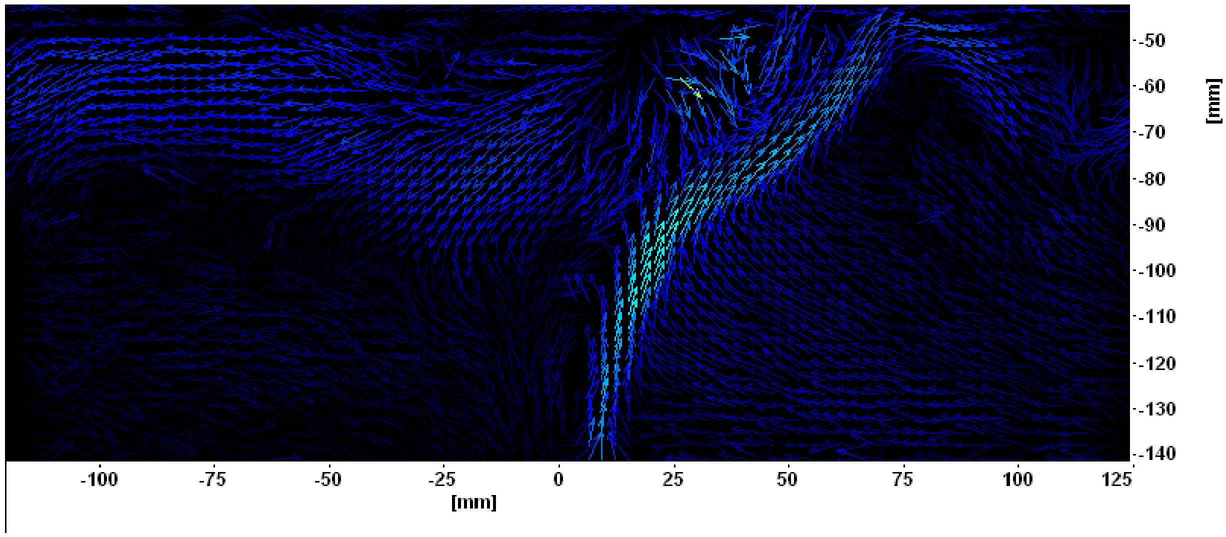

Figure 7

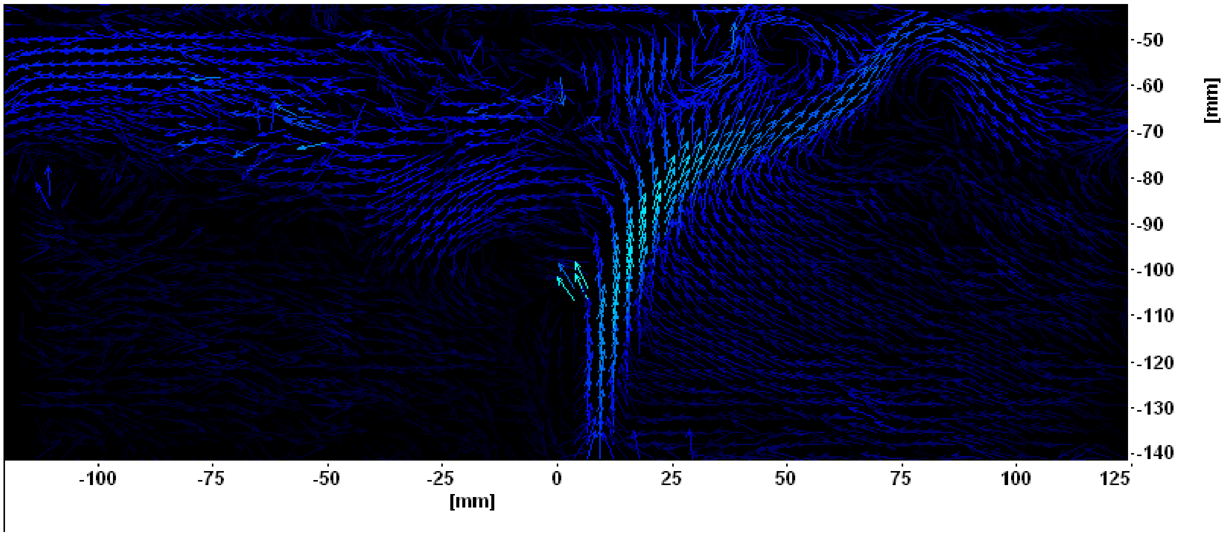

Figure 8

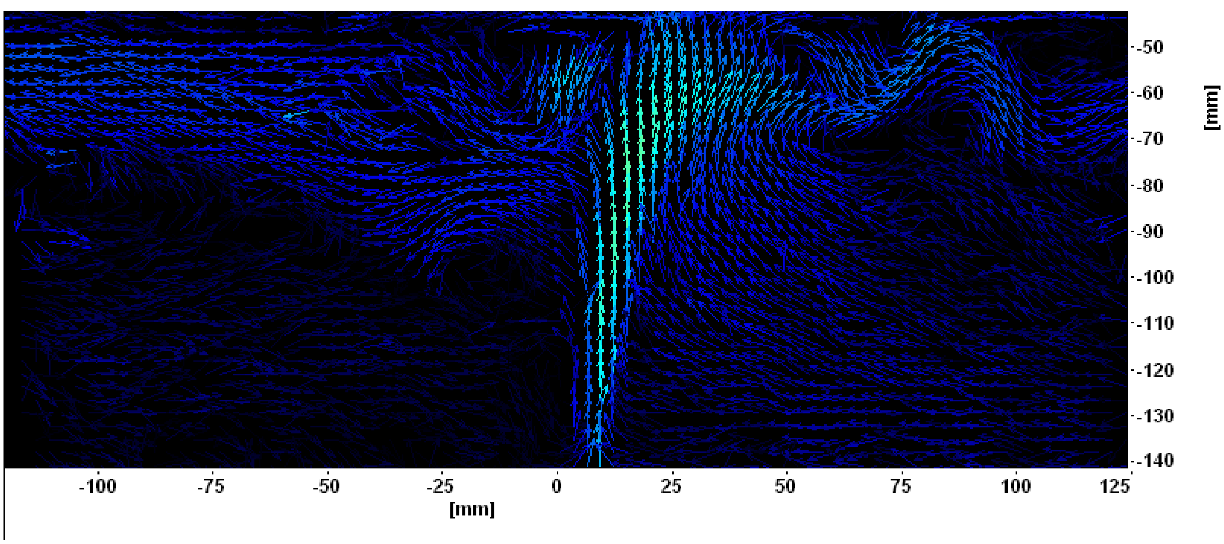

Figure 9

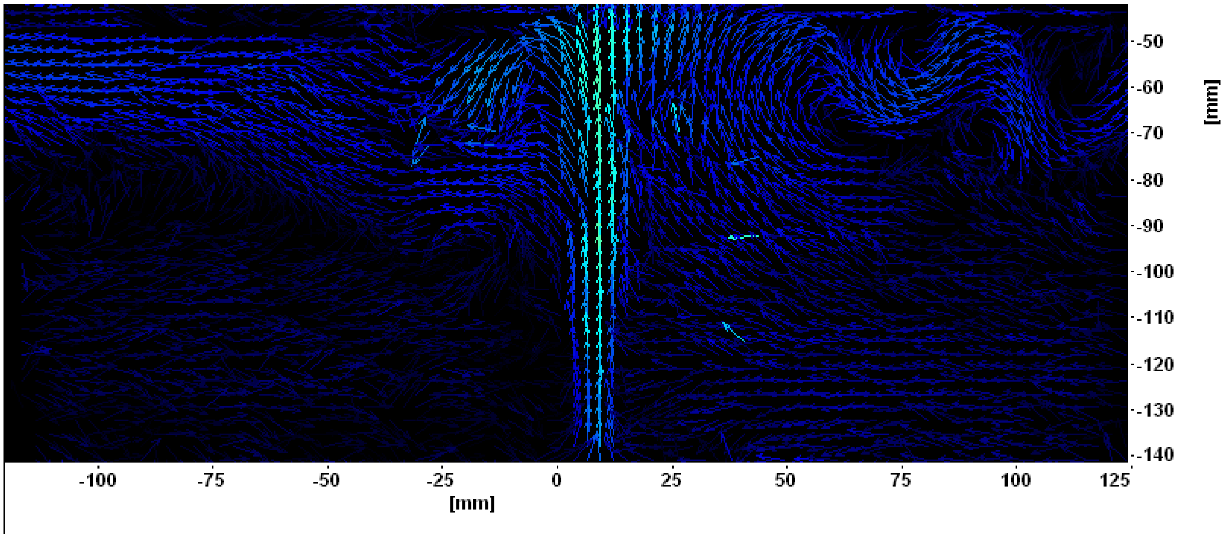

Figure 10

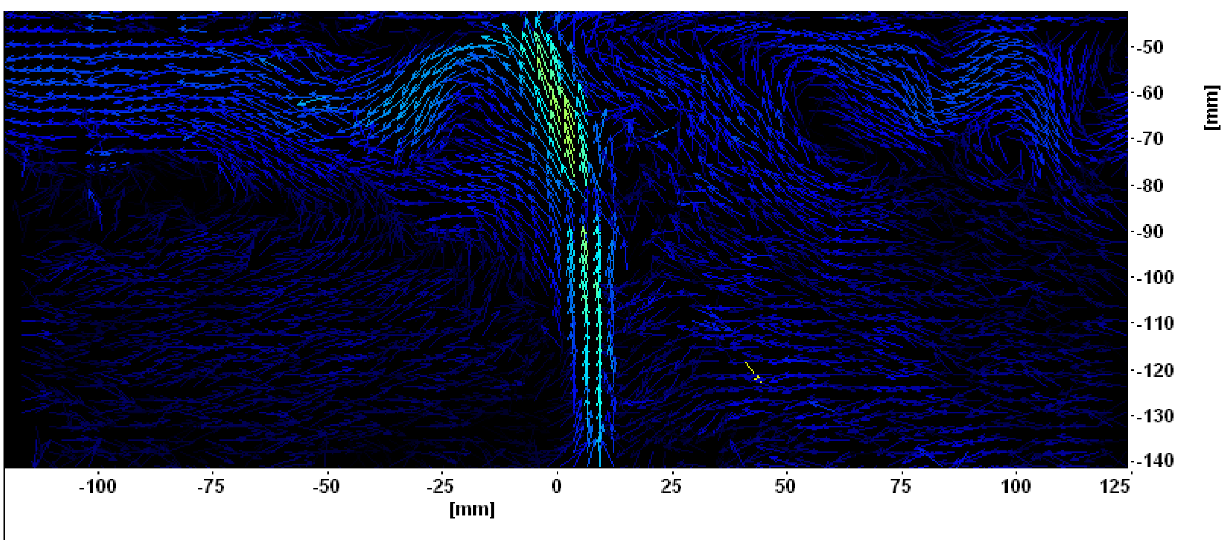

Figure 11

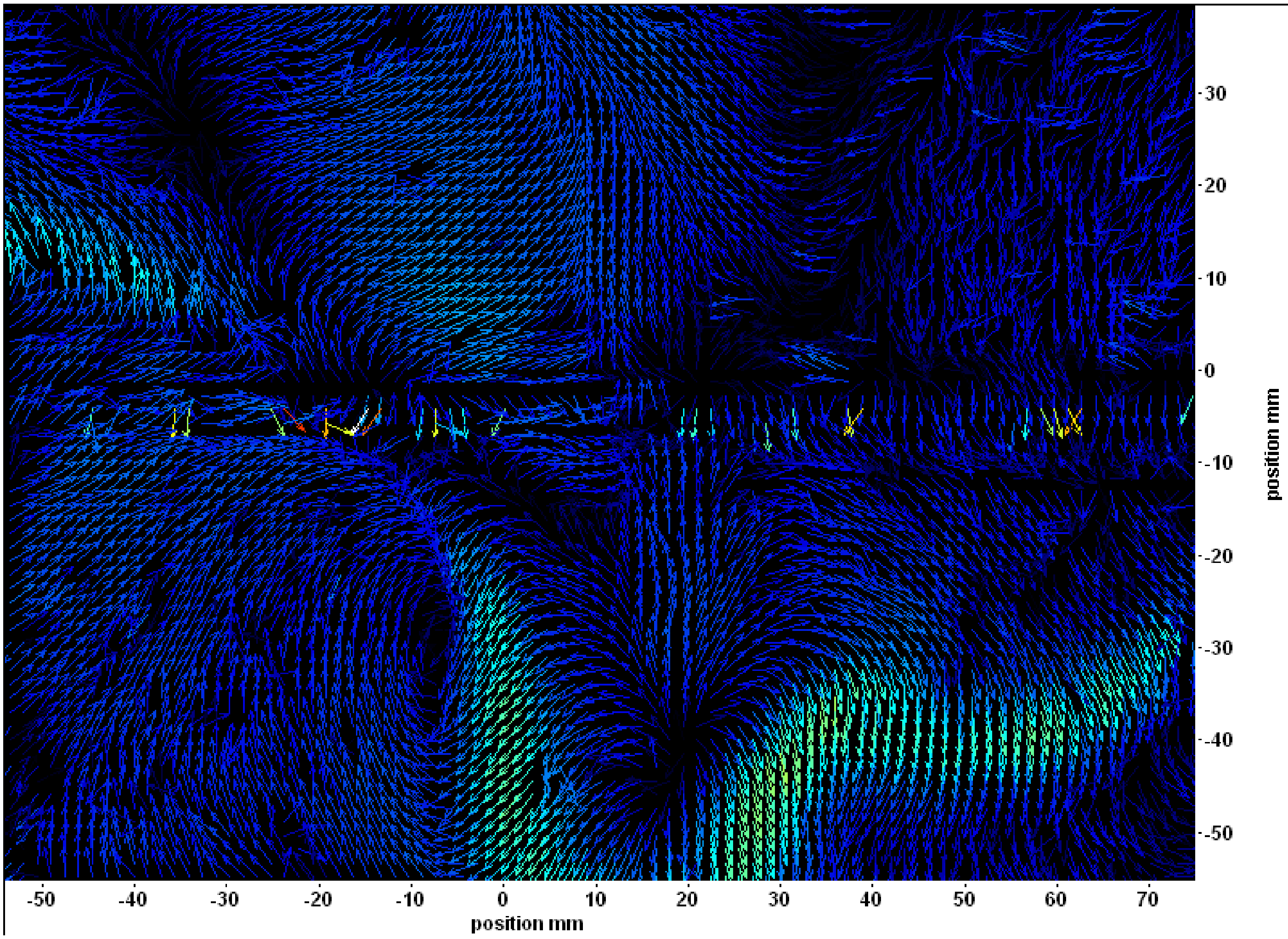

30
20
10
0
-10
-20
-30
-40
-50
position mm
-50
-40
-30
-20
-10
0
10
20
30
40
50
60
70
position mm

Figure 12

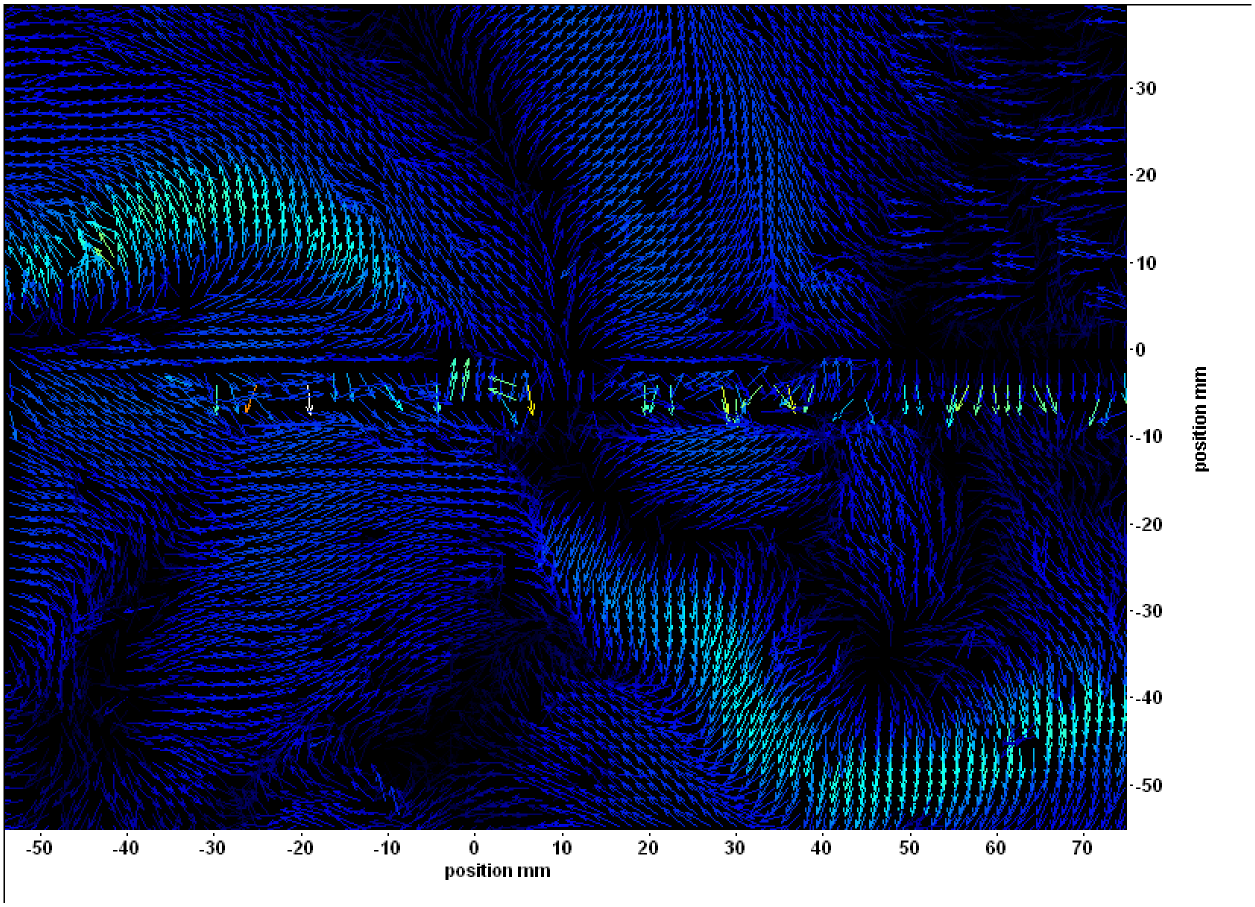

Figure 13

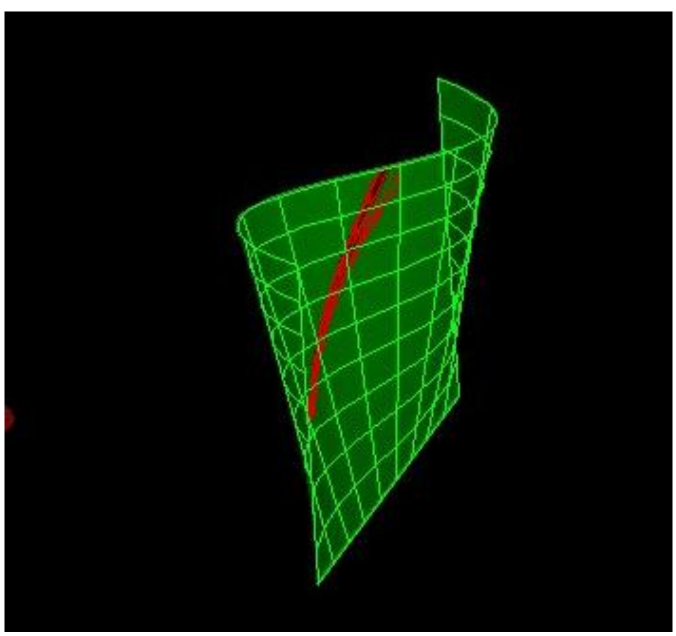

Figure 14

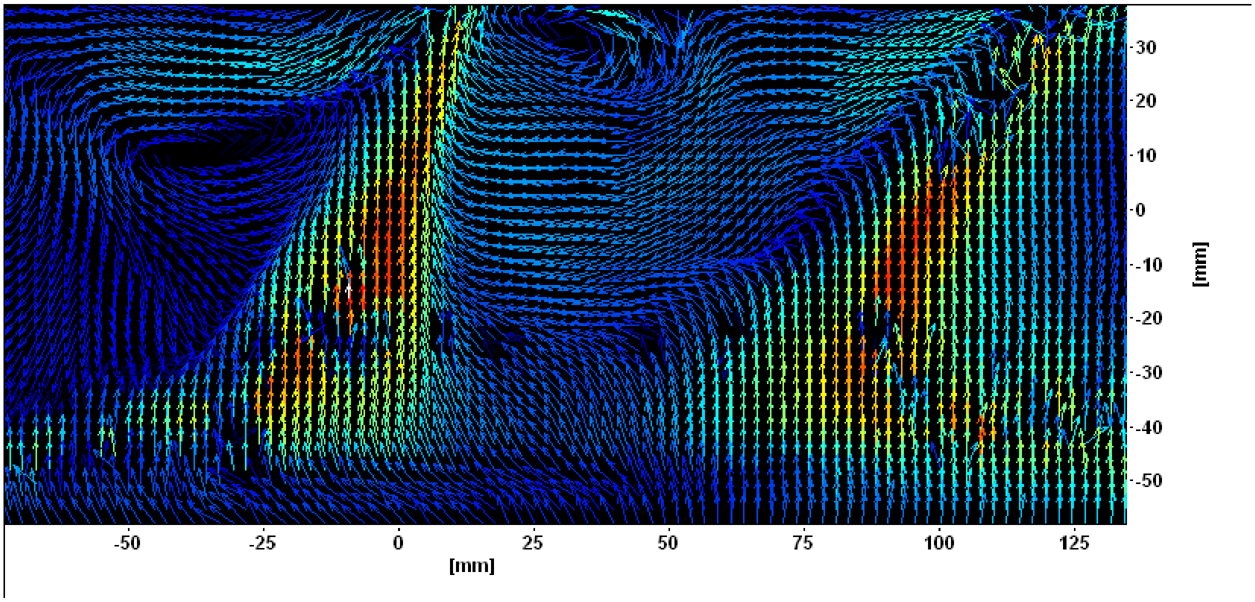

Figure 15

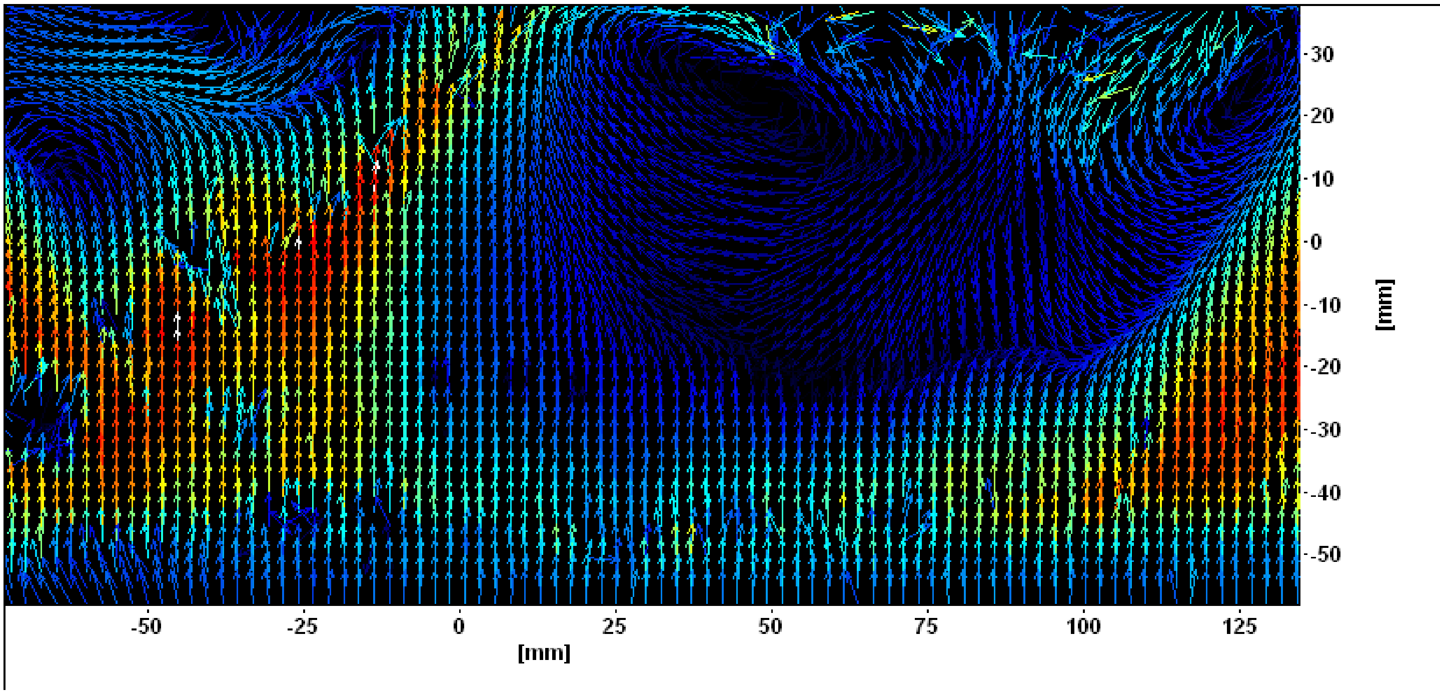

Figure 16

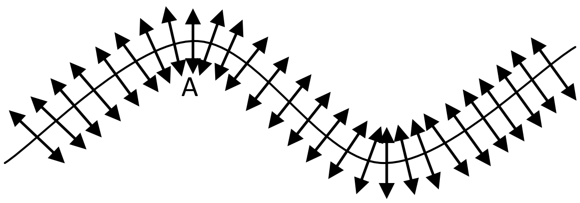

Figure 2-Overhead view of the plume. Point A references the area where water from the lip flows together far down the plume (out of plane).

Figure 17

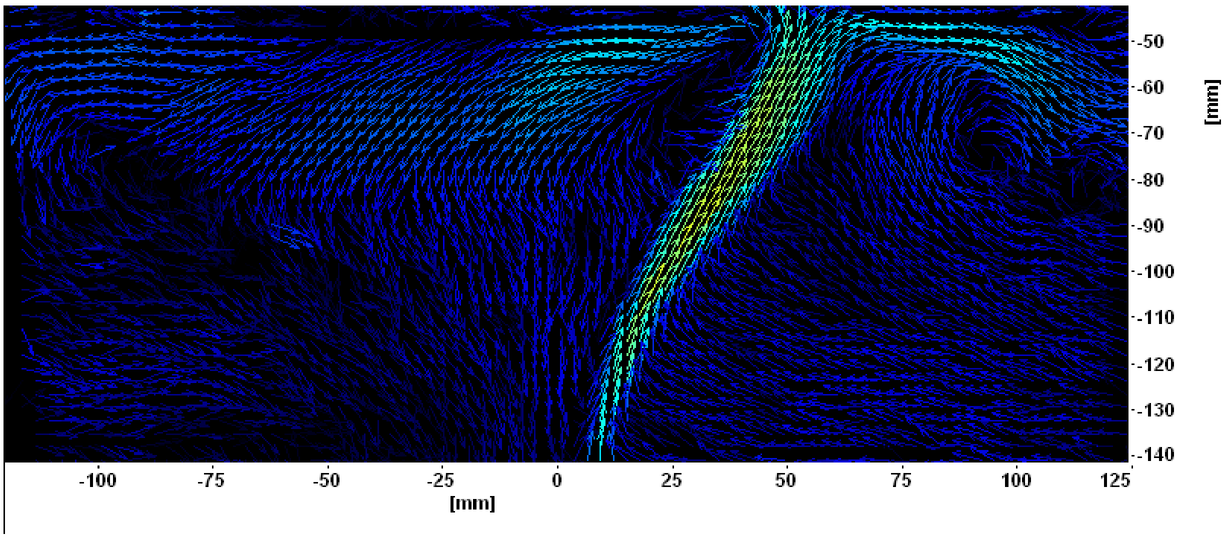

Figure 18

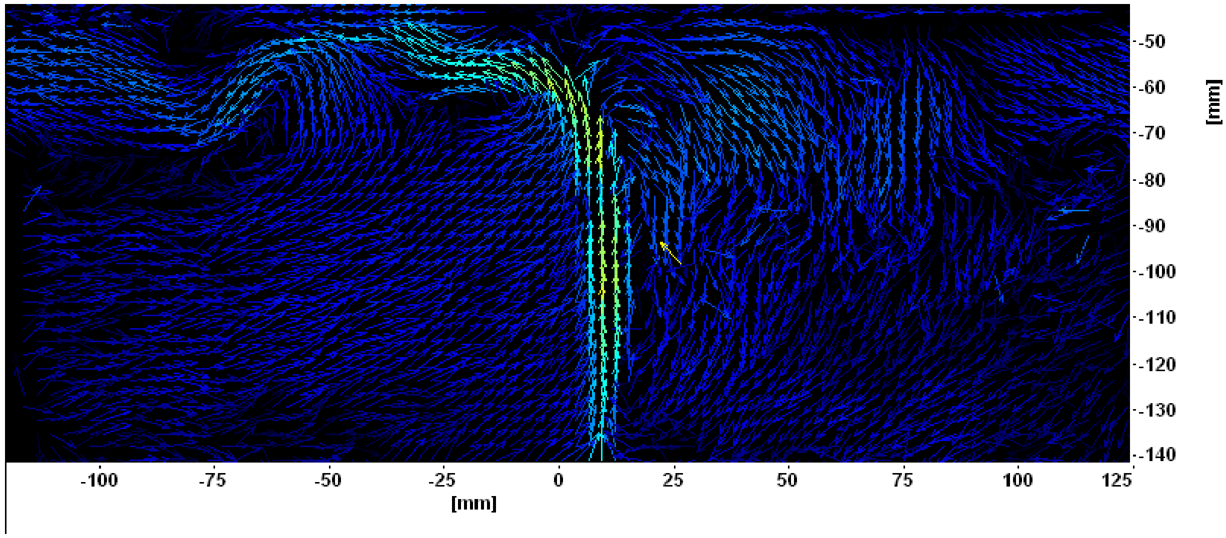

Figure 19

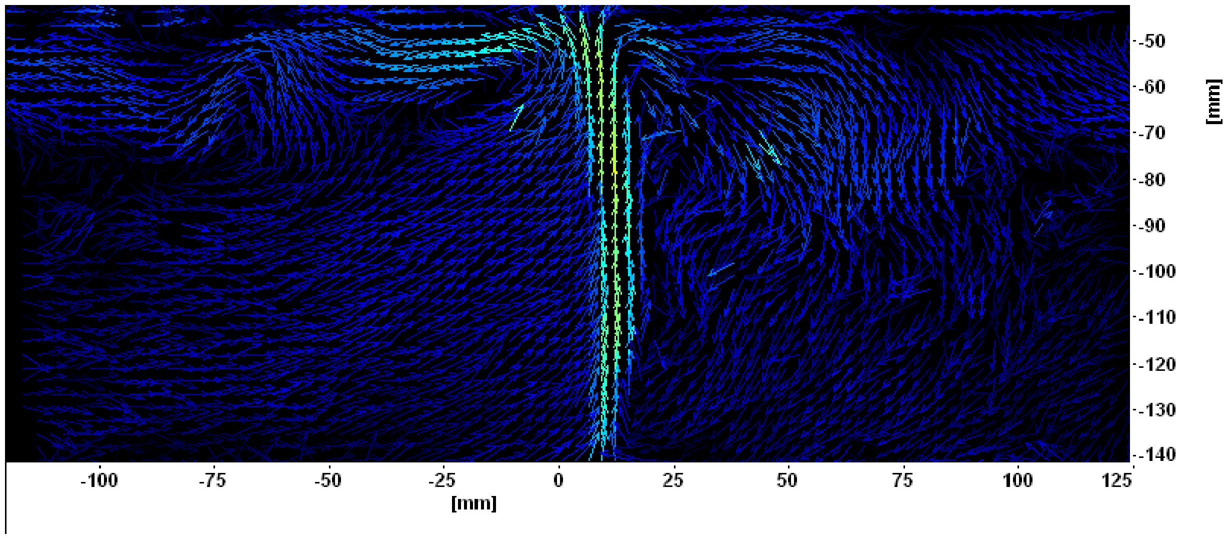

Figure 20

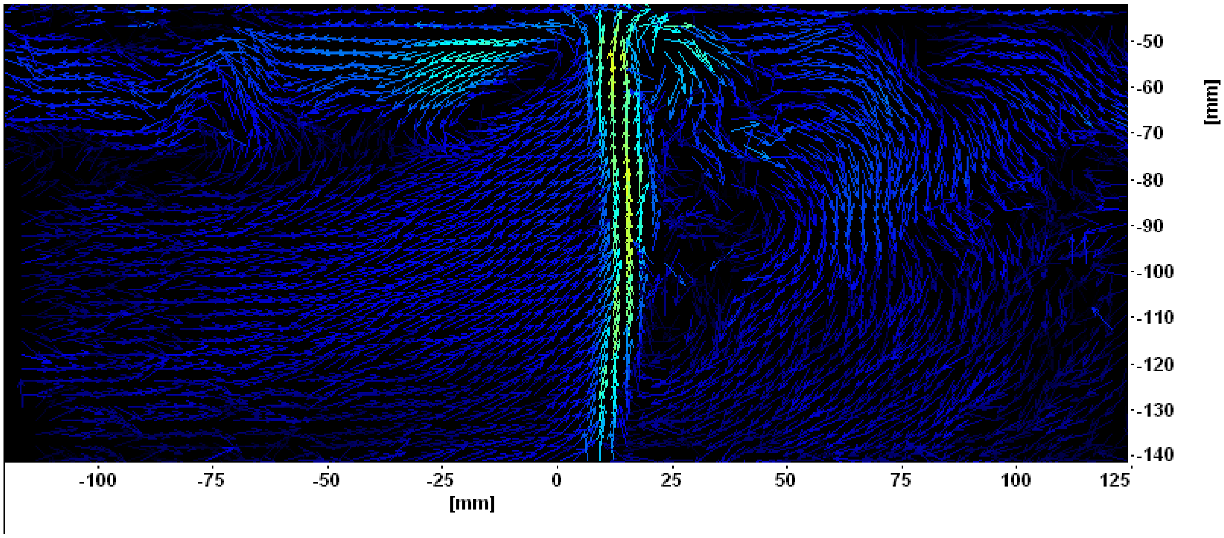

Figure 21

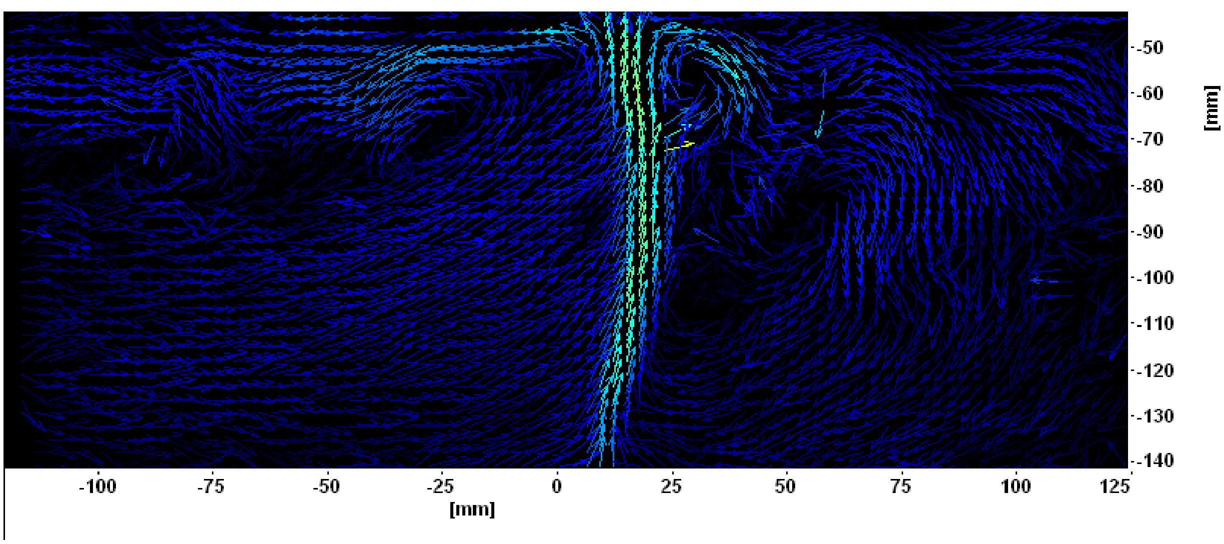

Figure 22

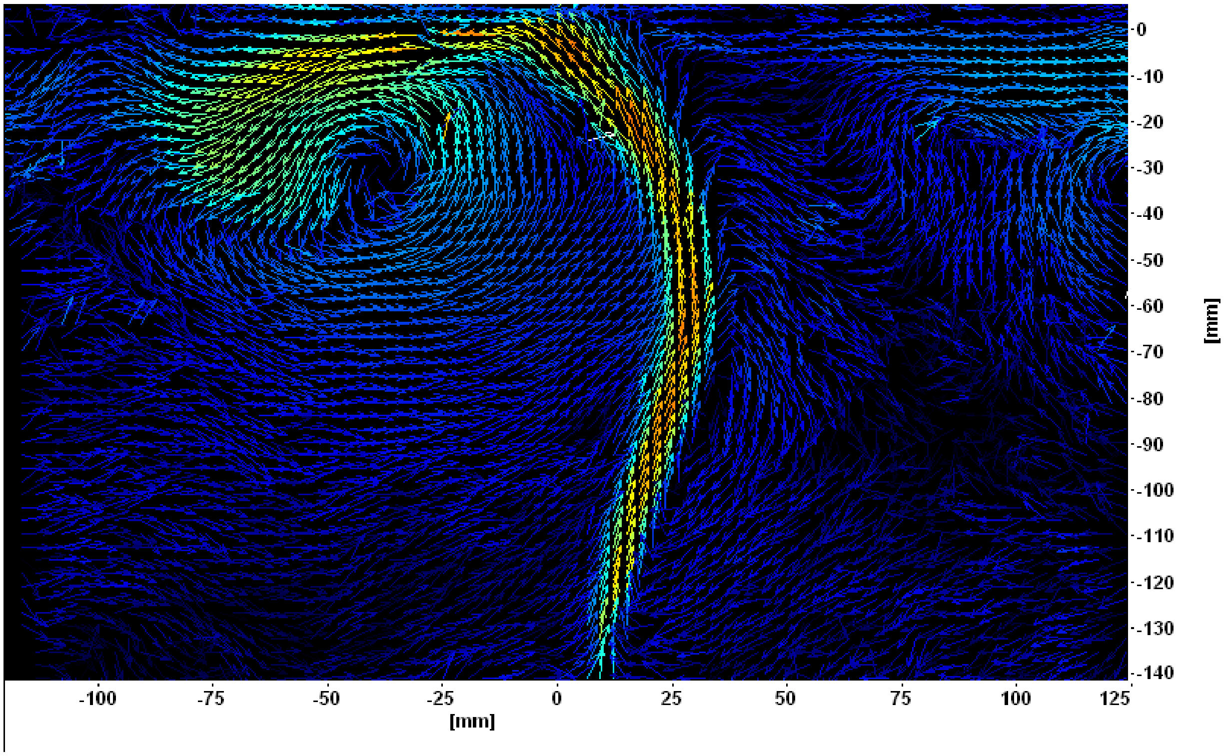

Figure 23

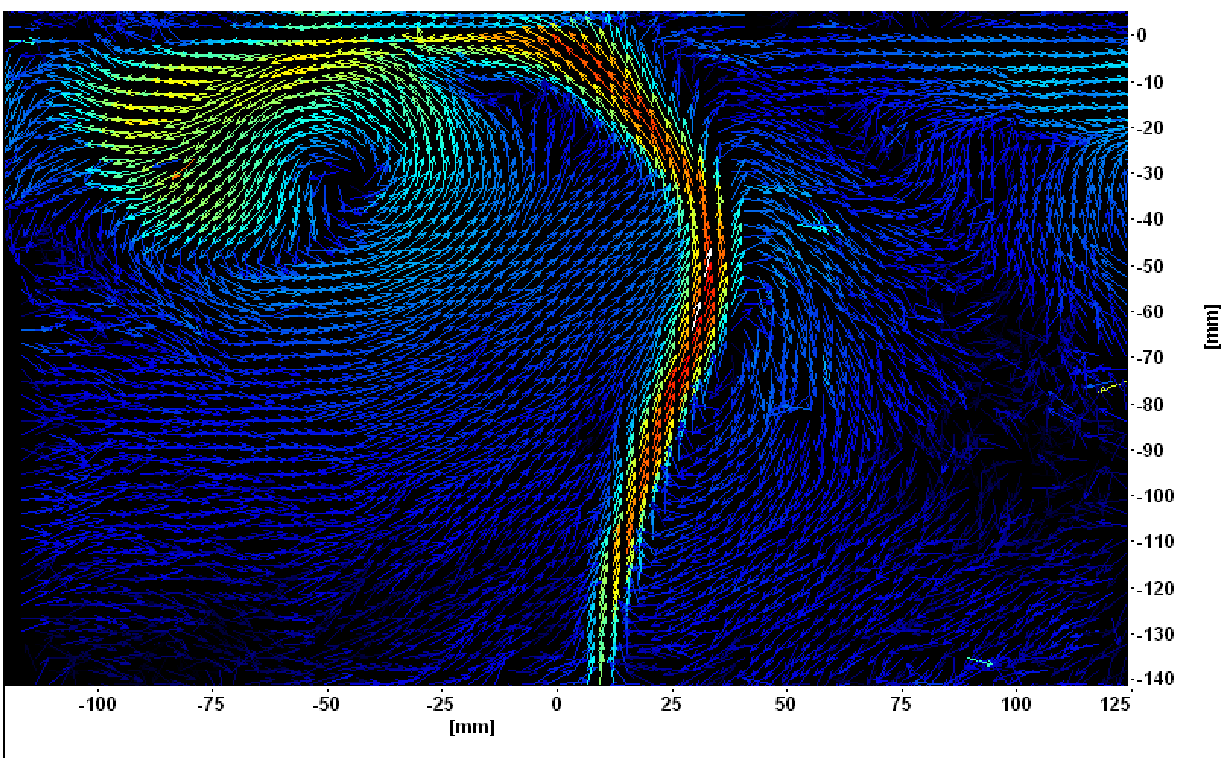

Figure 24

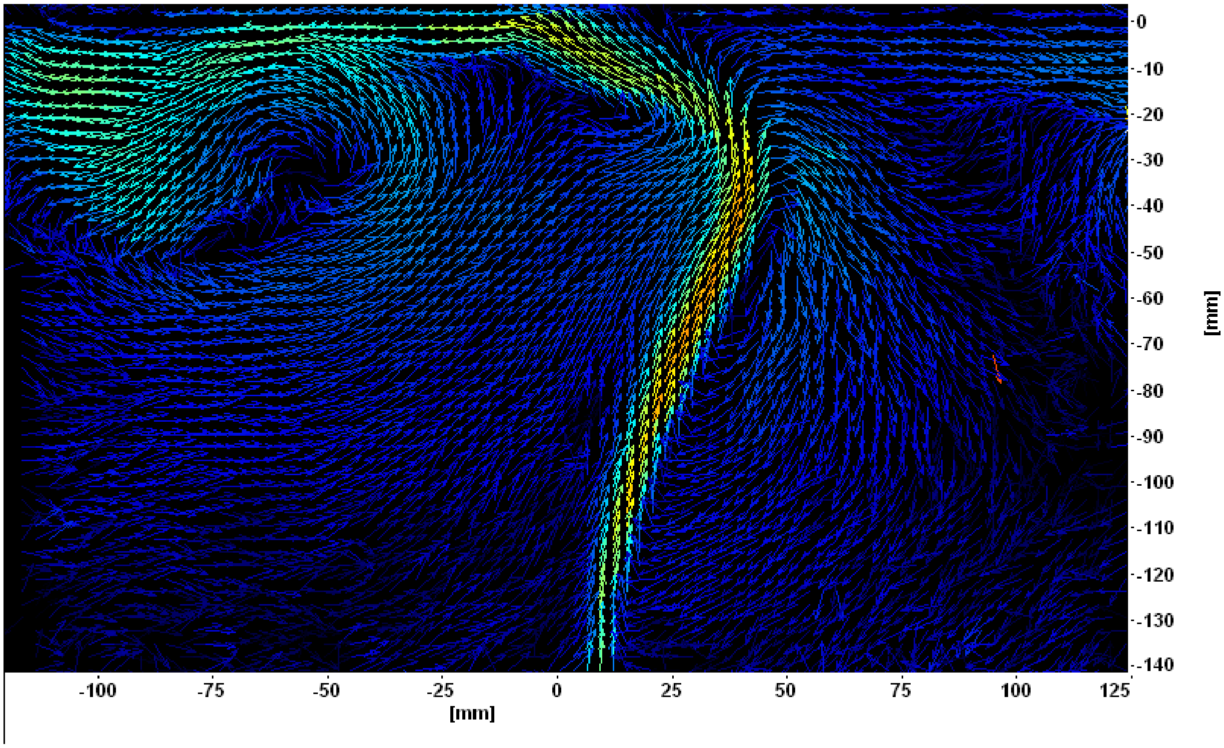

Figure 25

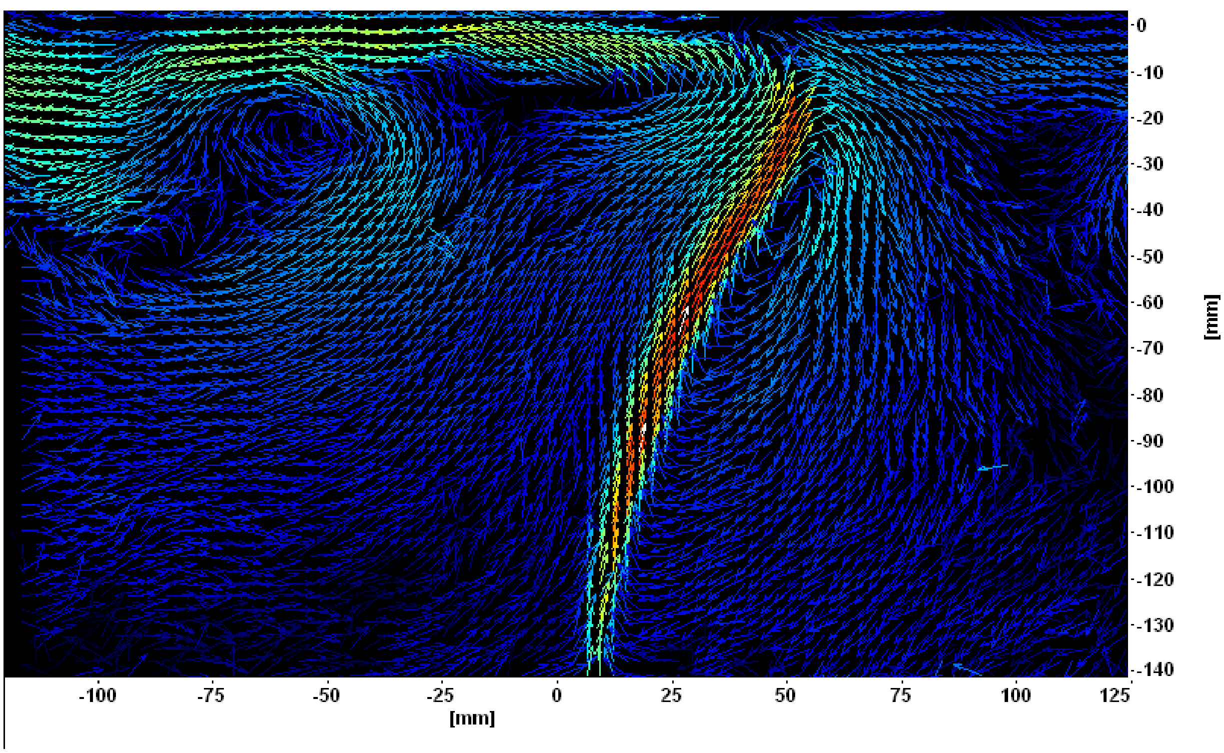

Figure 26

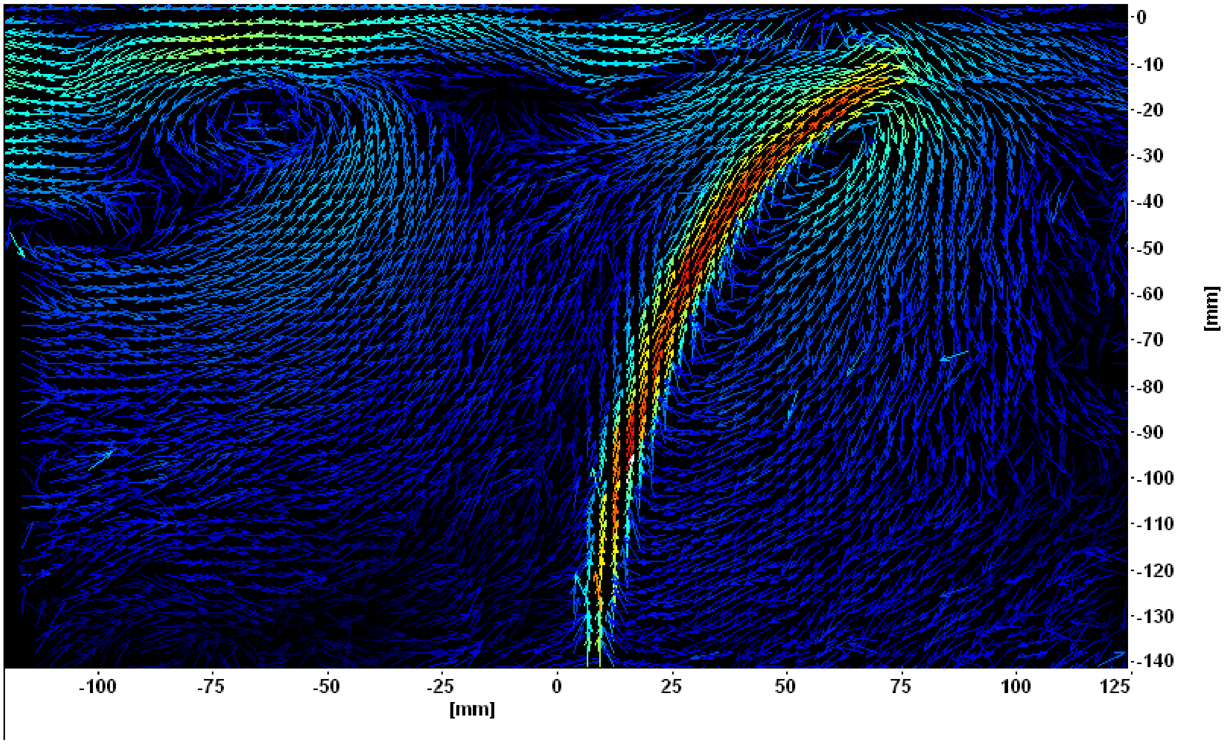

Figure 27

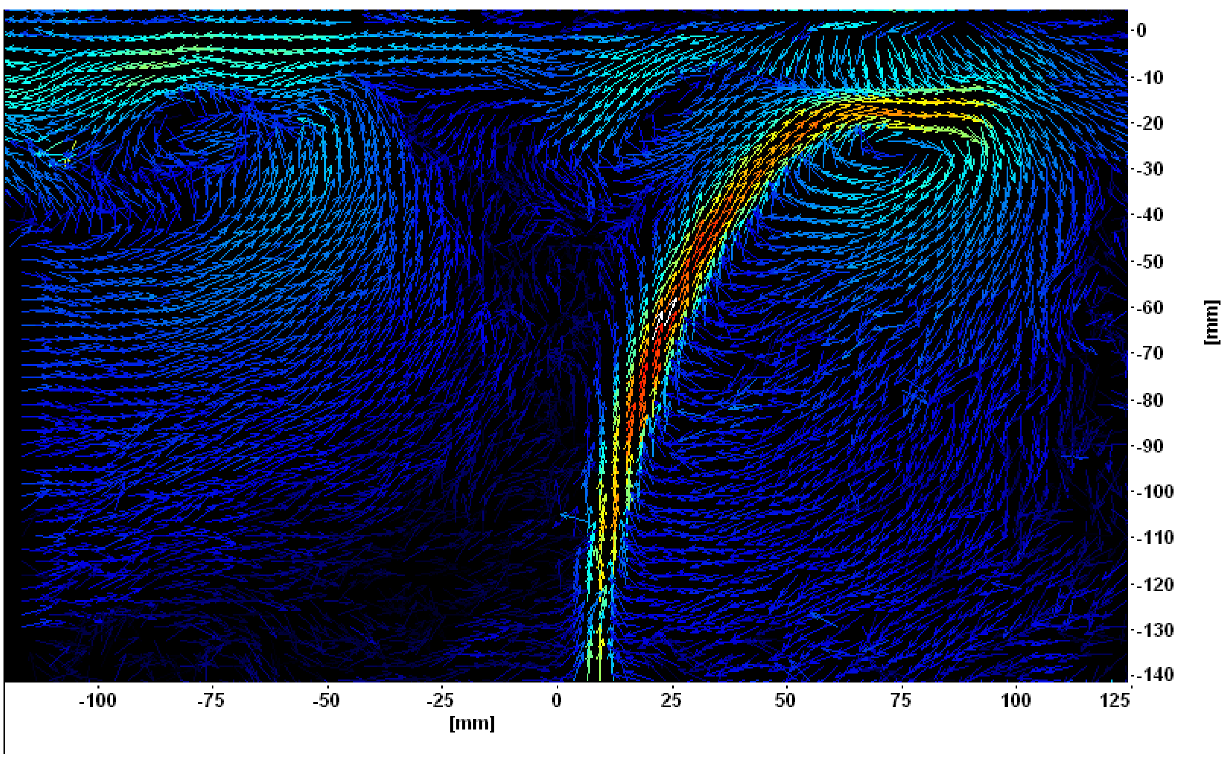

Figure 28

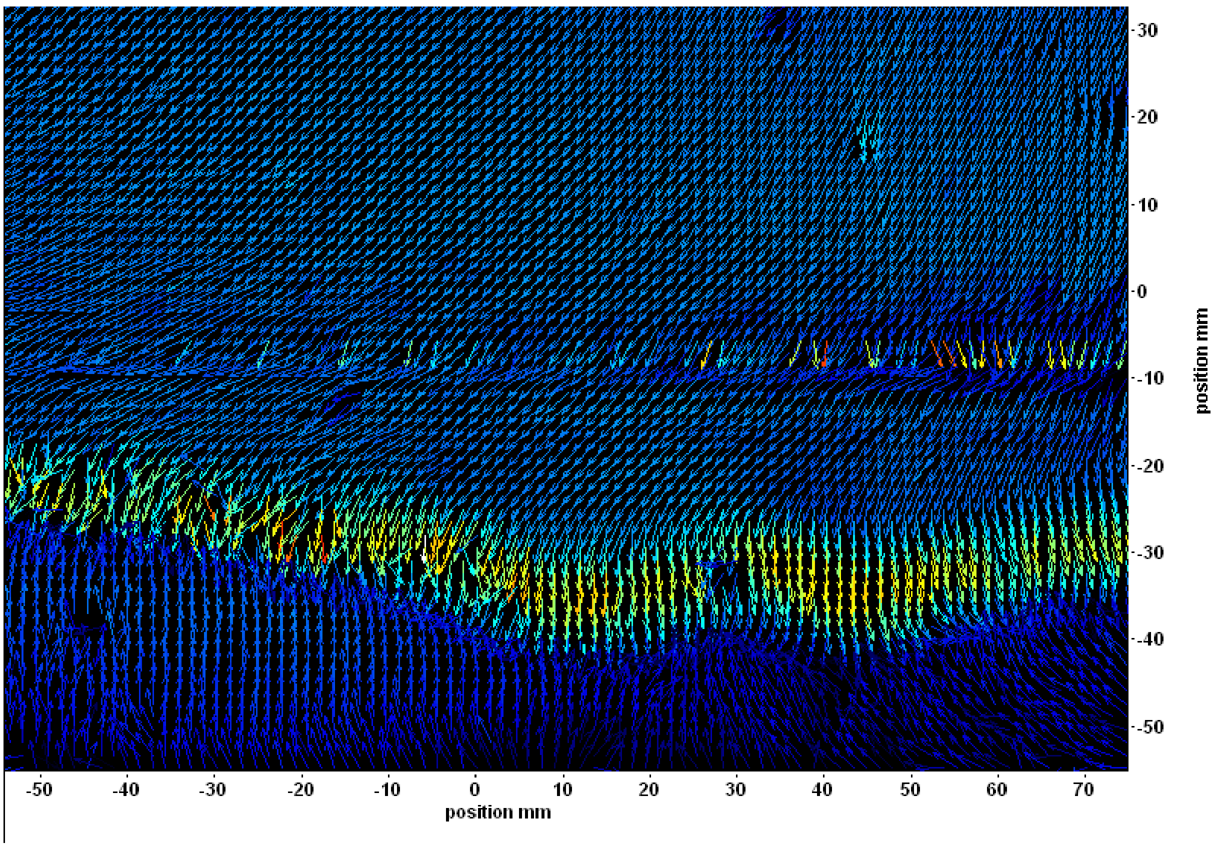
30
20
10
0
-10
-20
-30
-40
-50
position mm
-50
-40
-30
-20
-10
0
10
20
30
40
50
60
70
position mm

Figure 29

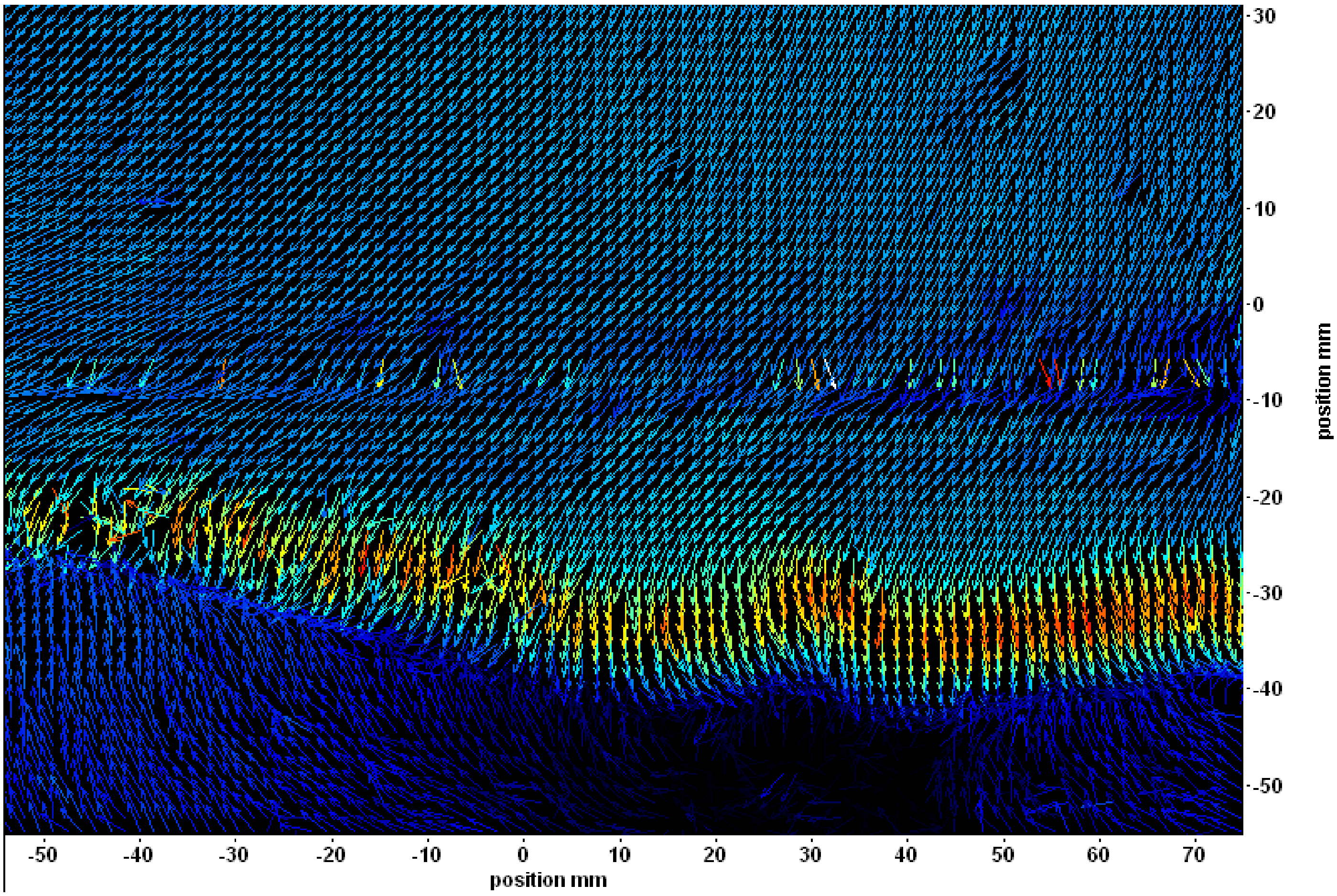
30
20
10
0
-10
-20
-30
-40
-50
position mm
-50
-40
-30
-20
-10
0
10
20
30
40
50
60
70
position mm

Figure 30

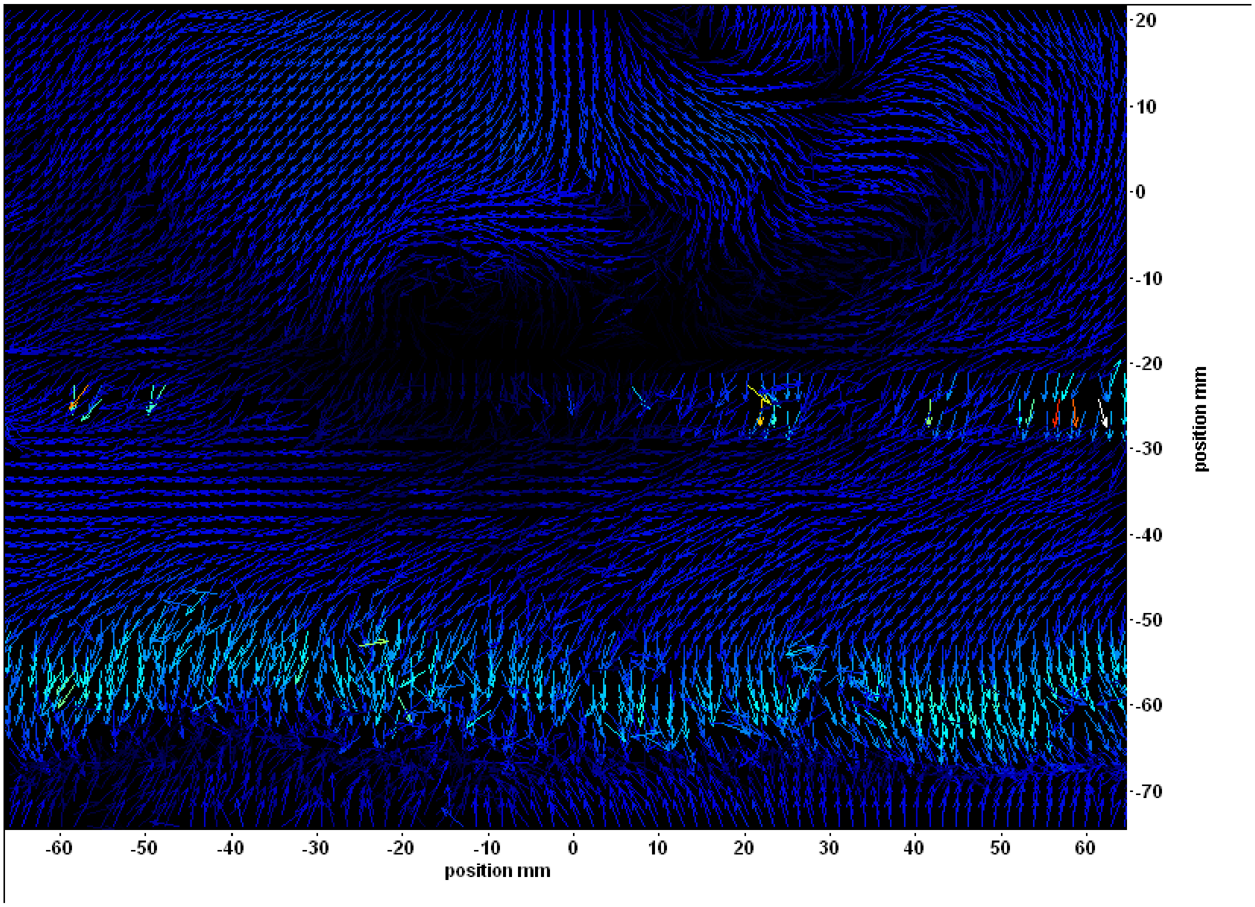

Figure 31

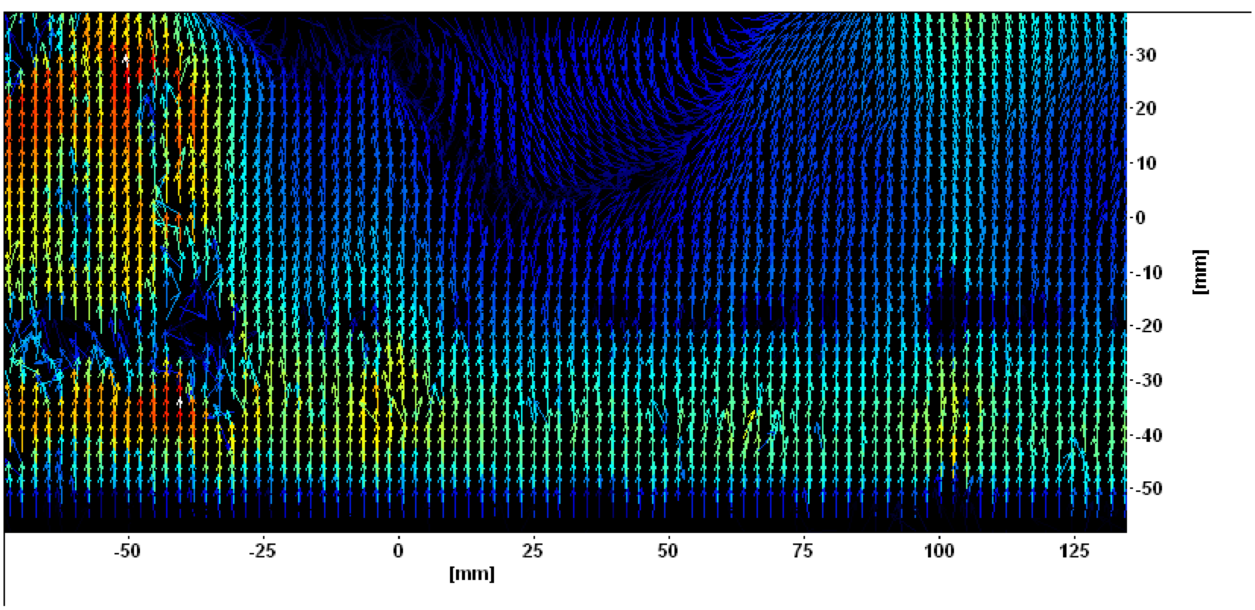

Figure 32

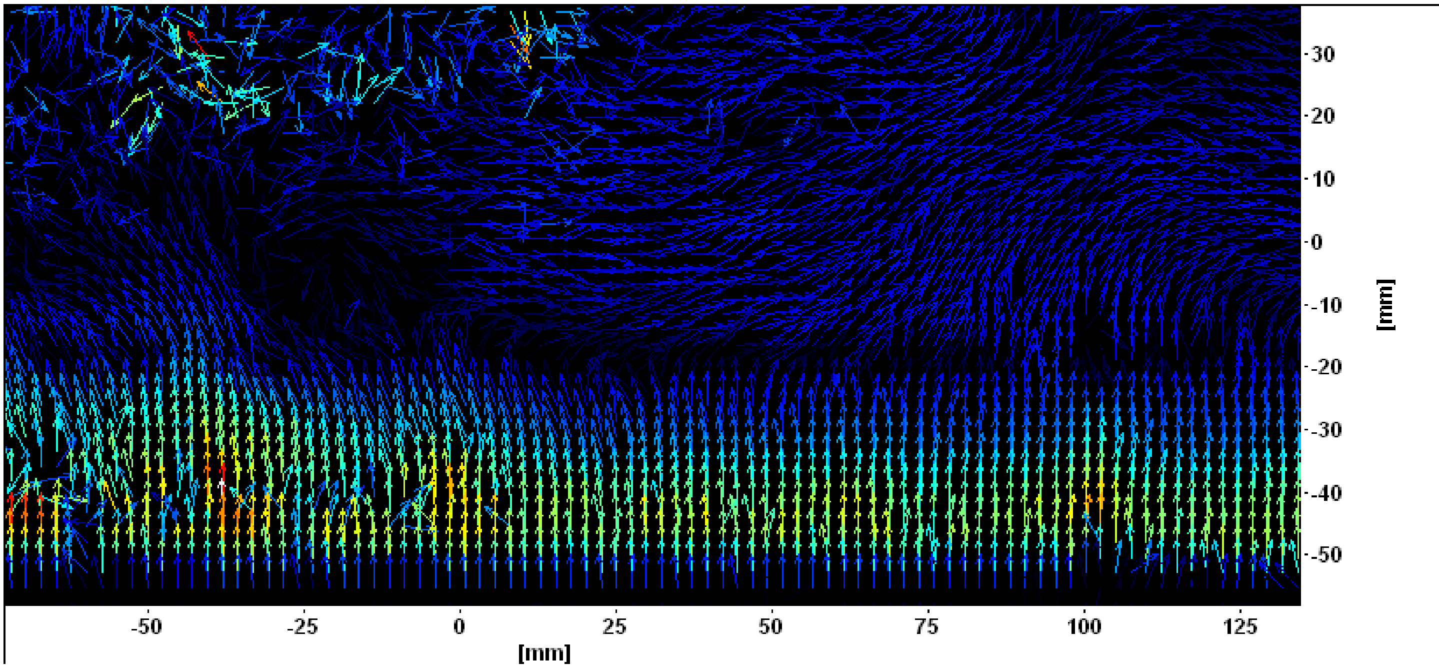

Figure 33

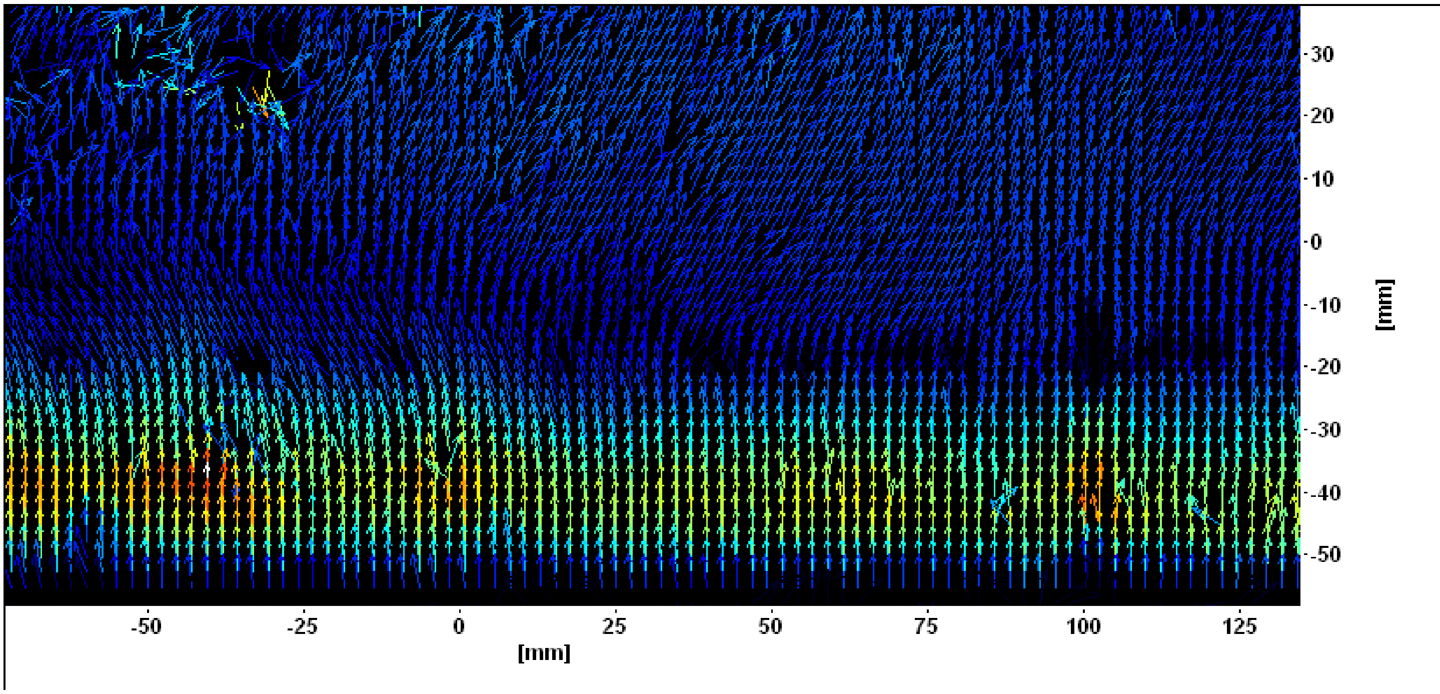

Figure 34

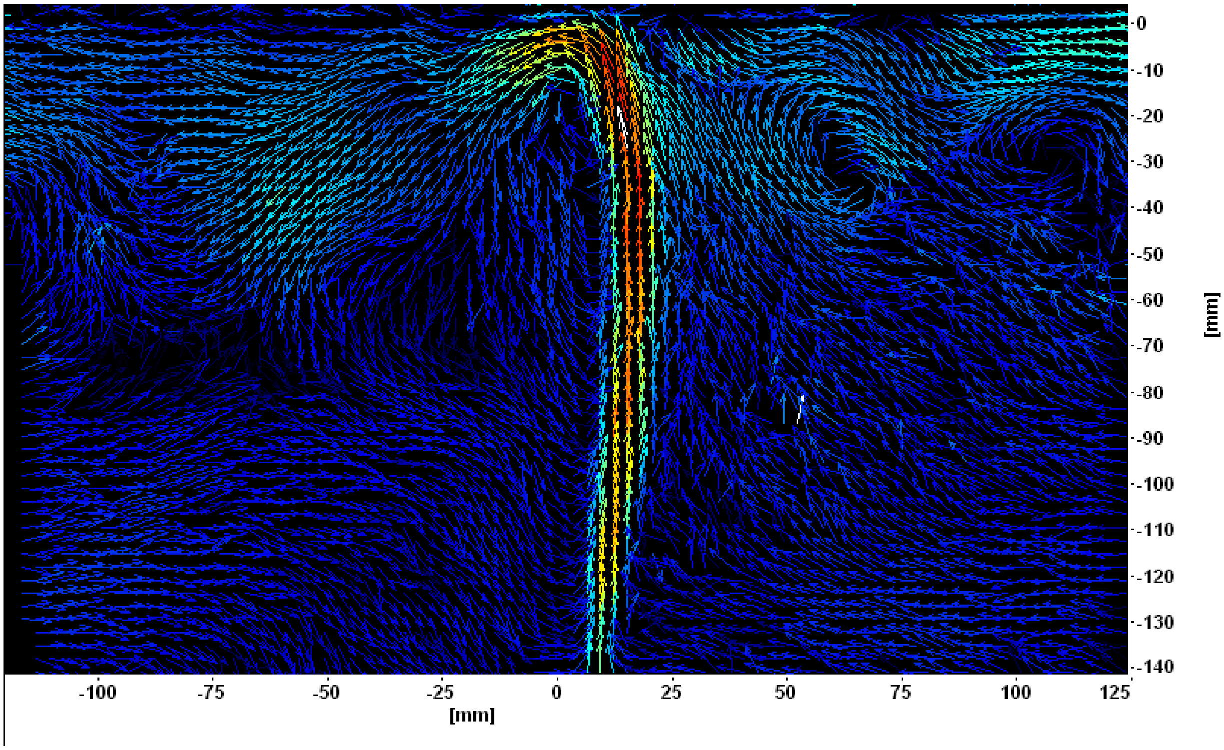

Figure 35

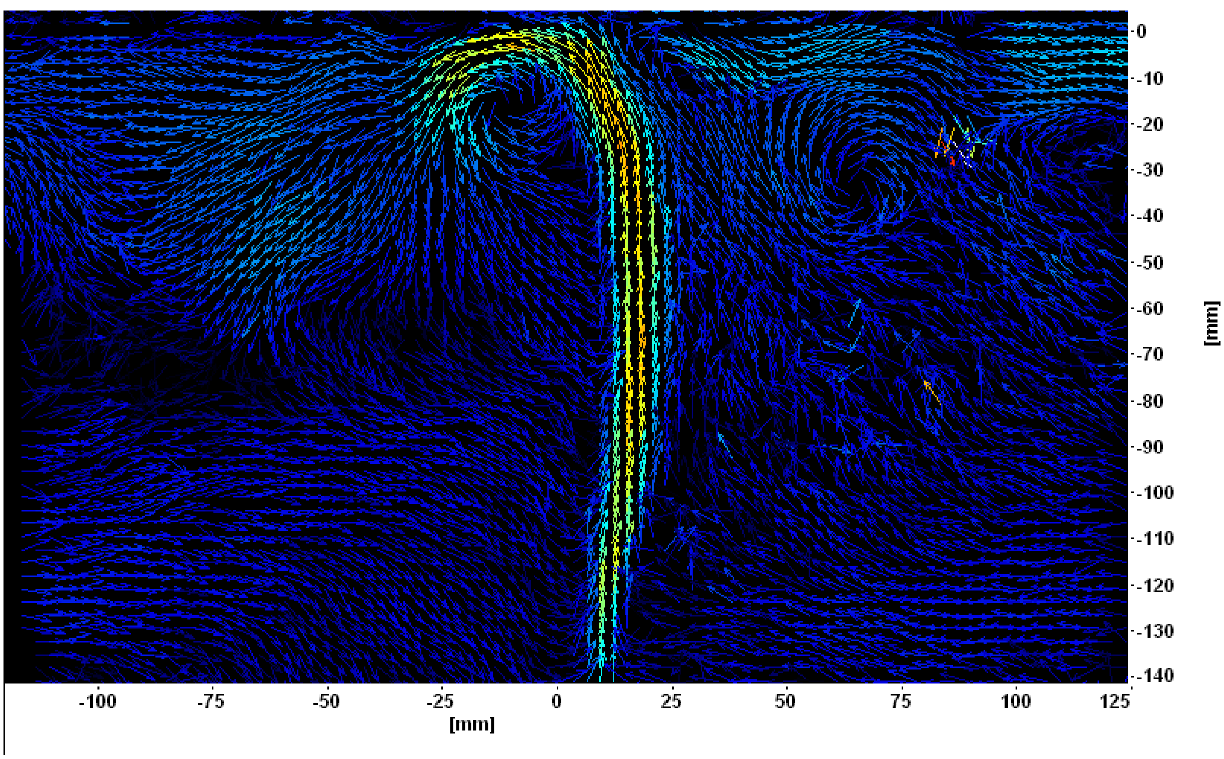

Figure 36

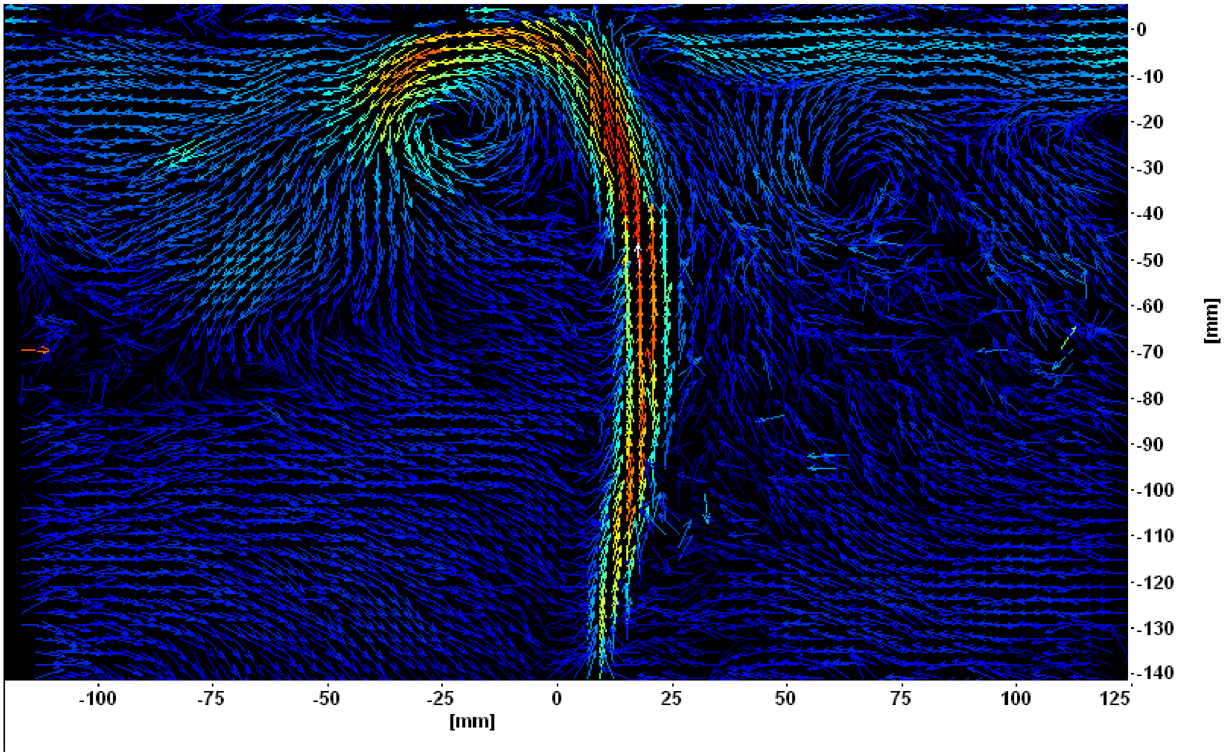

Figure 37

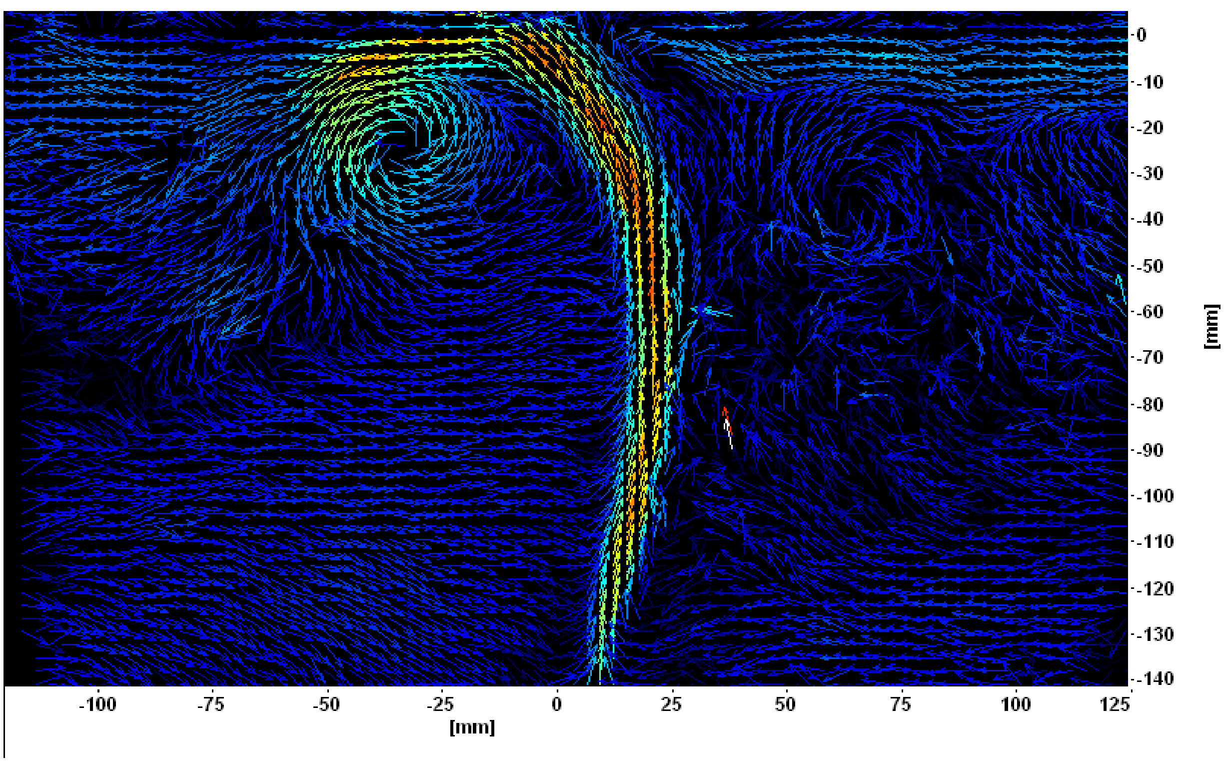

Figure 38

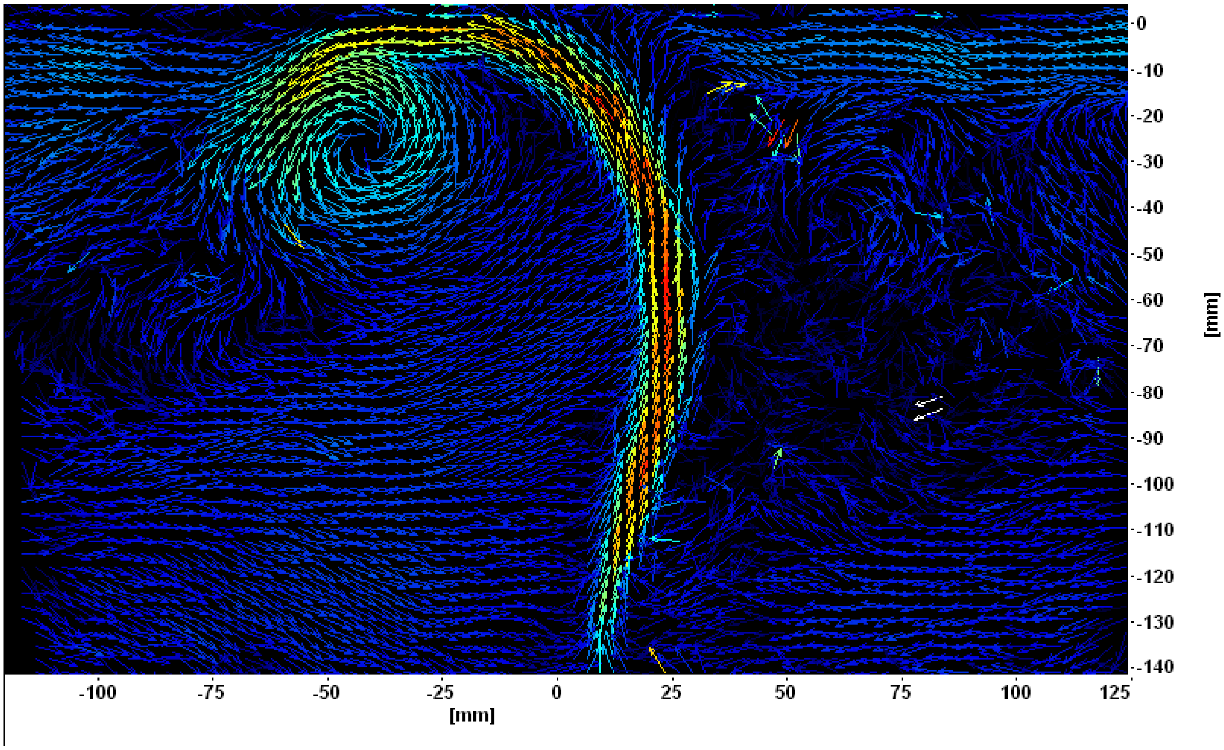

Figure 39

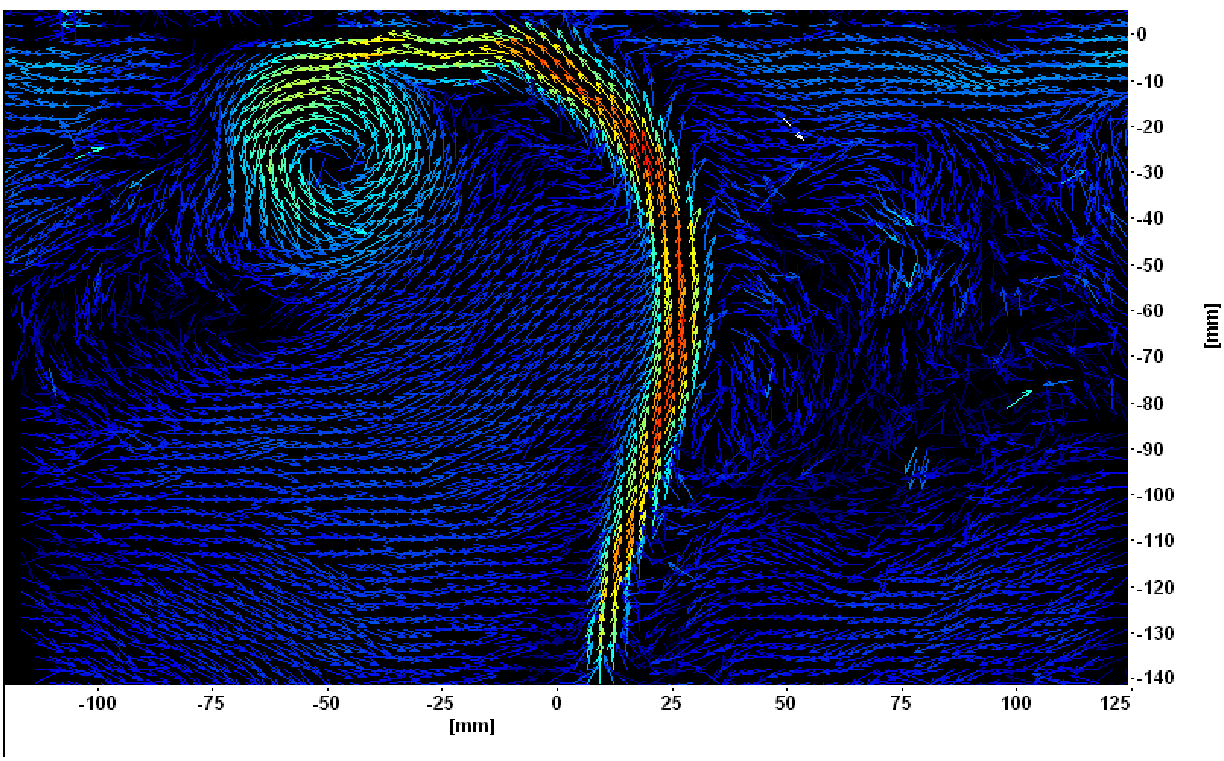

Figure 40

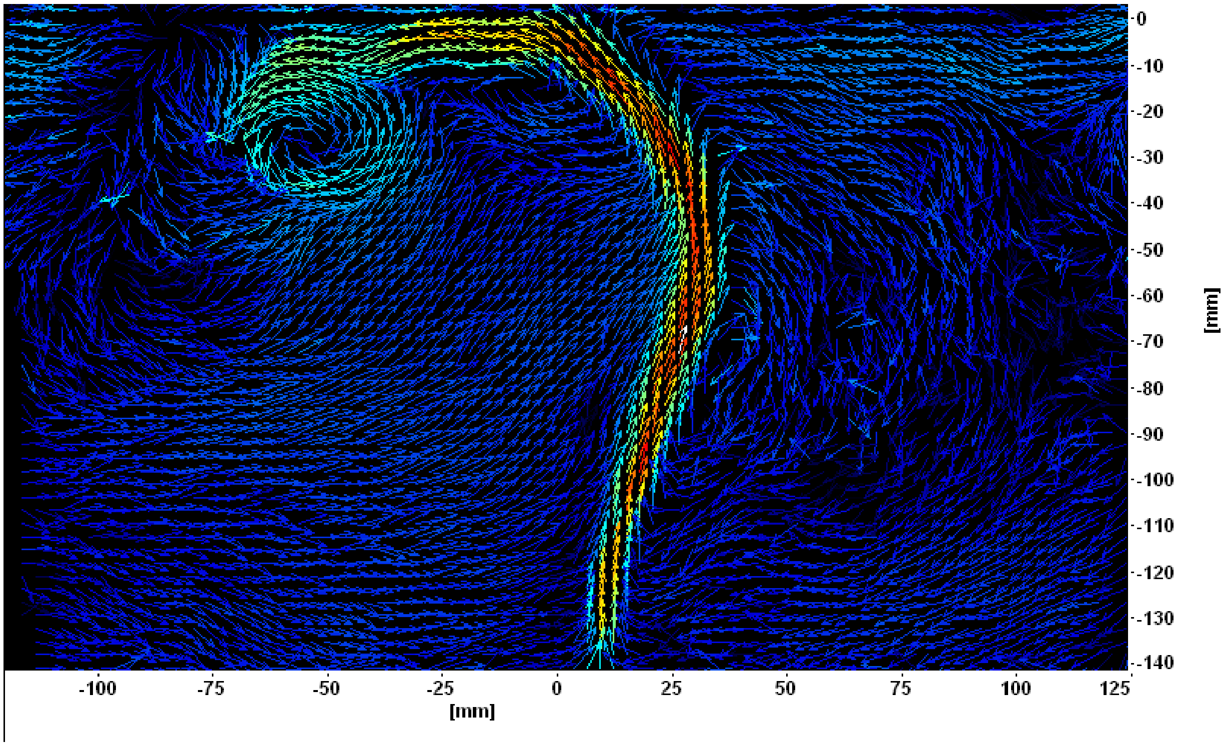

Figure 41

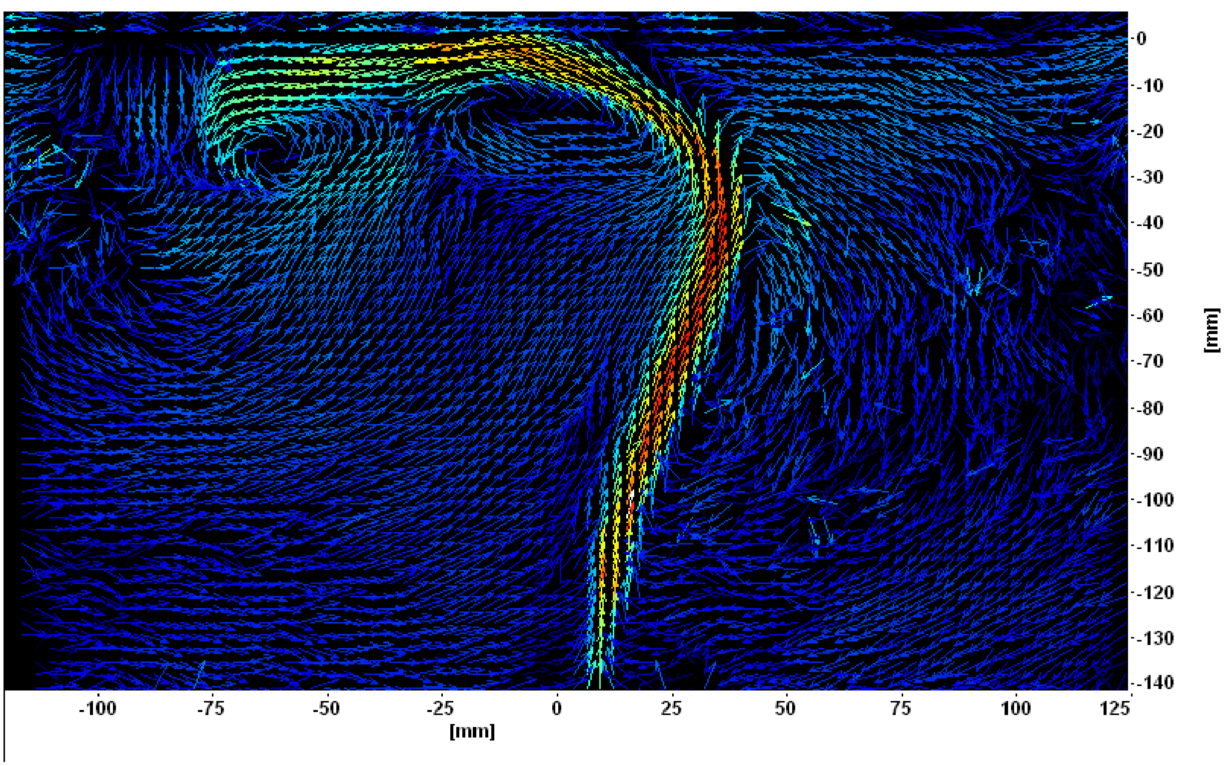

Figure 42

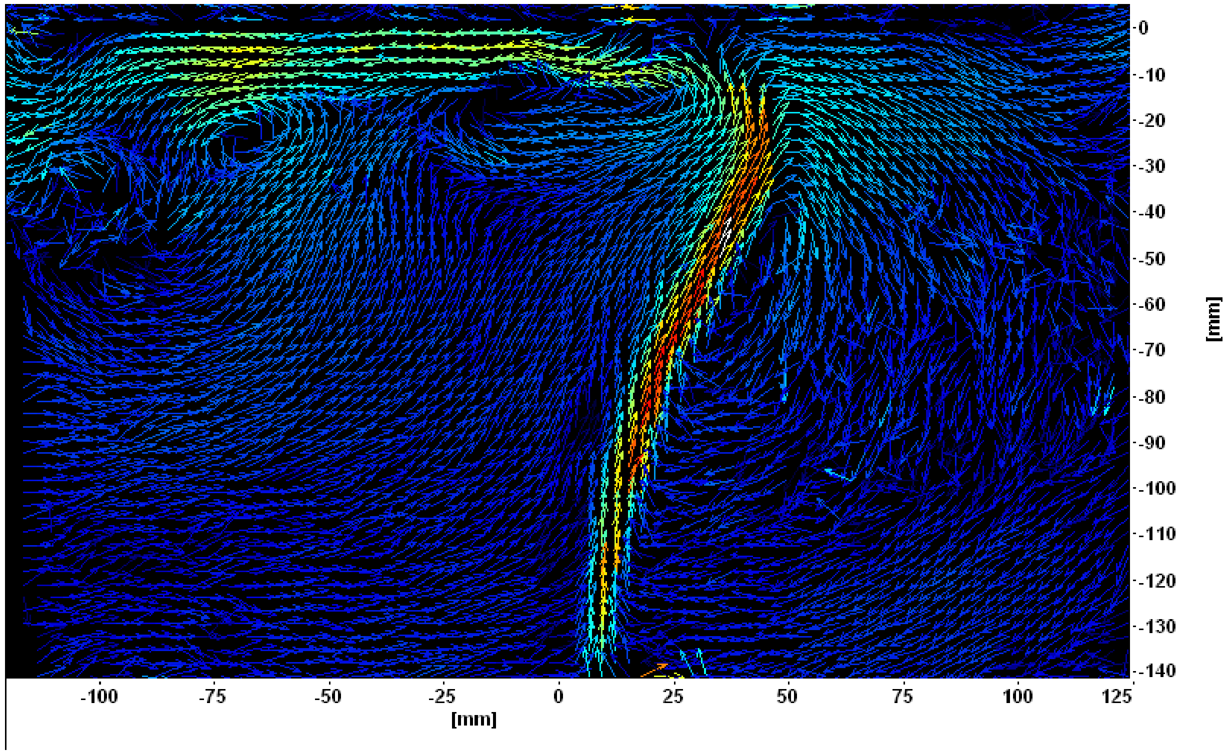

Figure 43

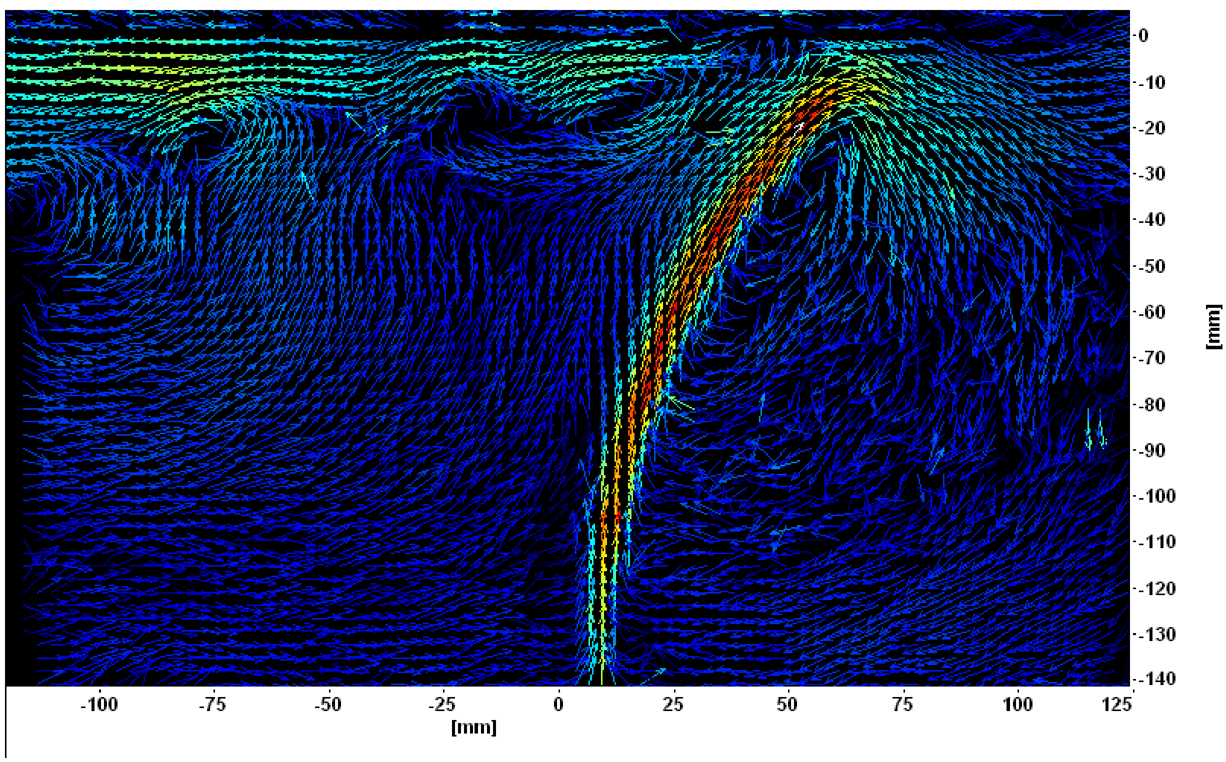

Figure 44

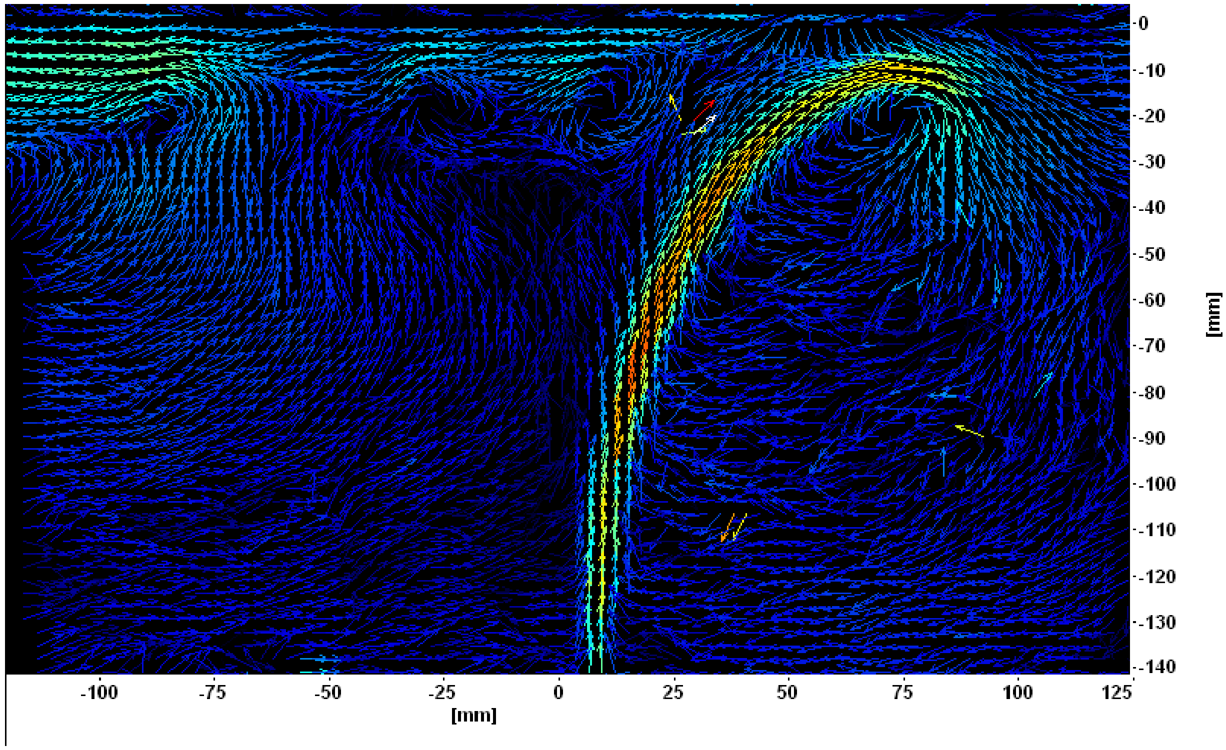

Figure 45

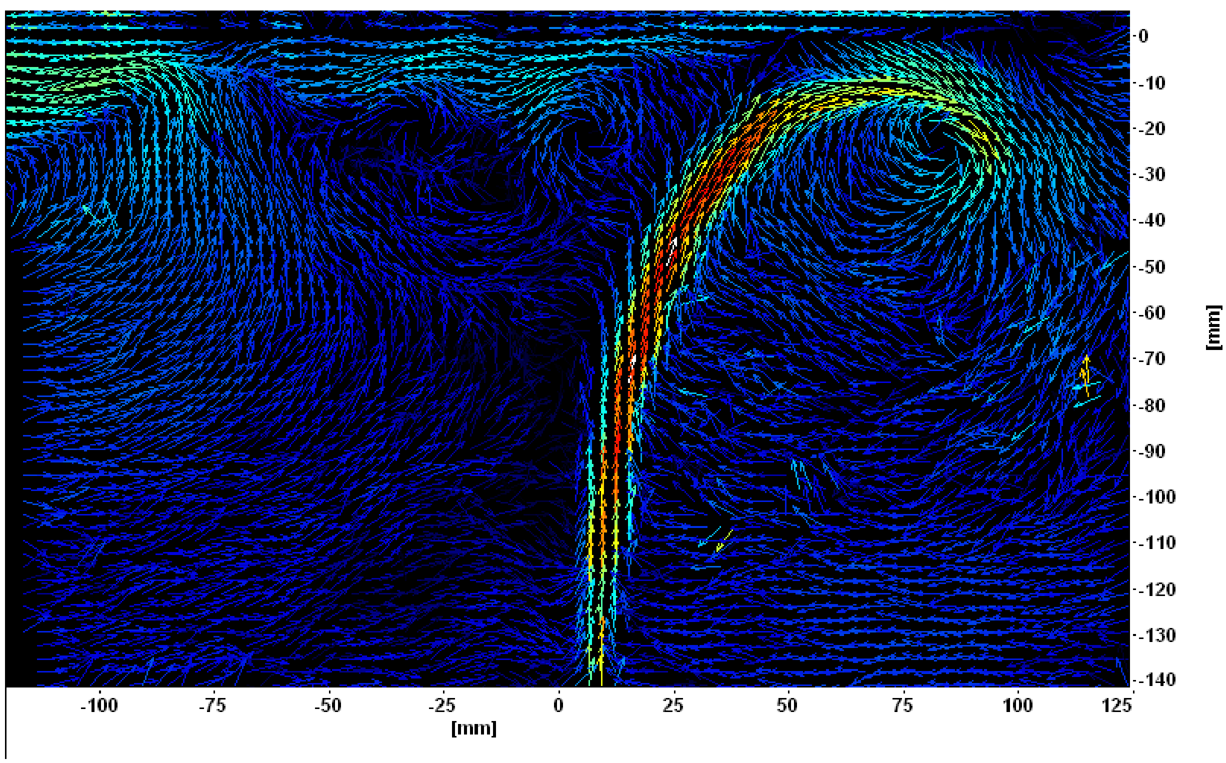

Figure 46

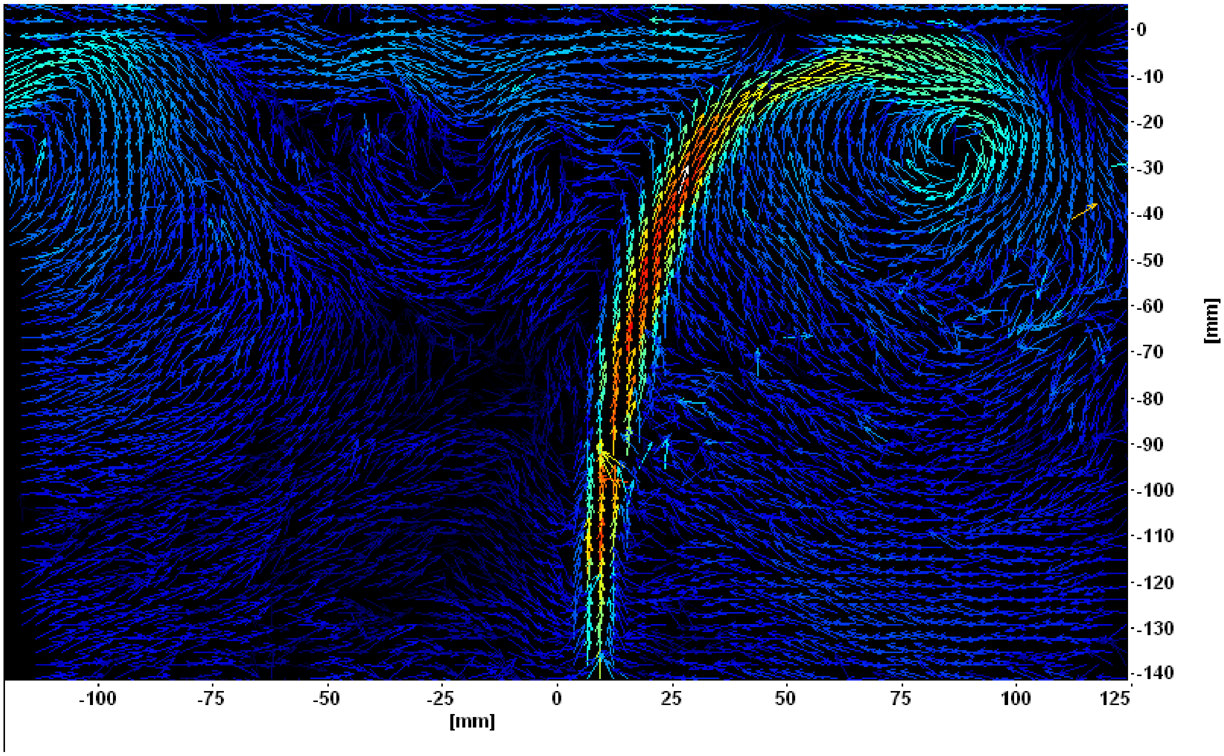

Figure 47

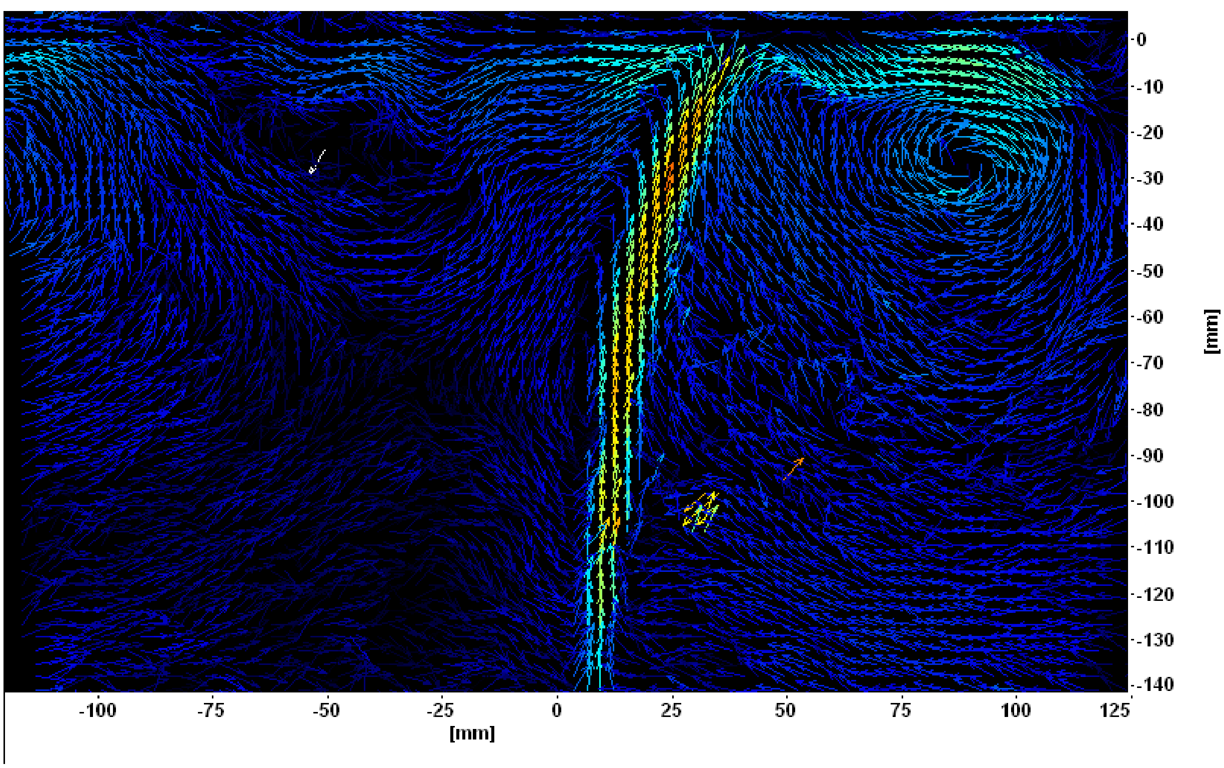

Figure 48

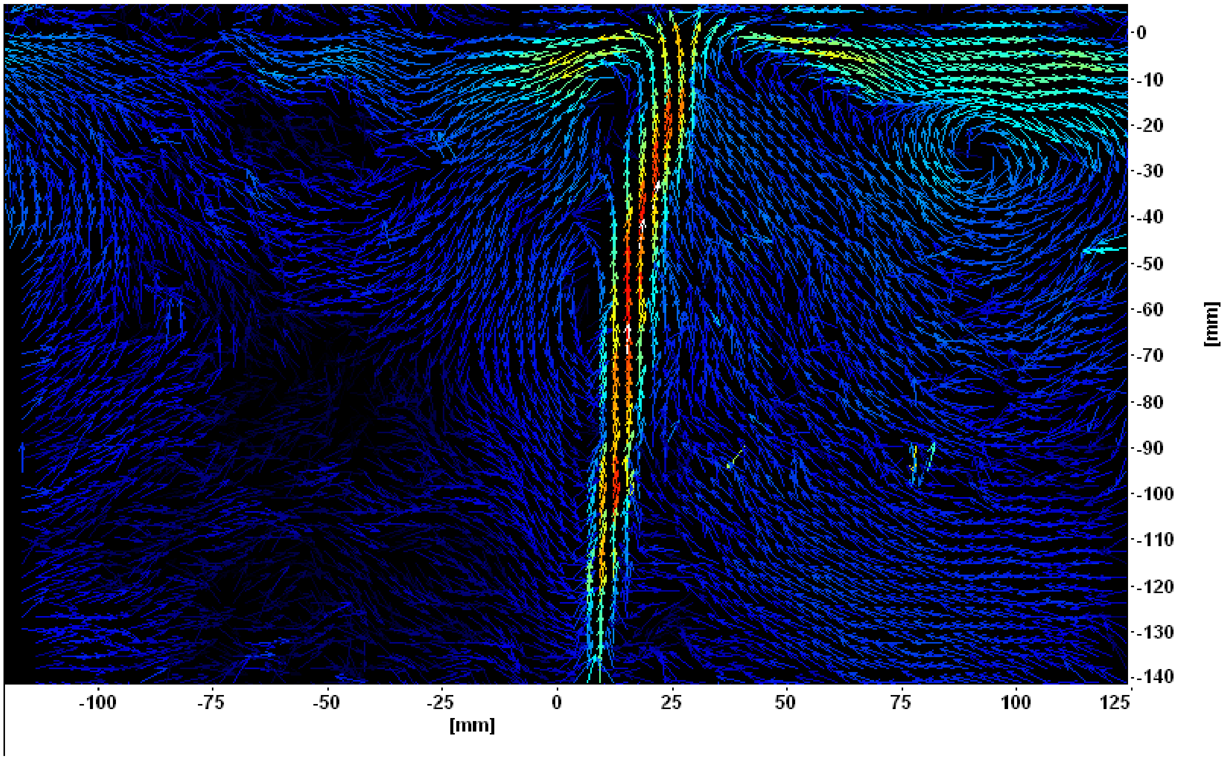

Figure 49

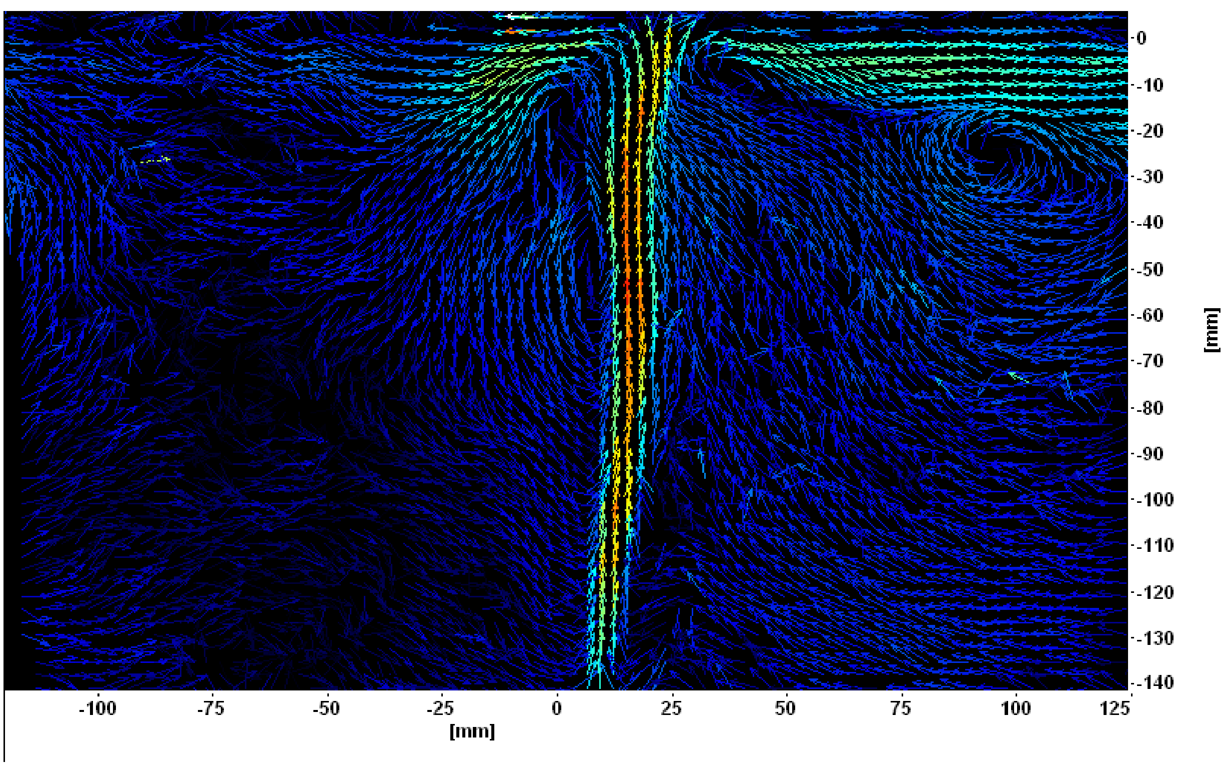

Figure 50

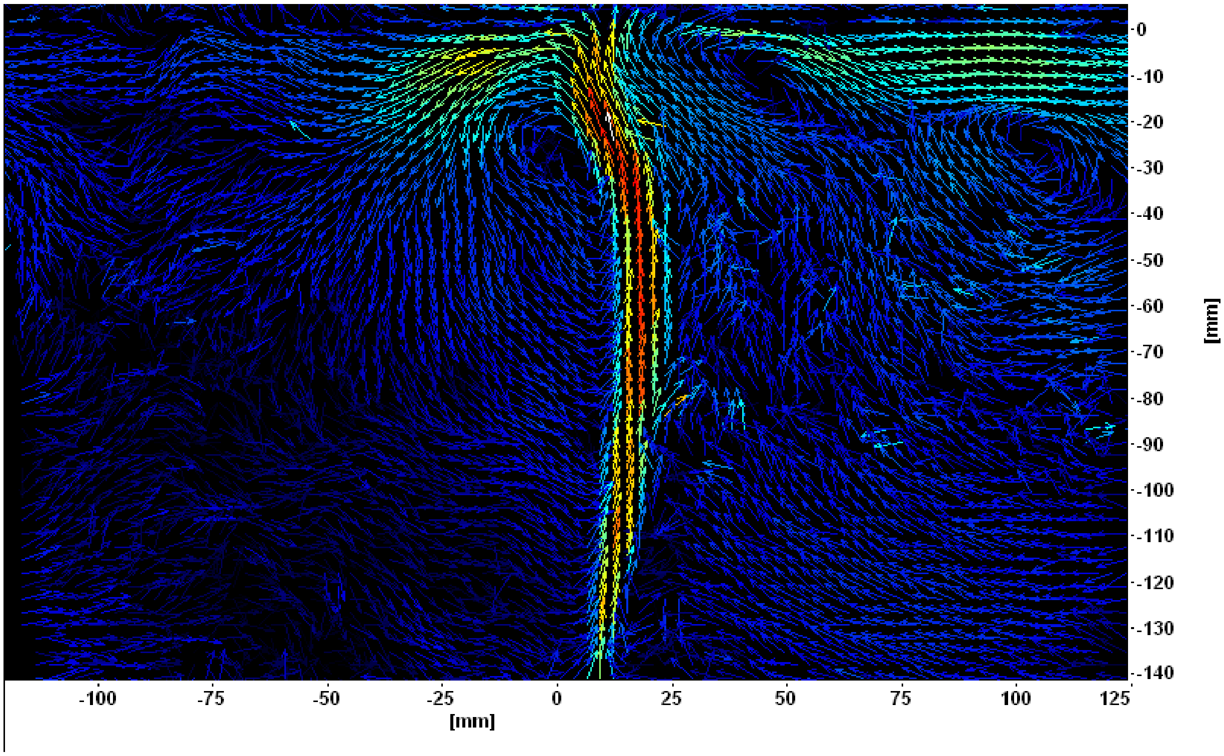

Figure 51

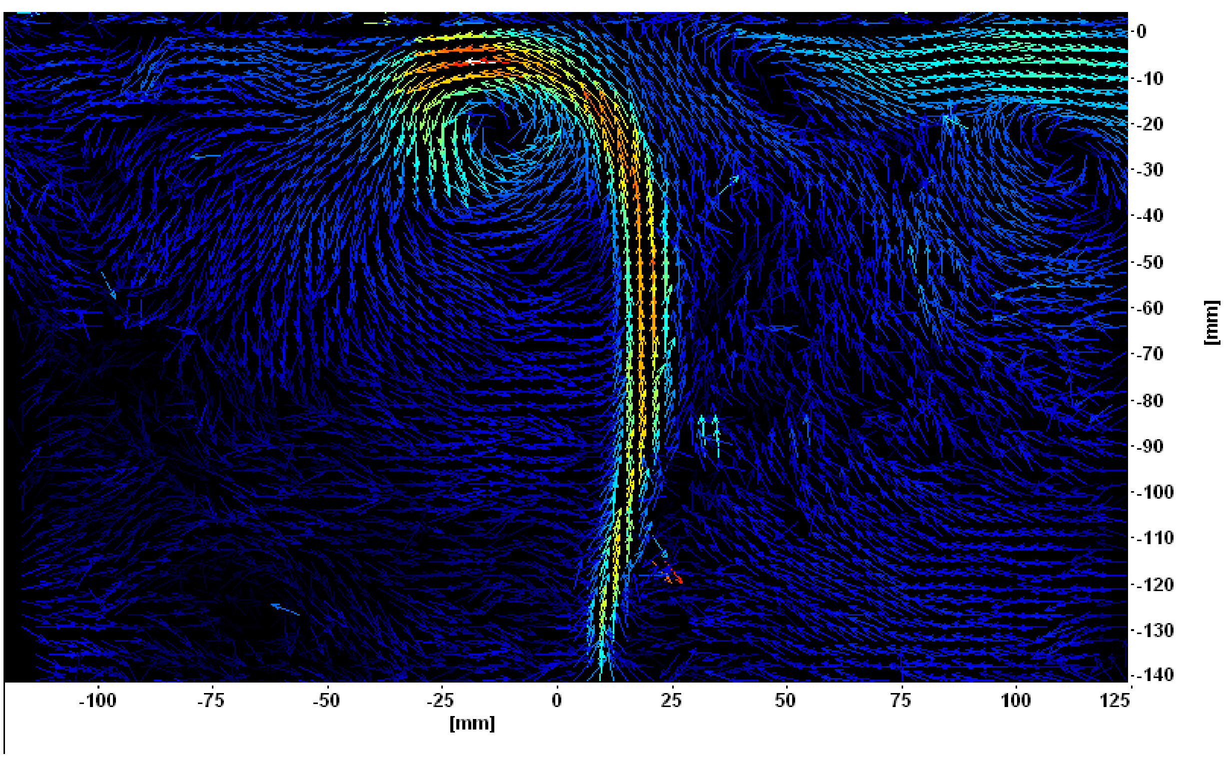

Figure 52

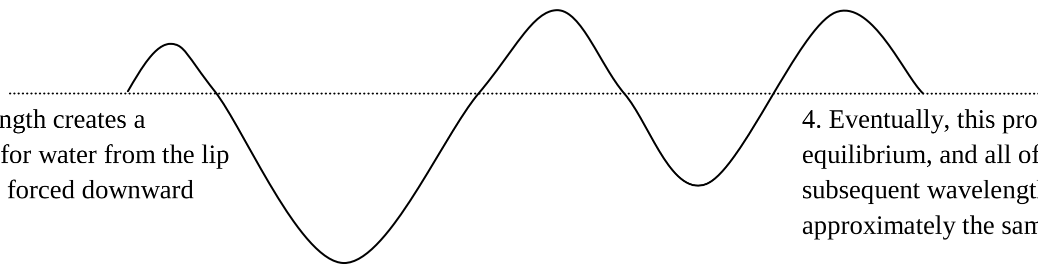
1. A small wavelength creates a concentrated area for water from the lip of the plume to be forced downward
2. Water is forced far down (in the negative Z) the plume, where it causes a disturbance, forming a B vortex. This vortex, since it must travel relatively far in the Z (up to the surface), takes longer to get to the surface (therefore longer in the X) and travels farther in the Y since B vortices tend to move in both the Y and Z. This creates a large wavelength.
3. The large wavelength does not create as concentrated of an area as the small wavelength does; consequently, it forces the water less far down. The water still creates a disturbance, though not as far down, creating a B vortex. This B vortex takes less time to get to the surface as the previous one, and creates a medium-sized wavelength.
4. Eventually, this process reaches equilibrium, and all of the subsequent wavelengths are approximately the same size.

Figure 53

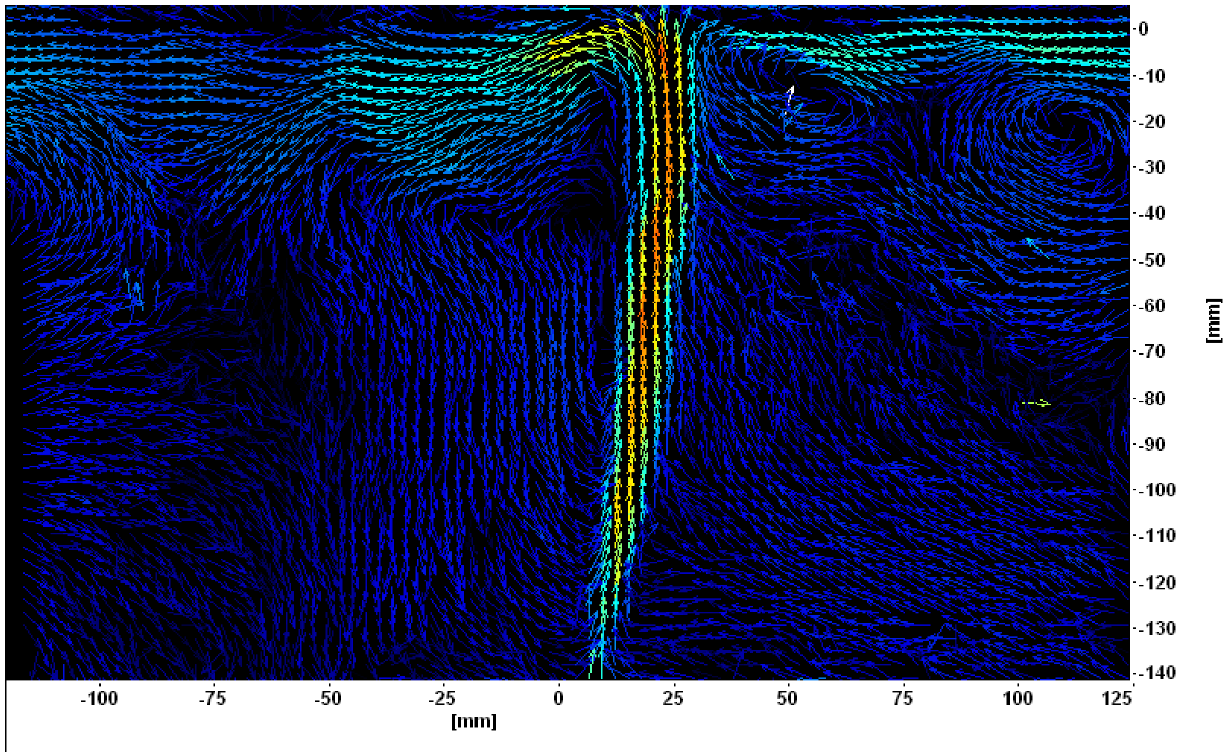

Figure 54

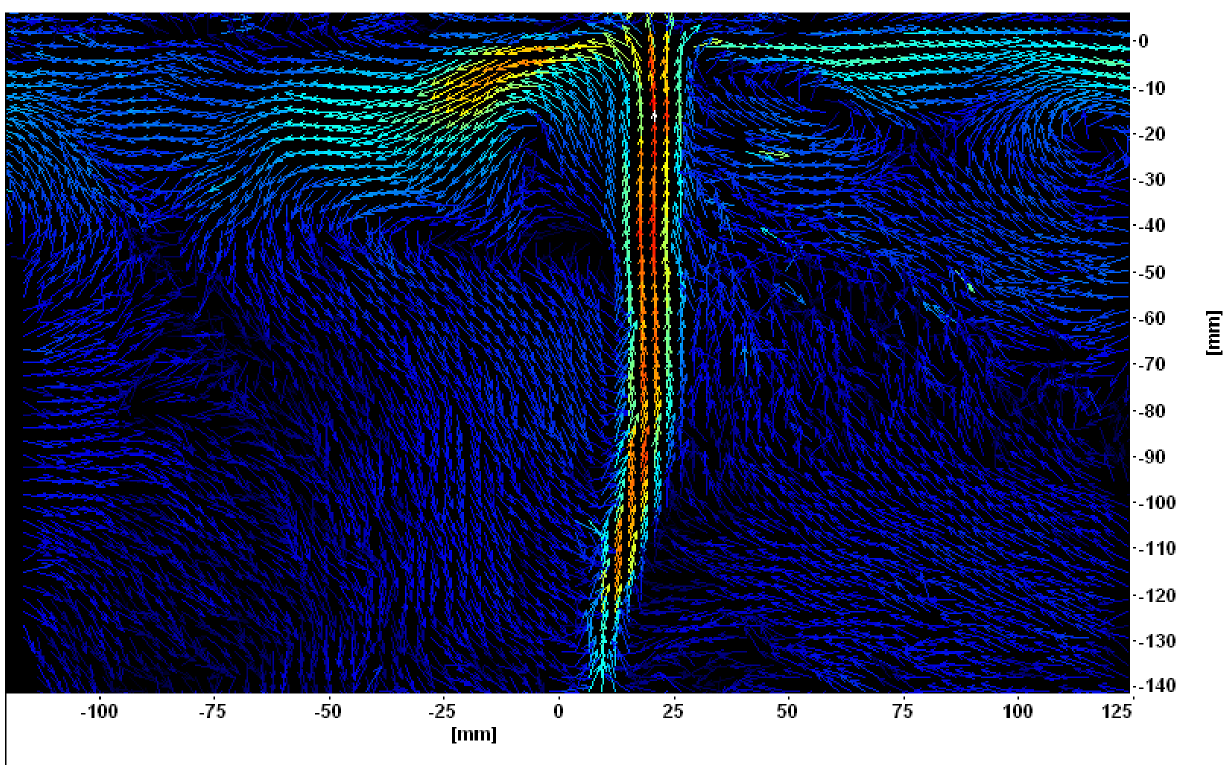

Figure 55

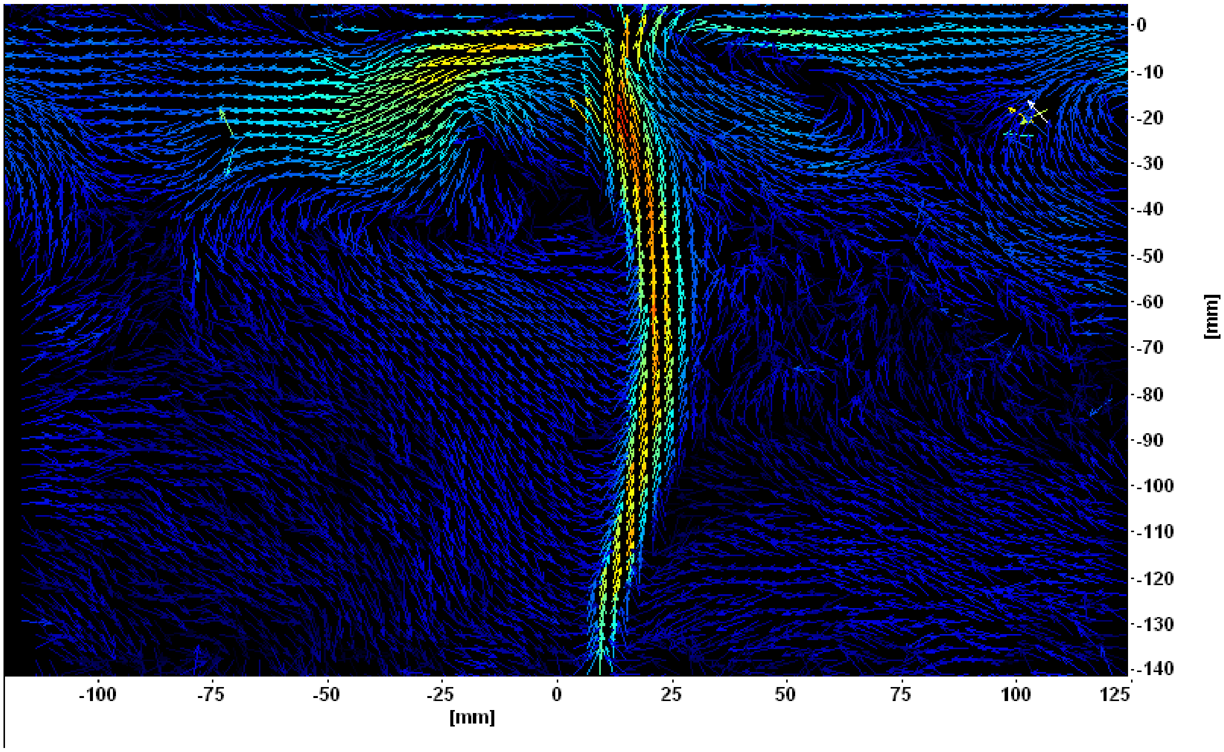

Figure 56

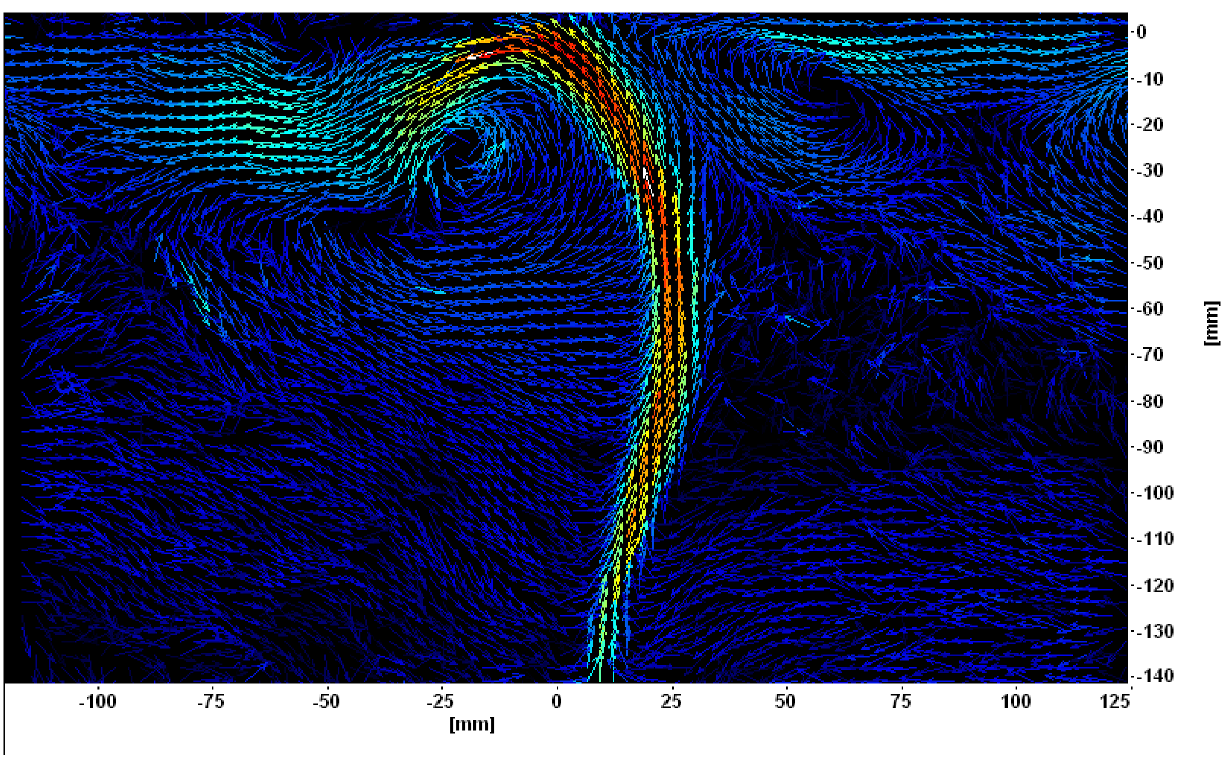

Figure 57

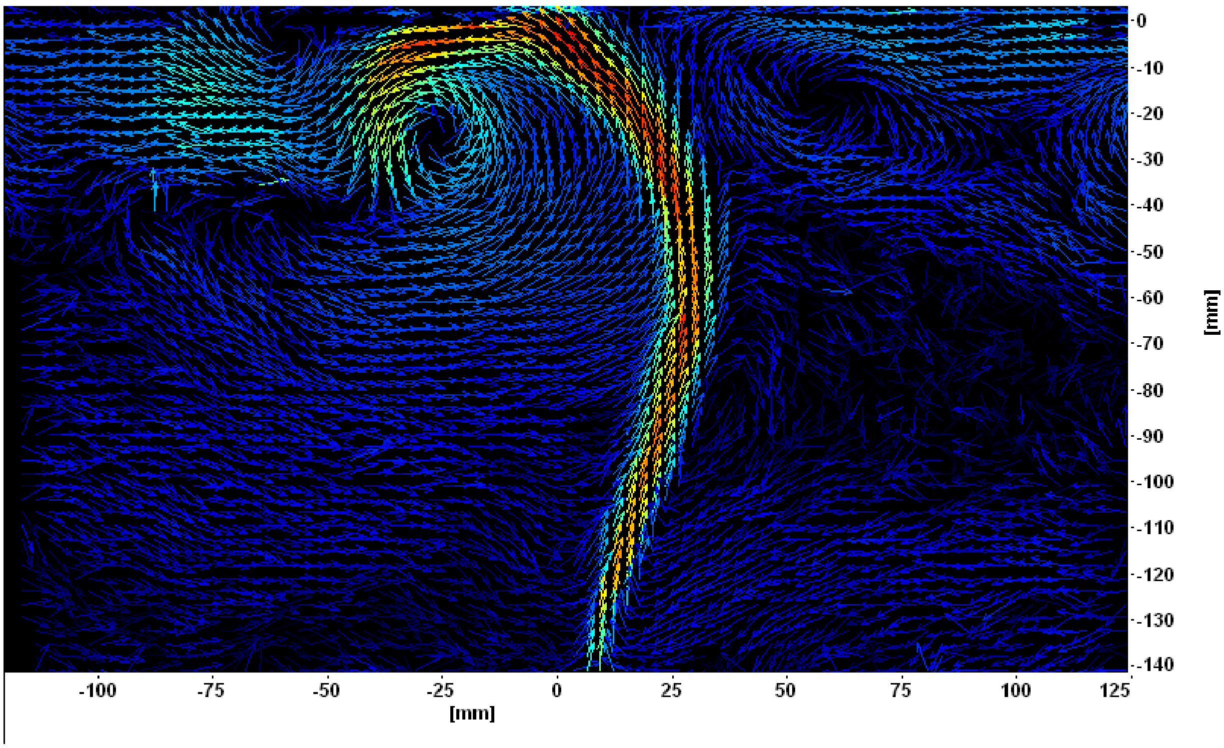

0
-10
-20
-30
-40
-50
-60
-70
-80
-90
-100
-110
-120
-130
-140
[mm]
-100
-75
-50
-25
0
25
50
75
100
125
[mm]

Figure 58

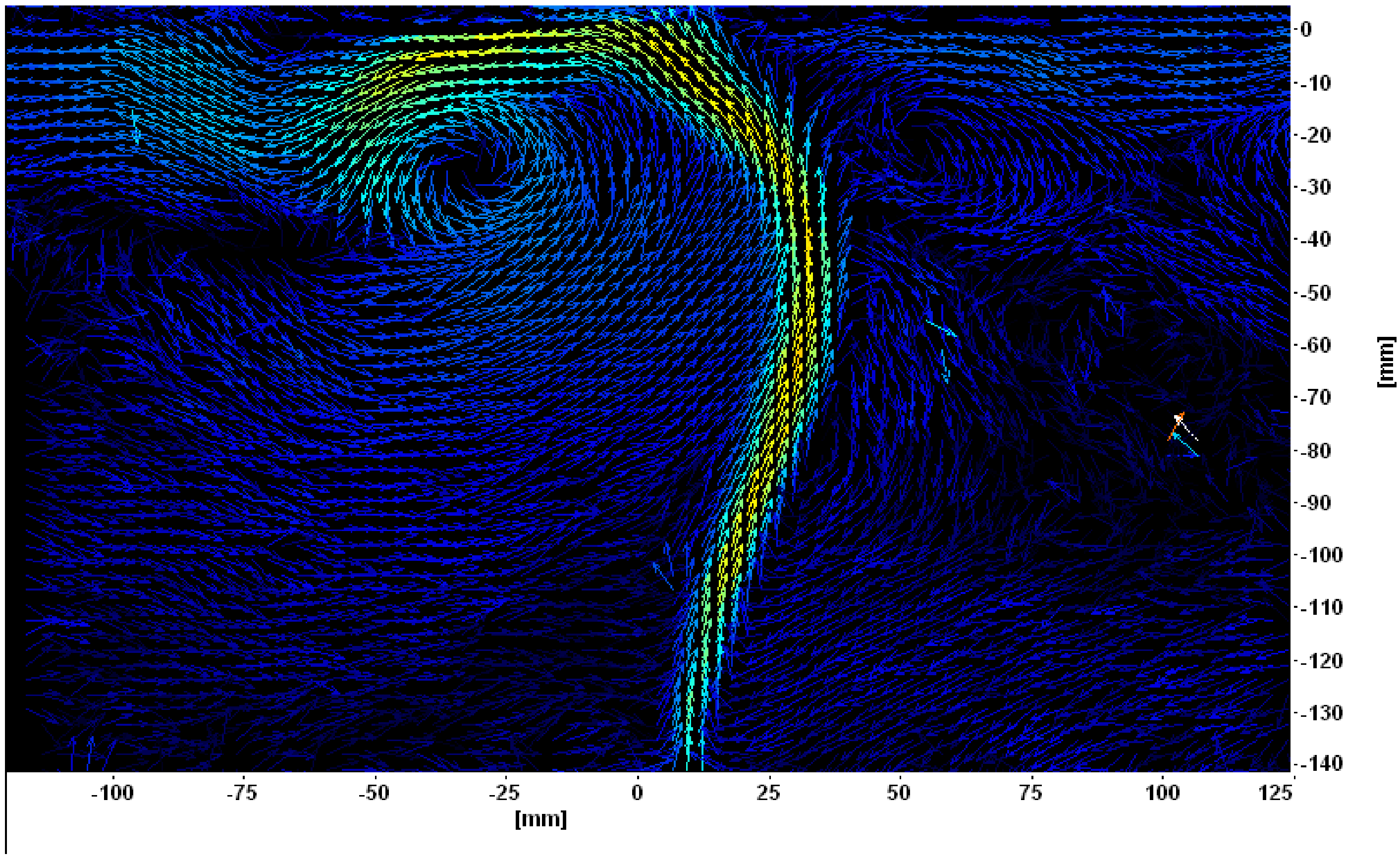

0
-10
-20
-30
-40
-50
-60
-70
-80
-90
-100
-110
-120
-130
-140
[mm]
-100
-75
-50
-25
0
25
50
75
100
125
[mm]

Figure 59

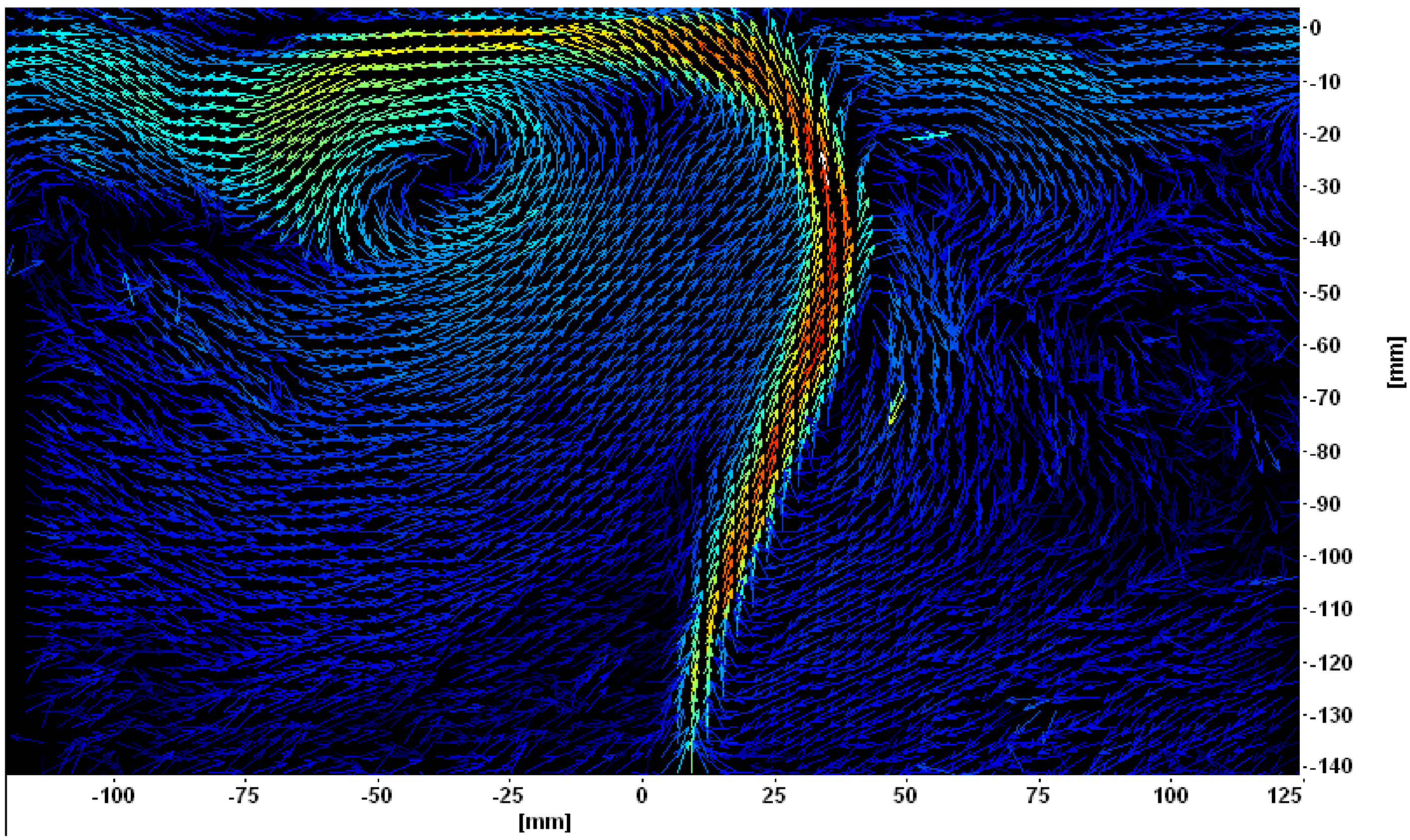
0
-10
-20
-30
-40
-50
-60
-70
-80
-90
-100
-110
-120
-130
-140
[mm]
-100
-75
-50
-25
0
25
50
75
100
125
[mm]

Figure 60

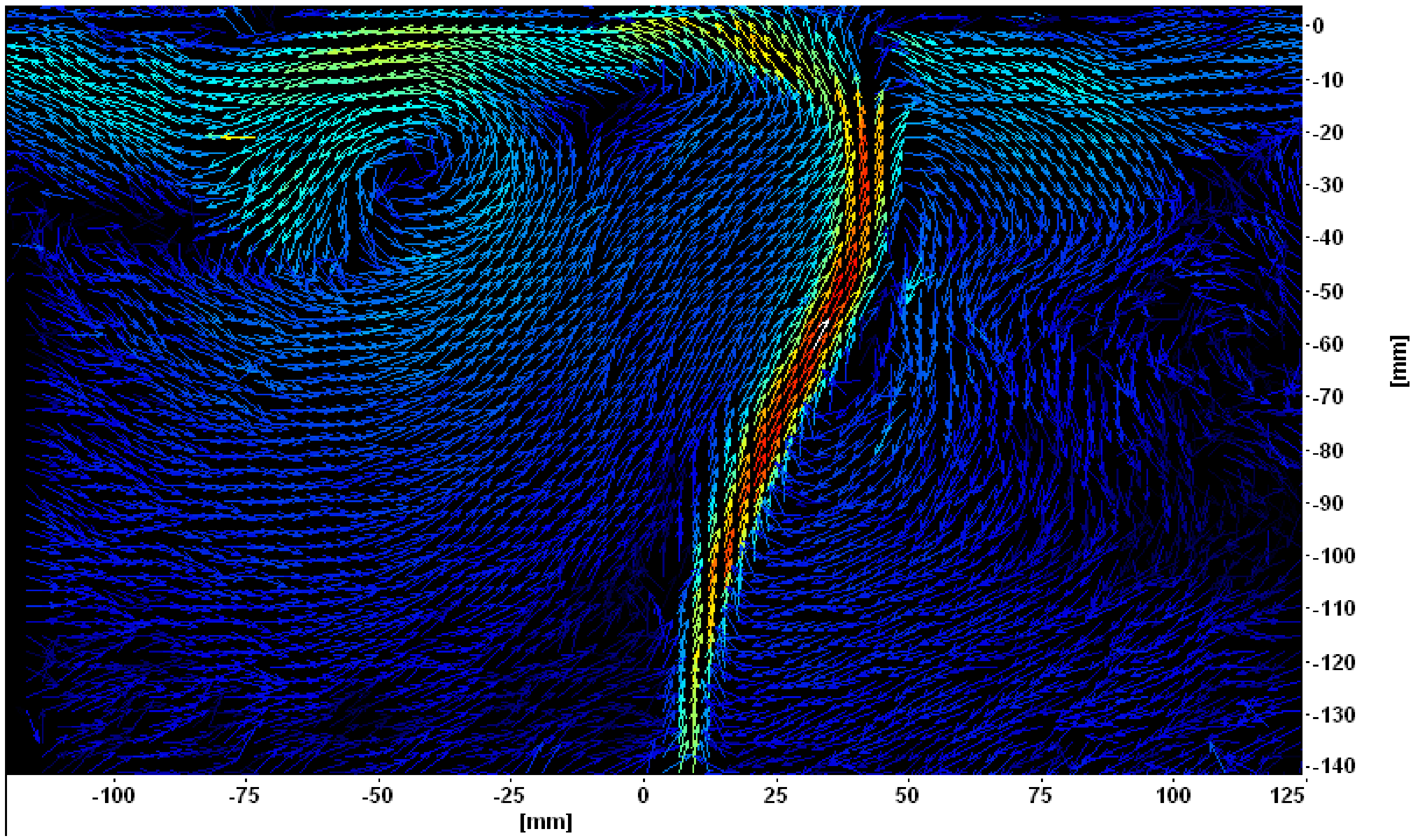
0
-10
-20
-30
-40
-50
-60
-70
-80
-90
-100
-110
-120
-130
-140
[mm]
-100
-75
-50
-25
0
25
50
75
100
125
[mm]

Figure 61

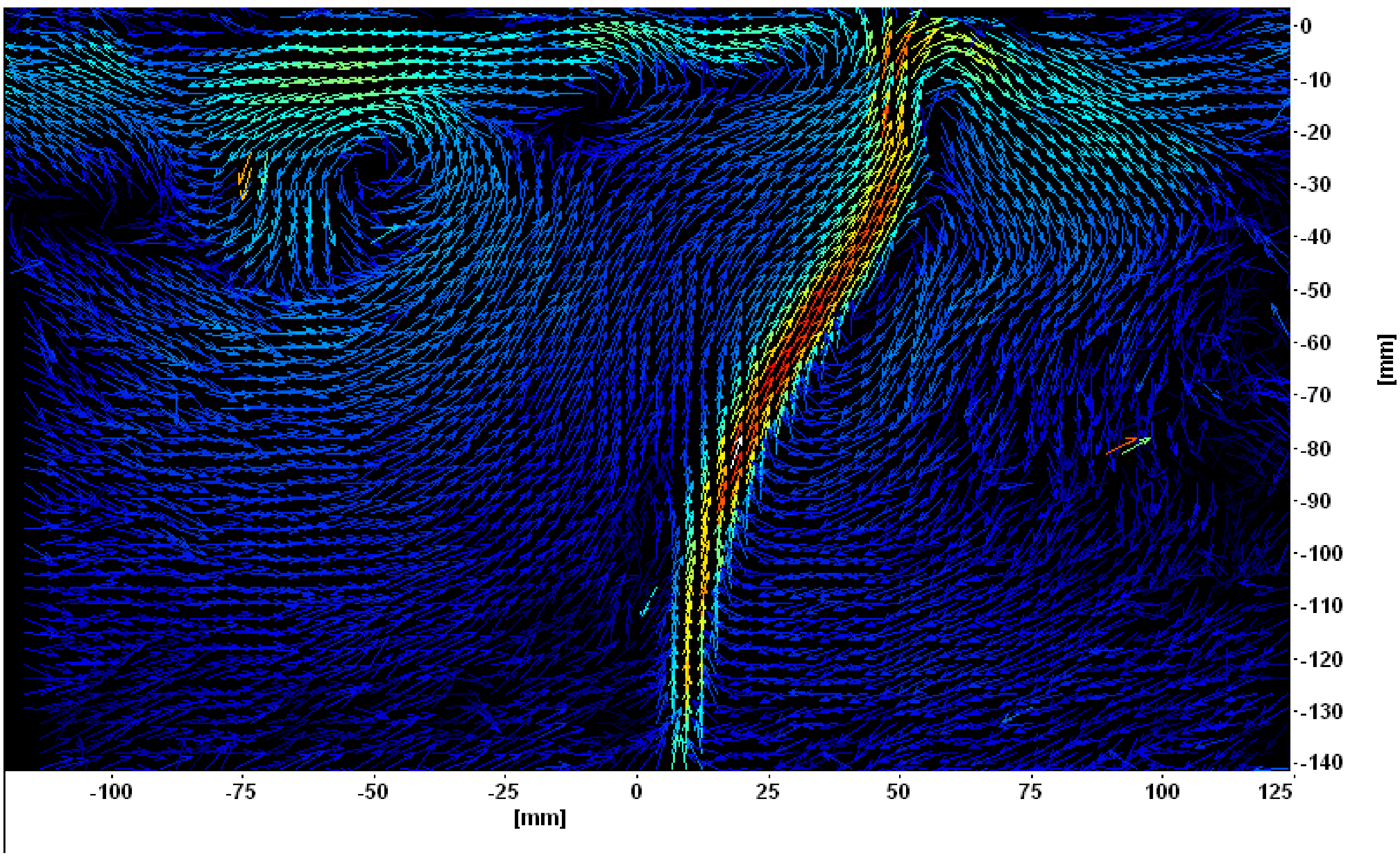

0
-10
-20
-30
-40
-50
-60
-70
-80
-90
-100
-110
-120
-130
-140
[mm]
-100
-75
-50
-25
0
25
50
75
100
125
[mm]

Figure 62

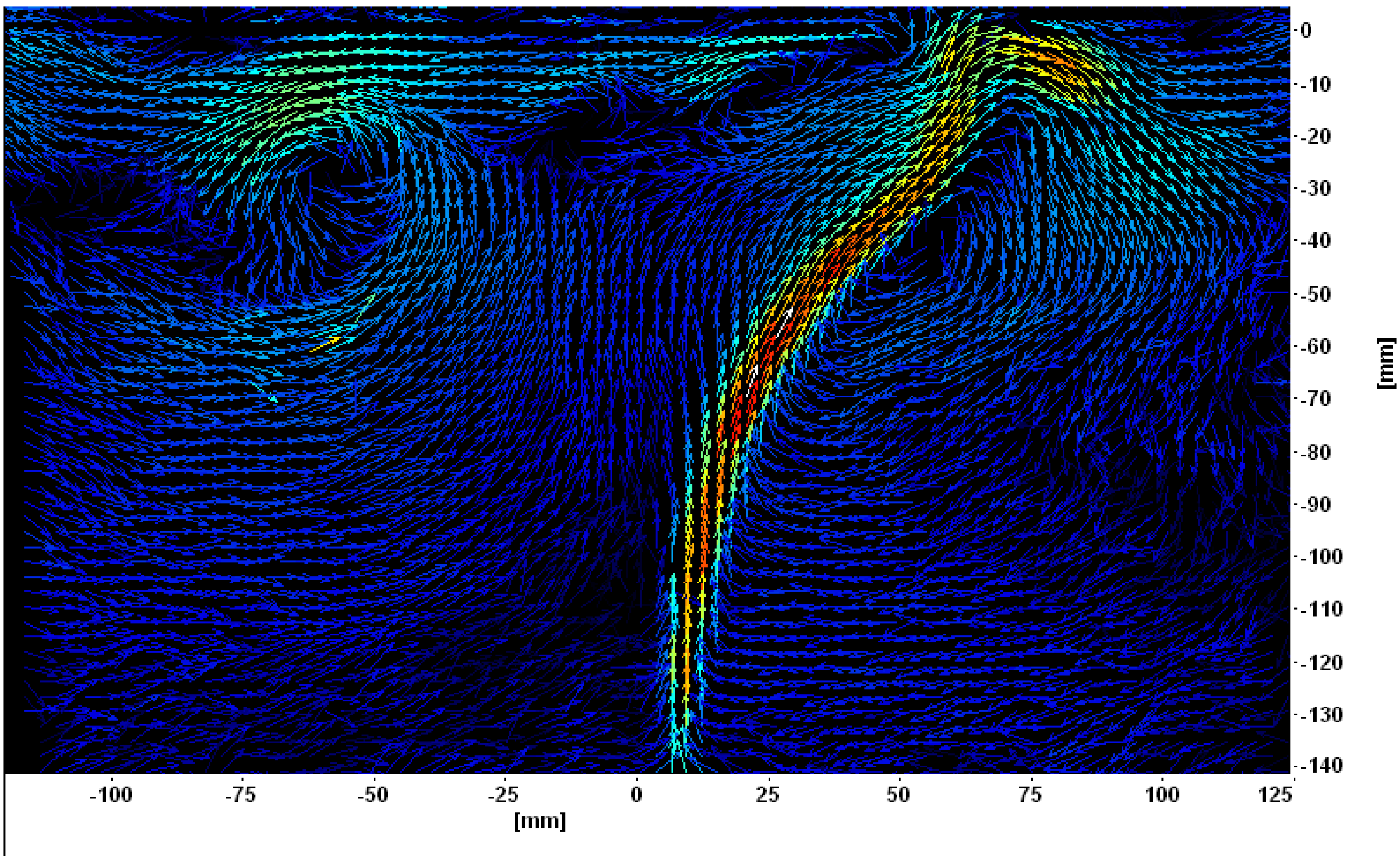

-100
-75
-50
-25
0
25
50
75
100
125
[mm]
0
-10
-20
-30
-40
-50
-60
-70
-80
-90
-100
-110
-120
-130
-140
[mm]

Figure 63

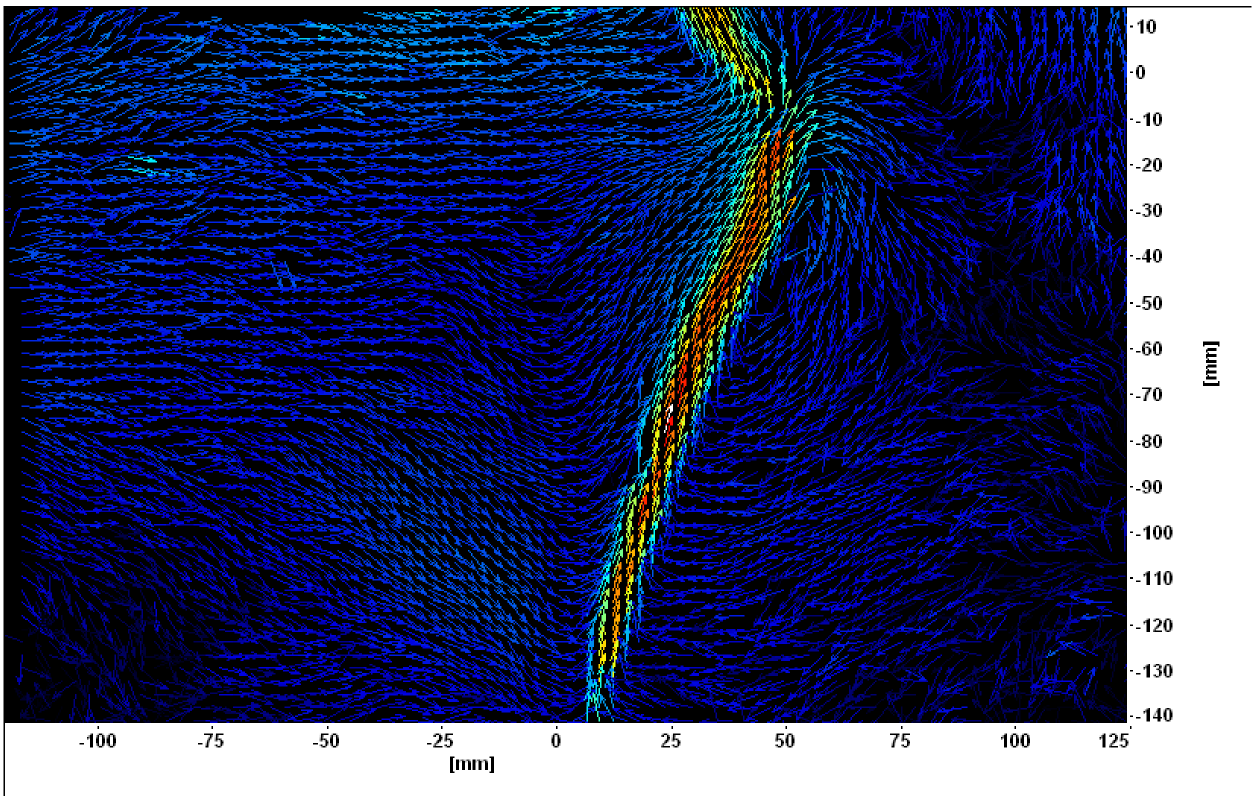

10
0
-10
-20
-30
-40
-50
-60
-70
-80
-90
-100
-110
-120
-130
-140
[mm]
-100
-75
-50
-25
0
25
50
75
100
125
[mm]

Figure 64

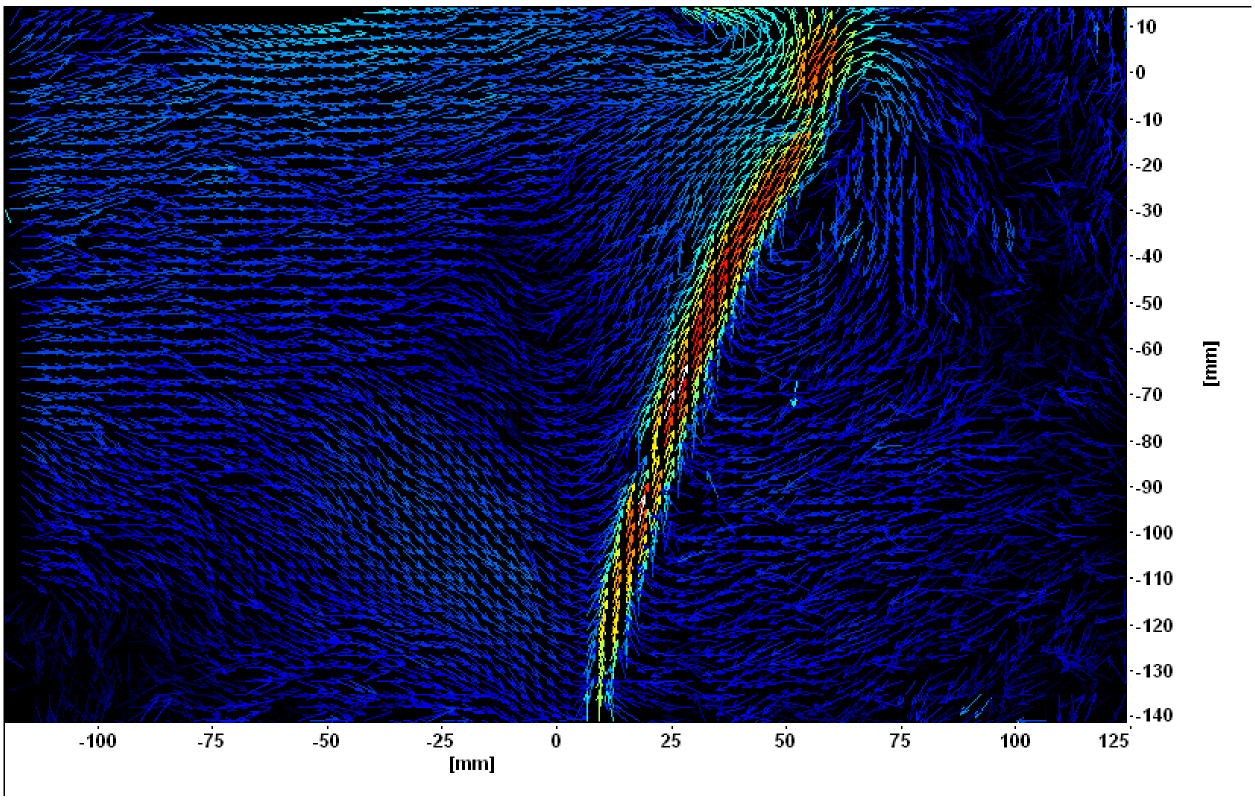

10
0
-10
-20
-30
-40
-50
-60
-70
-80
-90
-100
-110
-120
-130
-140
[mm]
-100
-75
-50
-25
0
25
50
75
100
125
[mm]

Figure 65

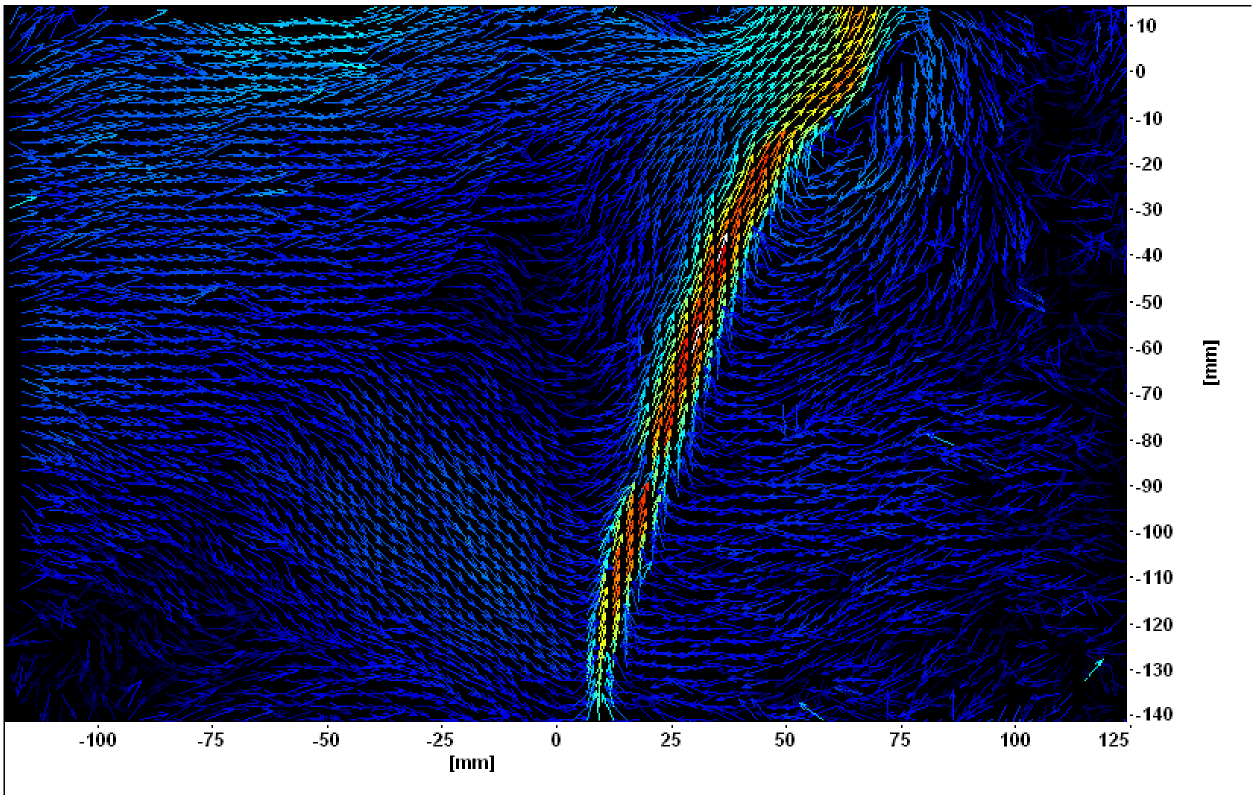
10
0
-10
-20
-30
-40
-50
-60
-70
-80
-90
-100
-110
-120
-130
-140
[mm]
-100
-75
-50
-25
0
25
50
75
100
125
[mm]

Figure 66

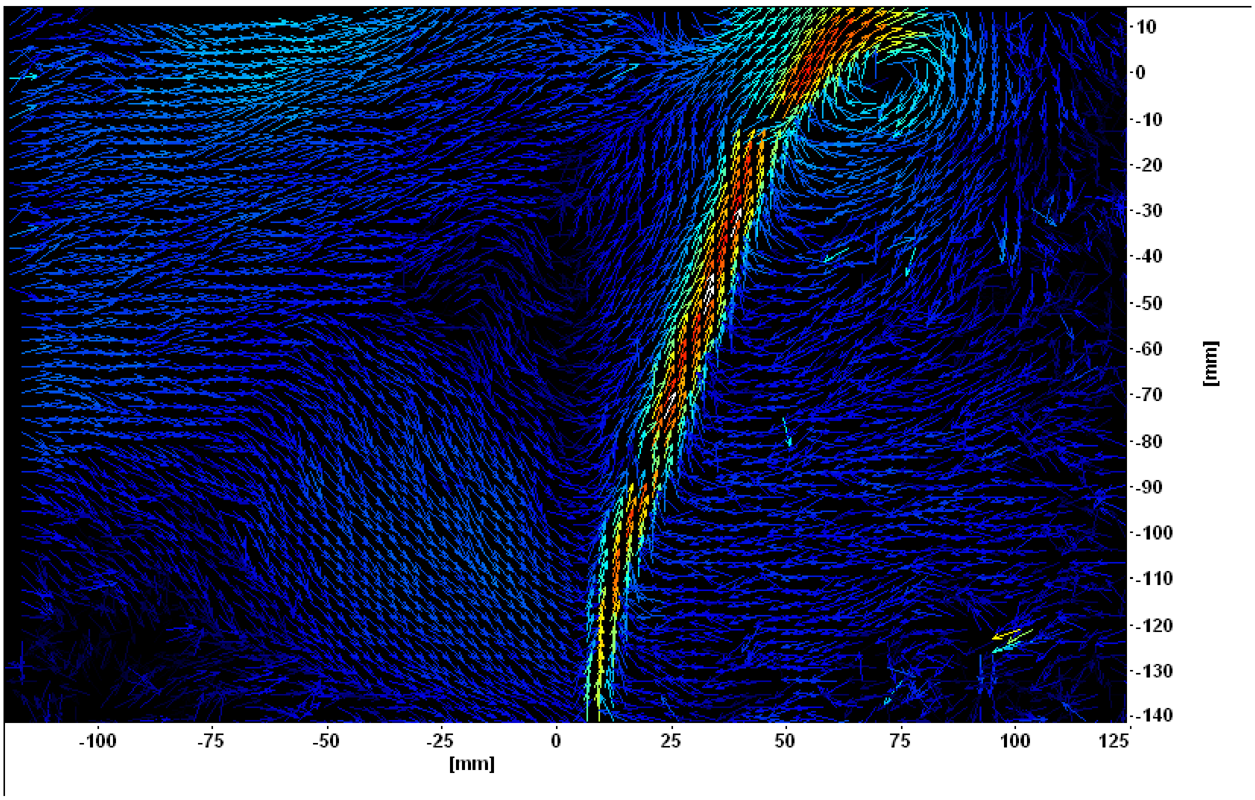

10
0
-10
-20
-30
-40
-50
-60
-70
-80
-90
-100
-110
-120
-130
-140
[mm]
-100
-75
-50
-25
0
25
50
75
100
125
[mm]

Figure 67

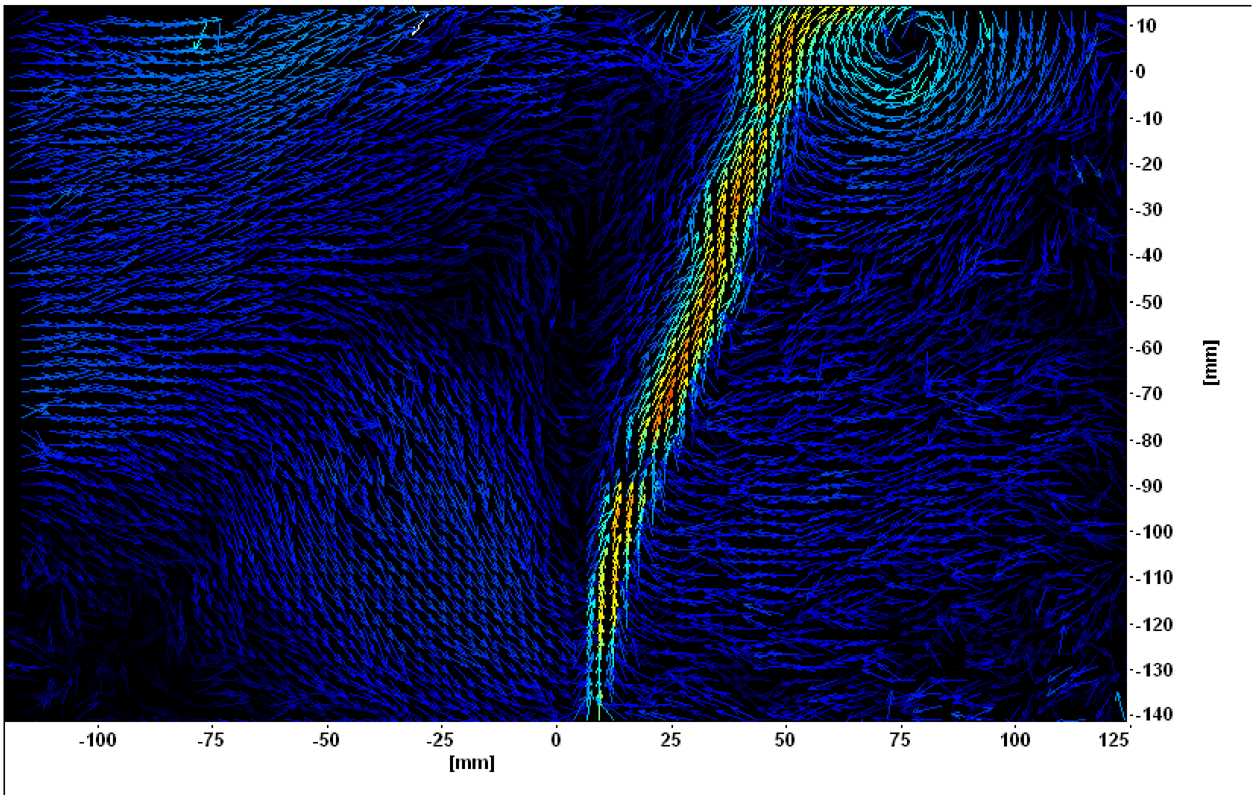

10
0
-10
-20
-30
-40
-50
-60
-70
-80
-90
-100
-110
-120
-130
-140
[mm]
-100
-75
-50
-25
0
25
50
75
100
125
[mm]

Figure 68

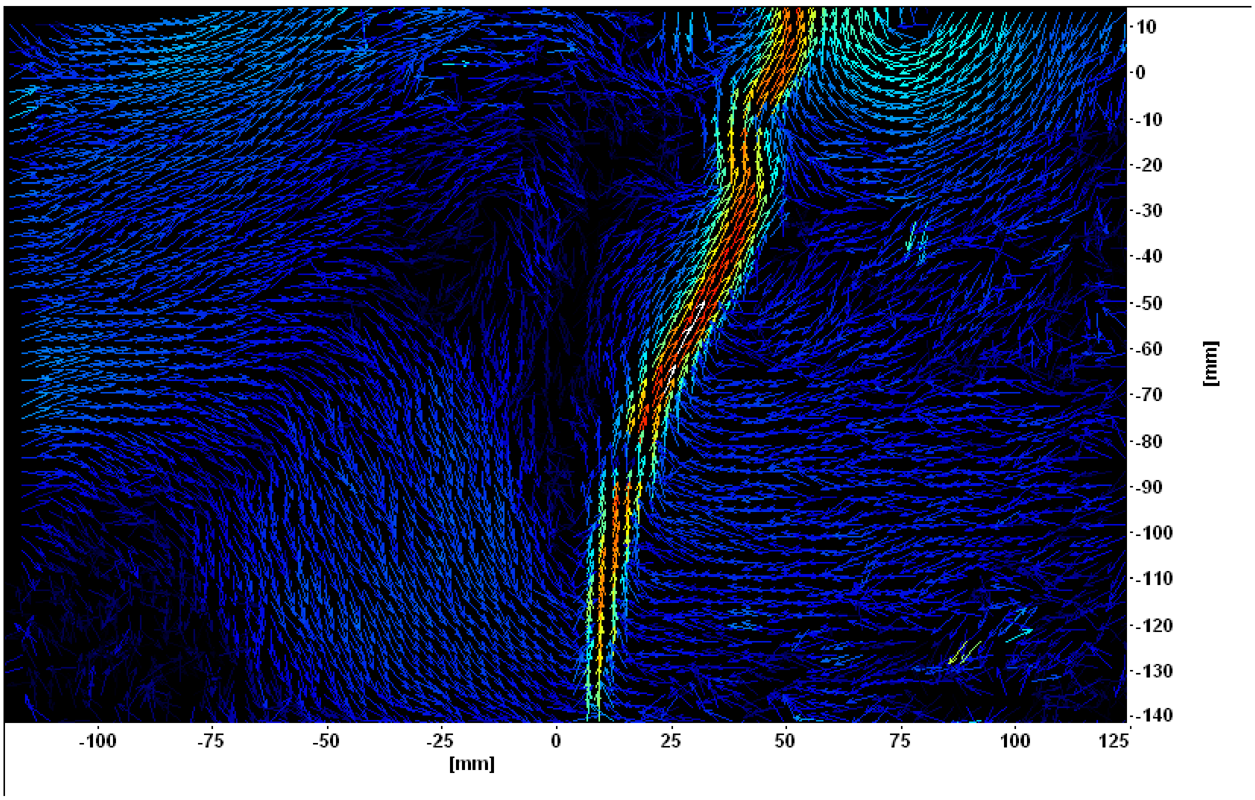
-100
-75
-50
-25
0
25
50
75
100
125
[mm]
10
0
-10
-20
-30
-40
-50
-60
-70
-80
-90
-100
-110
-120
-130
-140
[mm]

Figure 69

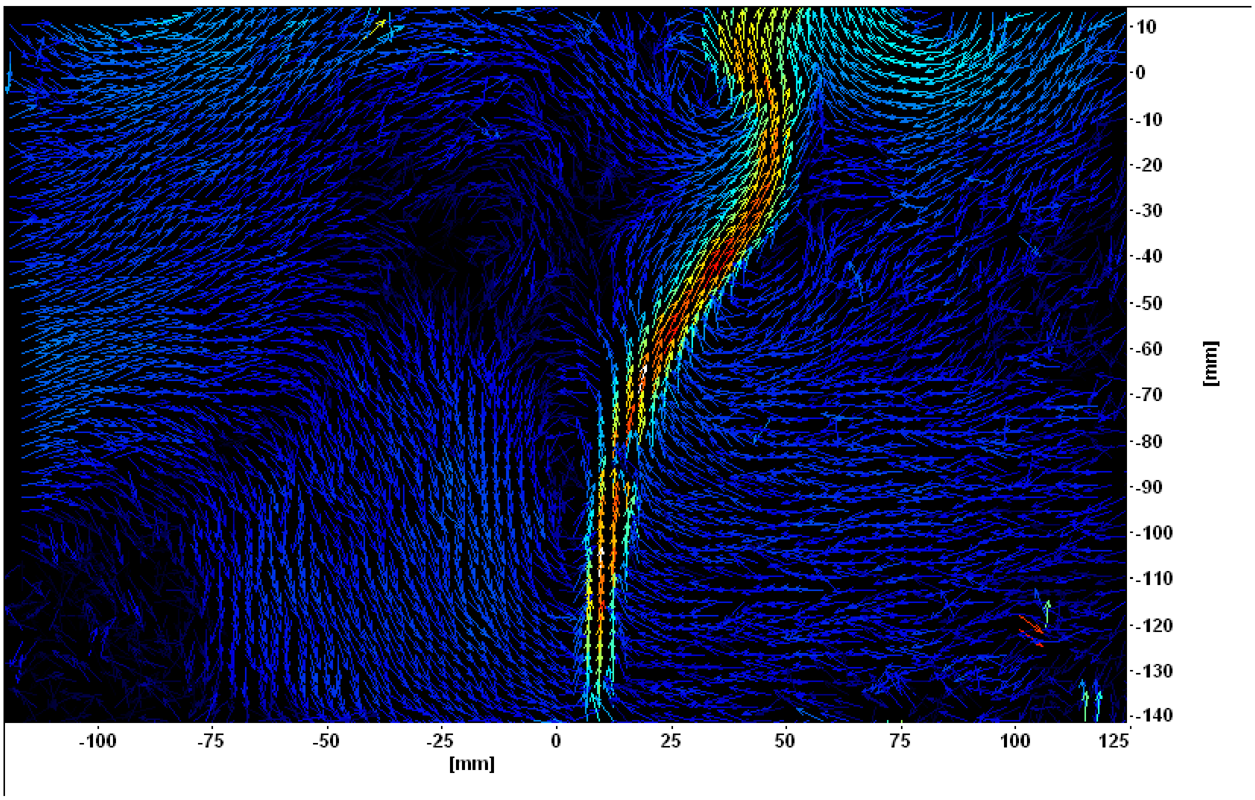

10
0
-10
-20
-30
-40
-50
-60
-70
-80
-90
-100
-110
-120
-130
-140
[mm]
-100
-75
-50
-25
0
25
50
75
100
125
[mm]

Figure 70

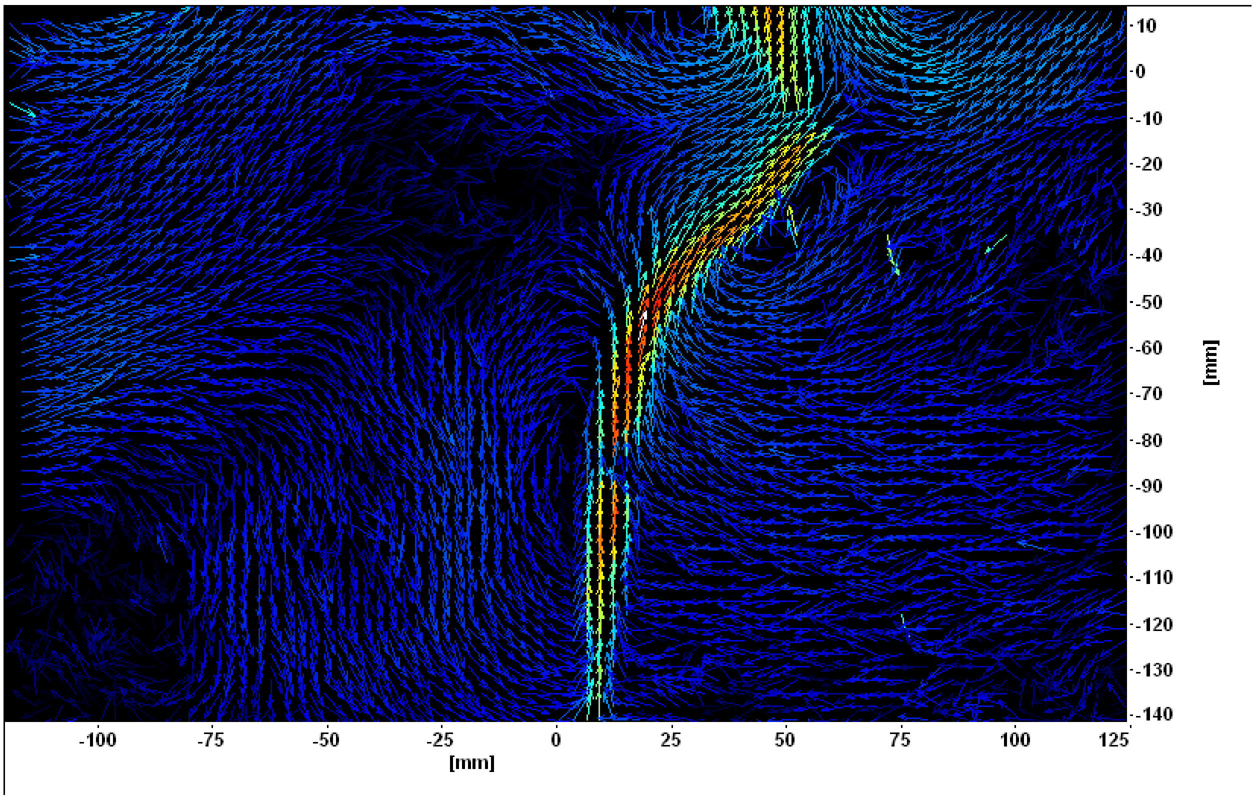

10
0
-10
-20
-30
-40
-50
-60
-70
-80
-90
-100
-110
-120
-130
-140
[mm]
-100
-75
-50
-25
0
25
50
75
100
125
[mm]

Figure 71

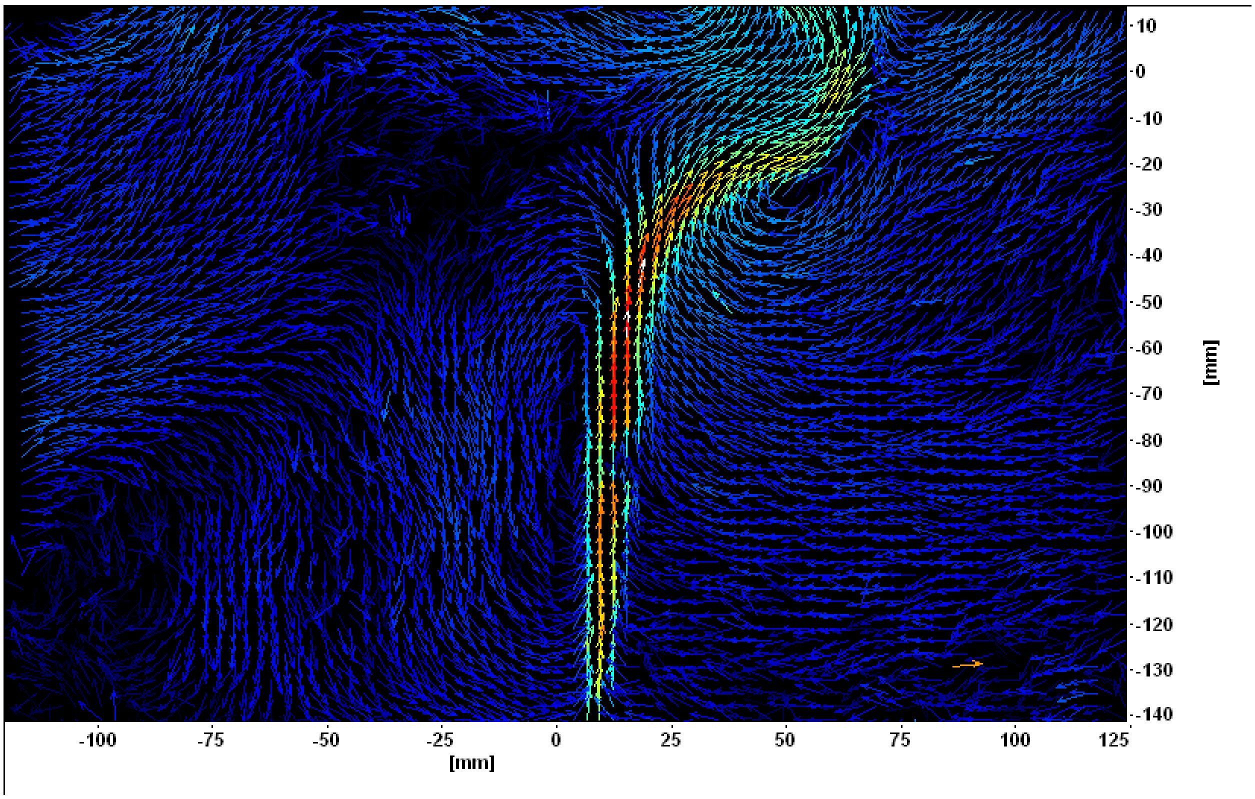
10
0
-10
-20
-30
-40
-50
-60
-70
-80
-90
-100
-110
-120
-130
-140
[mm]
-100
-75
-50
-25
0
25
50
75
100
125
[mm]

Figure 72

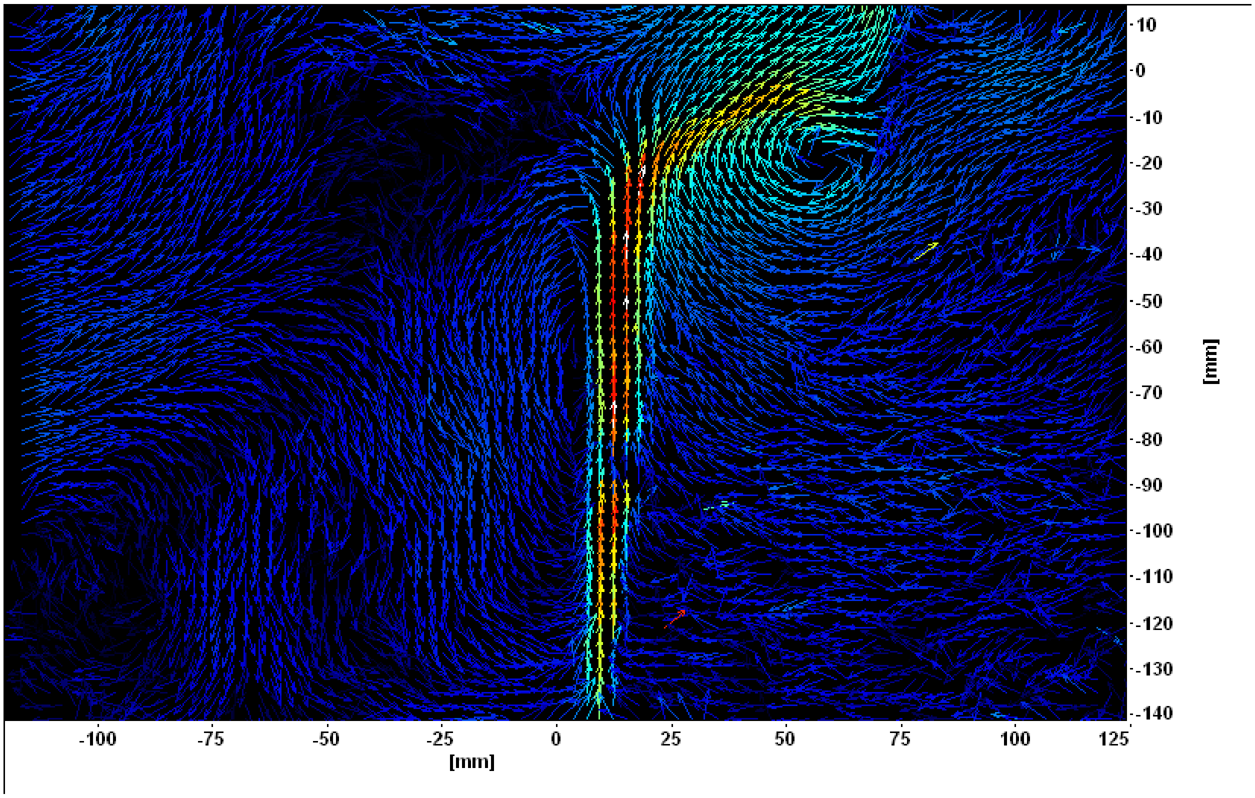
10
0
-10
-20
-30
-40
-50
-60
-70
-80
-90
-100
-110
-120
-130
-140
[mm]
-100
-75
-50
-25
0
25
50
75
100
125
[mm]

Figure 73

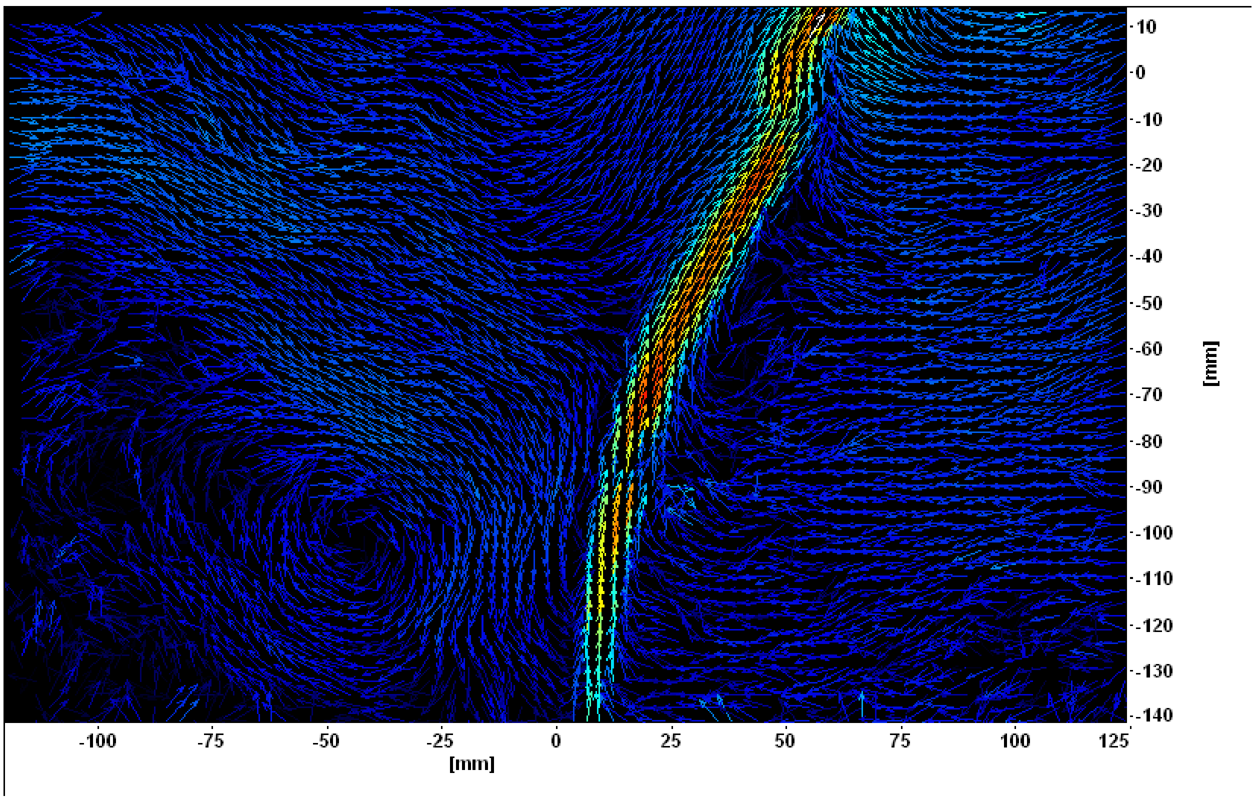

10
0
-10
-20
-30
-40
-50
-60
-70
-80
-90
-100
-110
-120
-130
-140
[mm]
-100
-75
-50
-25
0
25
50
75
100
125
[mm]

Figure 74

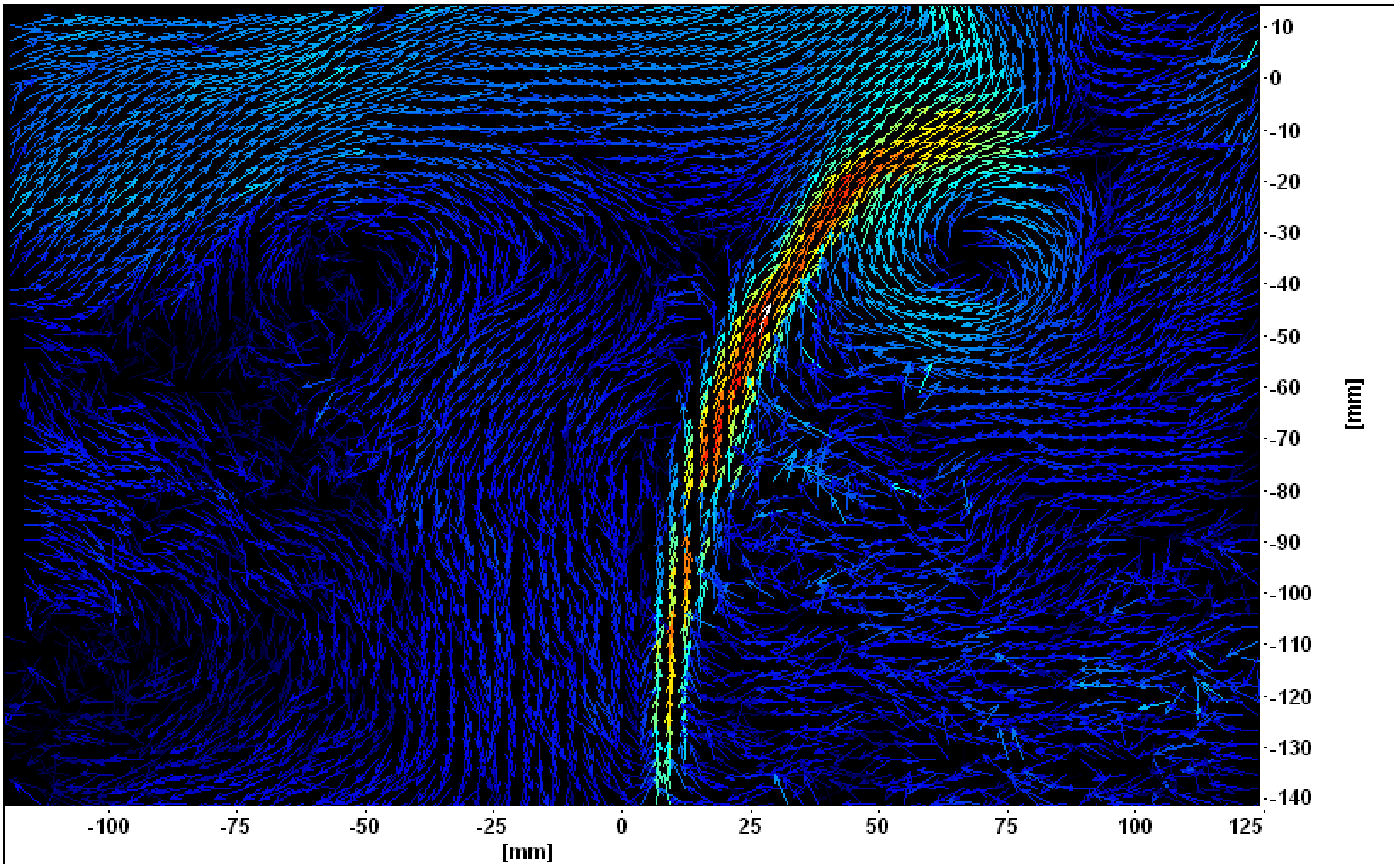
10
0
-10
-20
-30
-40
-50
-60
-70
-80
-90
-100
-110
-120
-130
-140
[mm]
-100
-75
-50
-25
0
25
50
75
100
125
[mm]

Figure 75

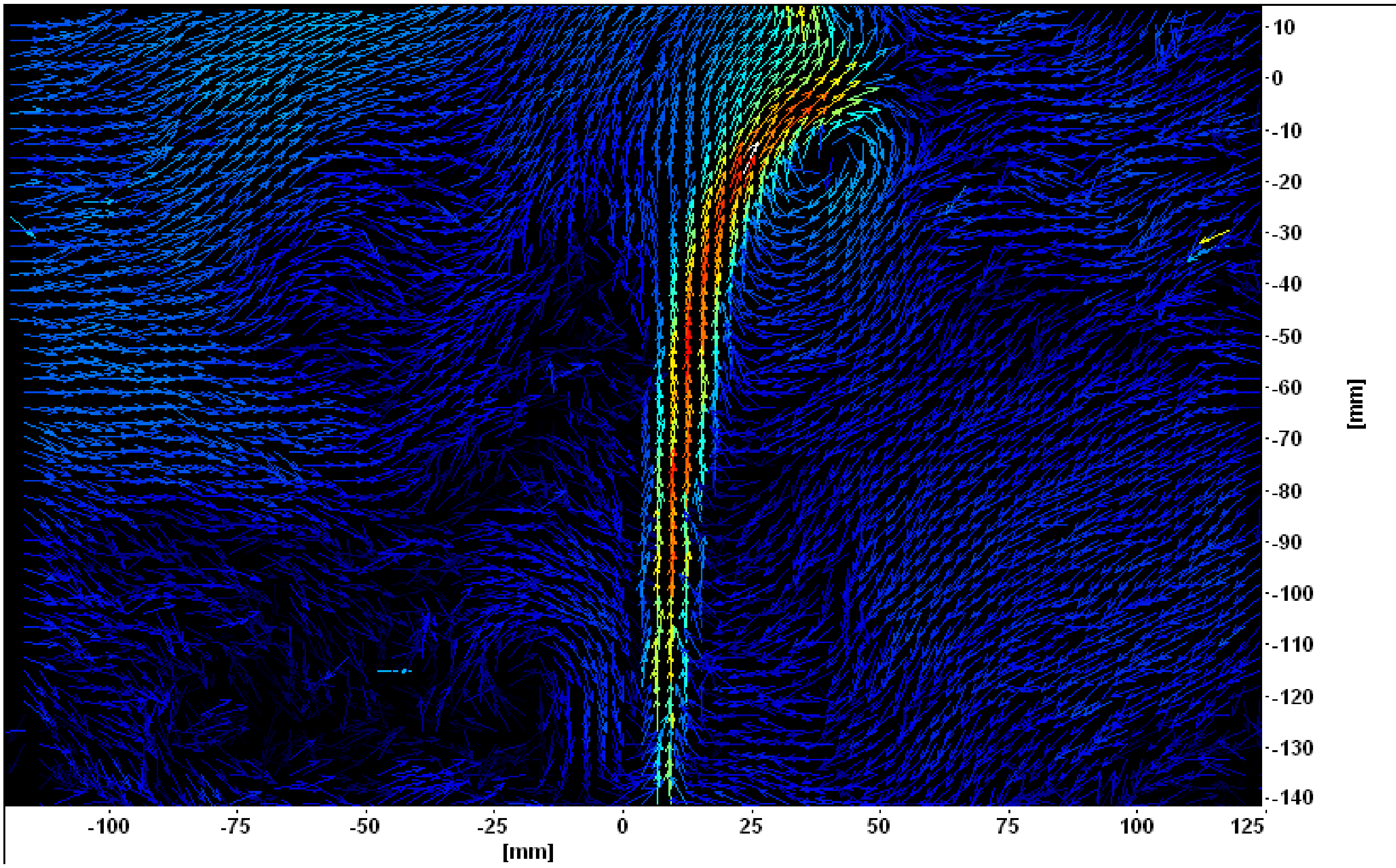

10
0
-10
-20
-30
-40
-50
-60
-70
-80
-90
-100
-110
-120
-130
-140
[mm]
-100
-75
-50
-25
0
25
50
75
100
125
[mm]

Figure 76

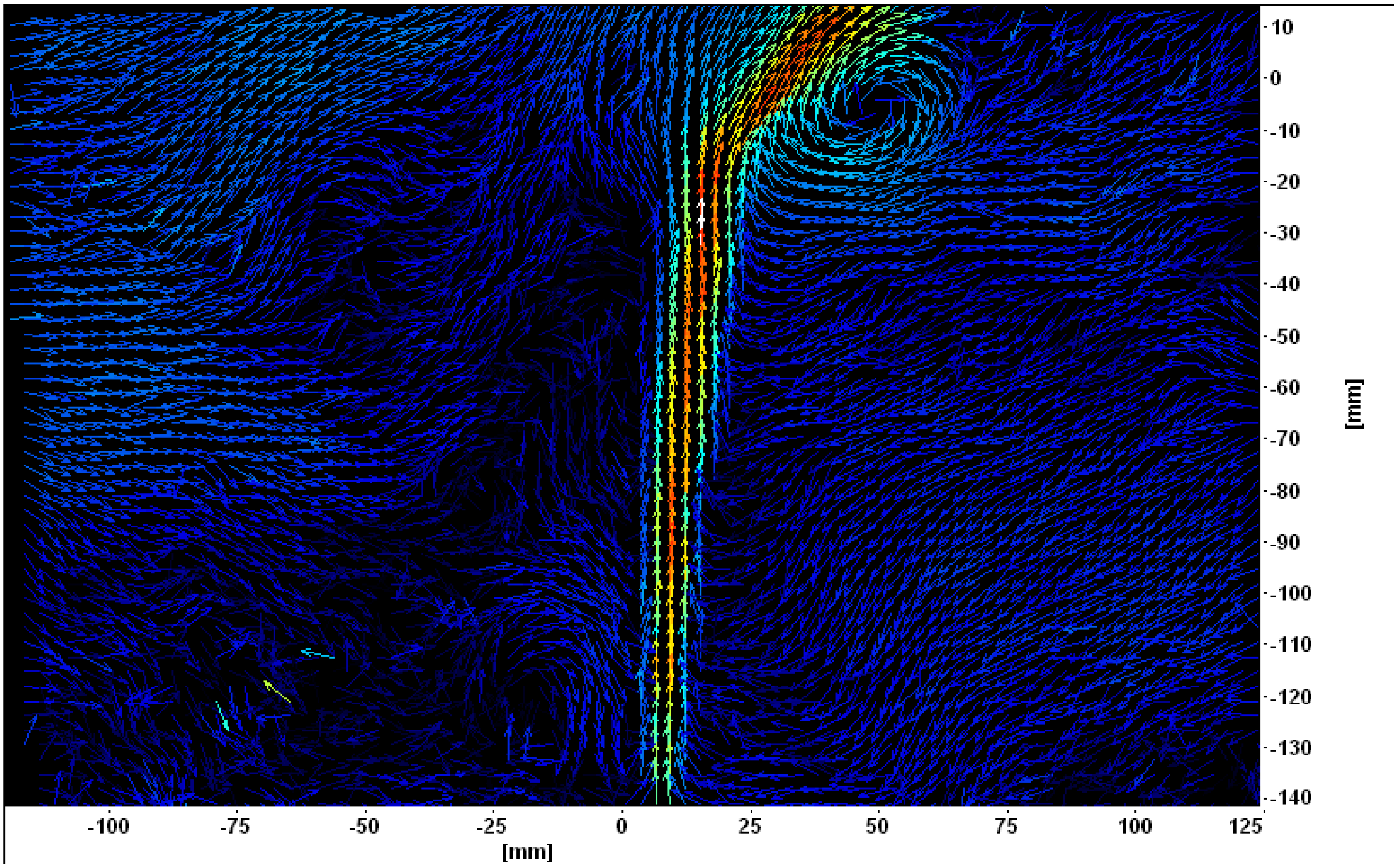

10
0
-10
-20
-30
-40
-50
-60
-70
-80
-90
-100
-110
-120
-130
-140
[mm]
-100
-75
-50
-25
0
25
50
75
100
125
[mm]

Figure 77

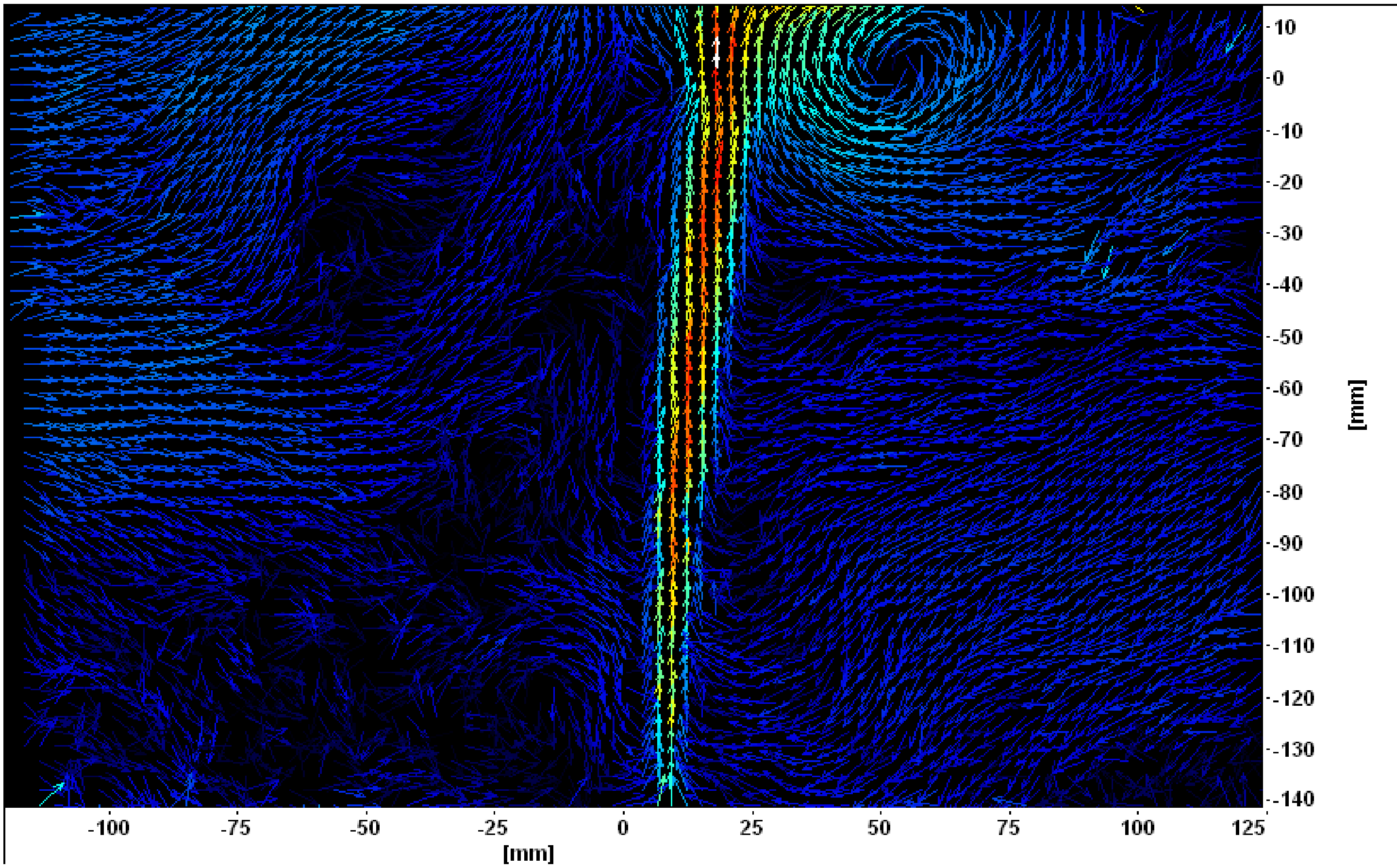

10
0
-10
-20
-30
-40
-50
-60
-70
-80
-90
-100
-110
-120
-130
-140
[mm]
-100
-75
-50
-25
0
25
50
75
100
125
[mm]

Figure 78

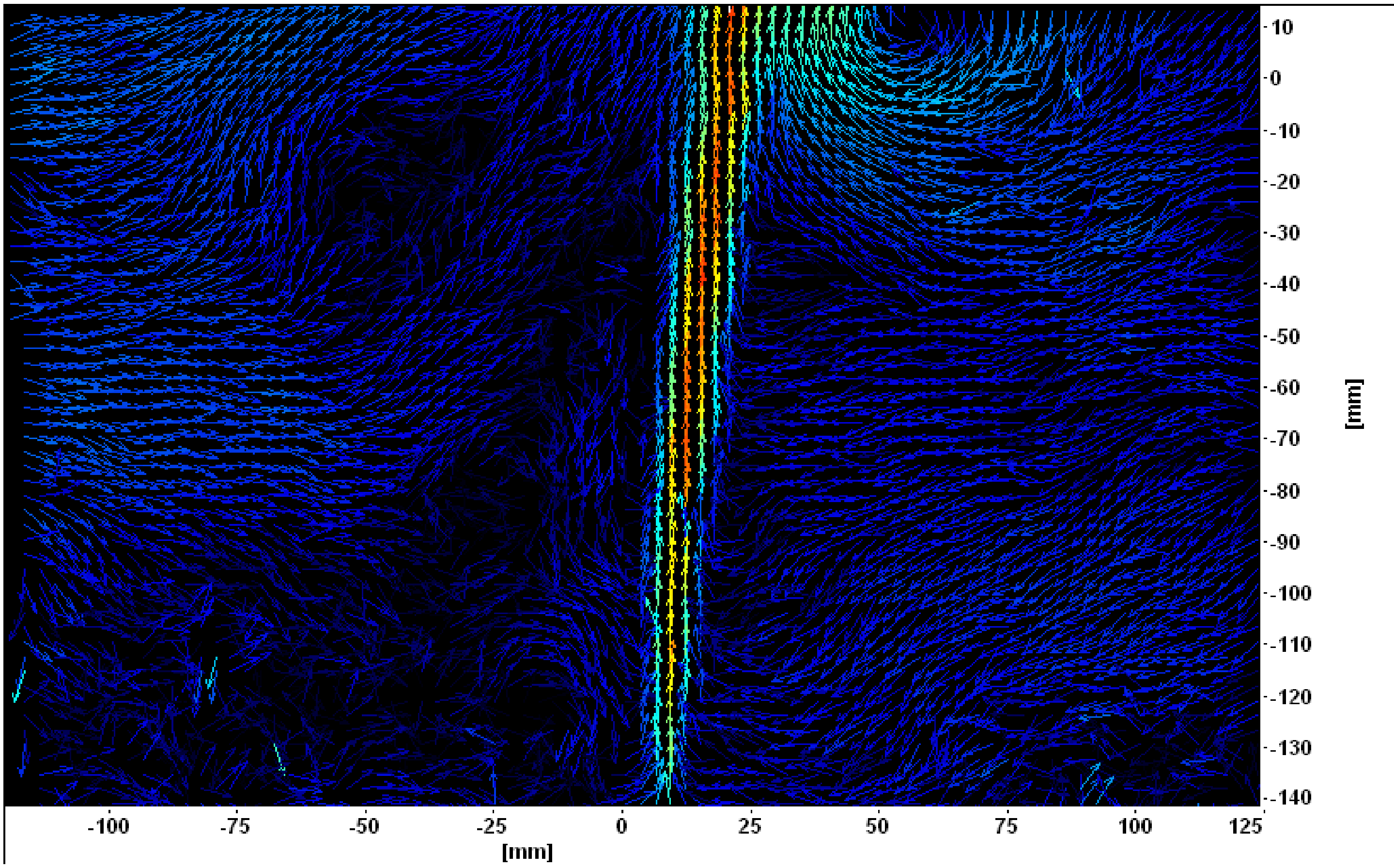

10
0
-10
-20
-30
-40
-50
-60
-70
-80
-90
-100
-110
-120
-130
-140
[mm]
-100
-75
-50
-25
0
25
50
75
100
125
[mm]

Figure 79

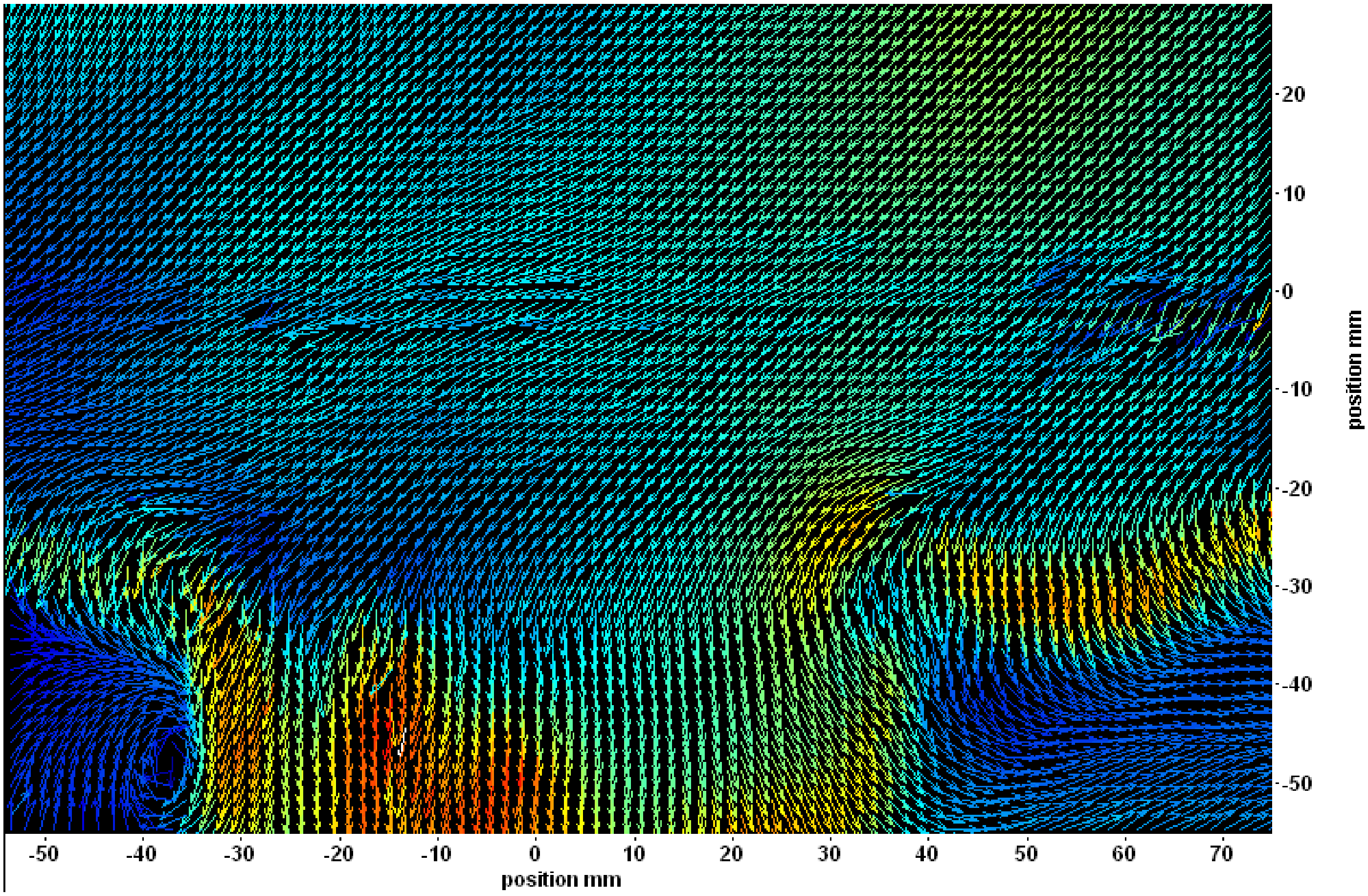

Figure 80

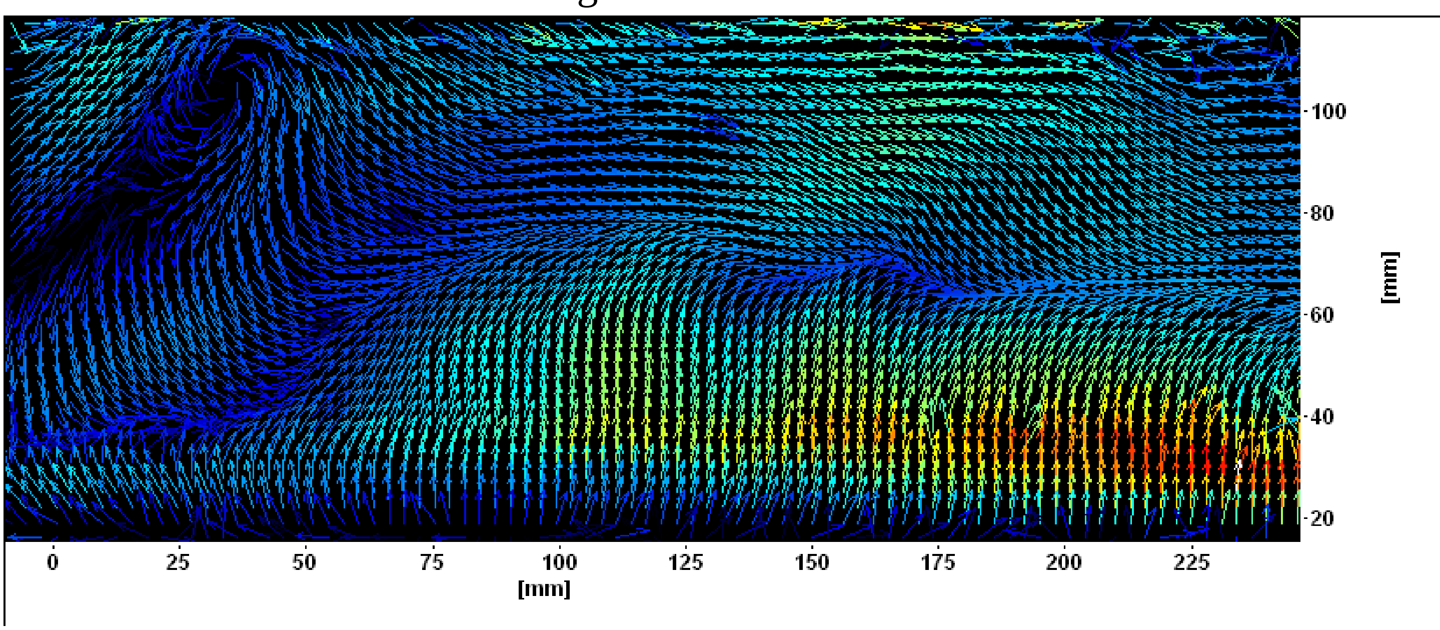

Figure 81

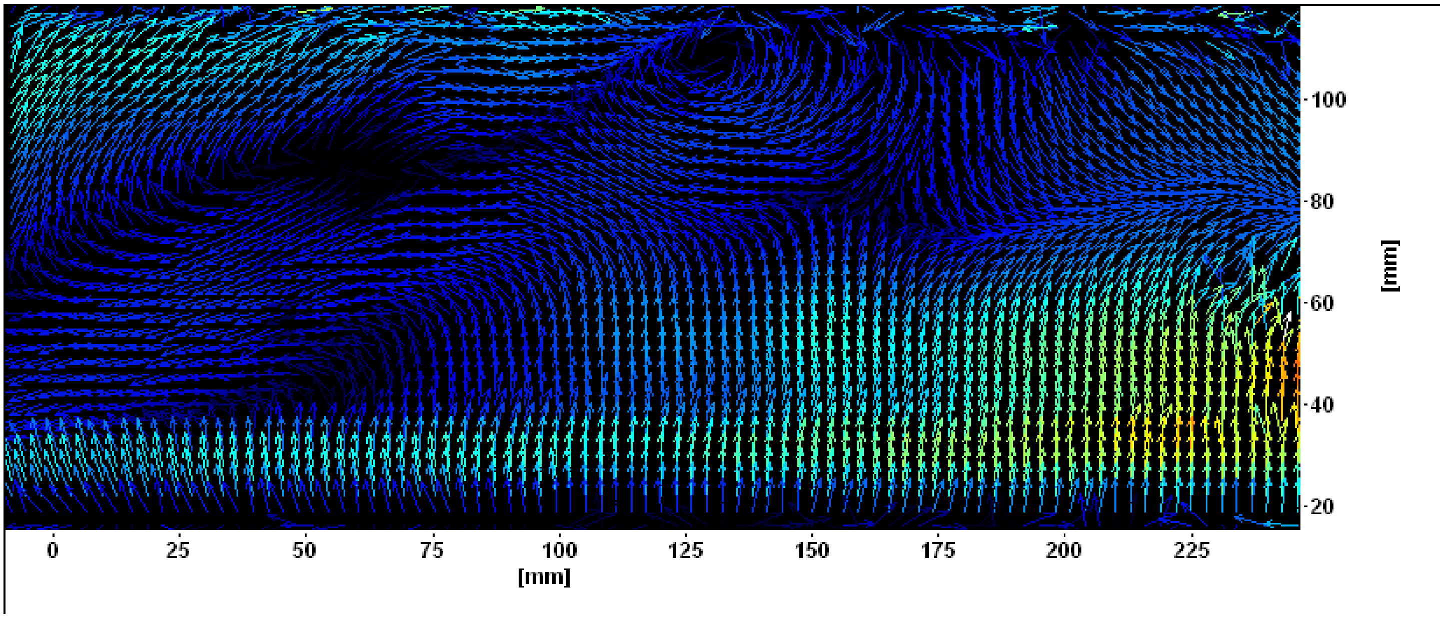

Figure 82

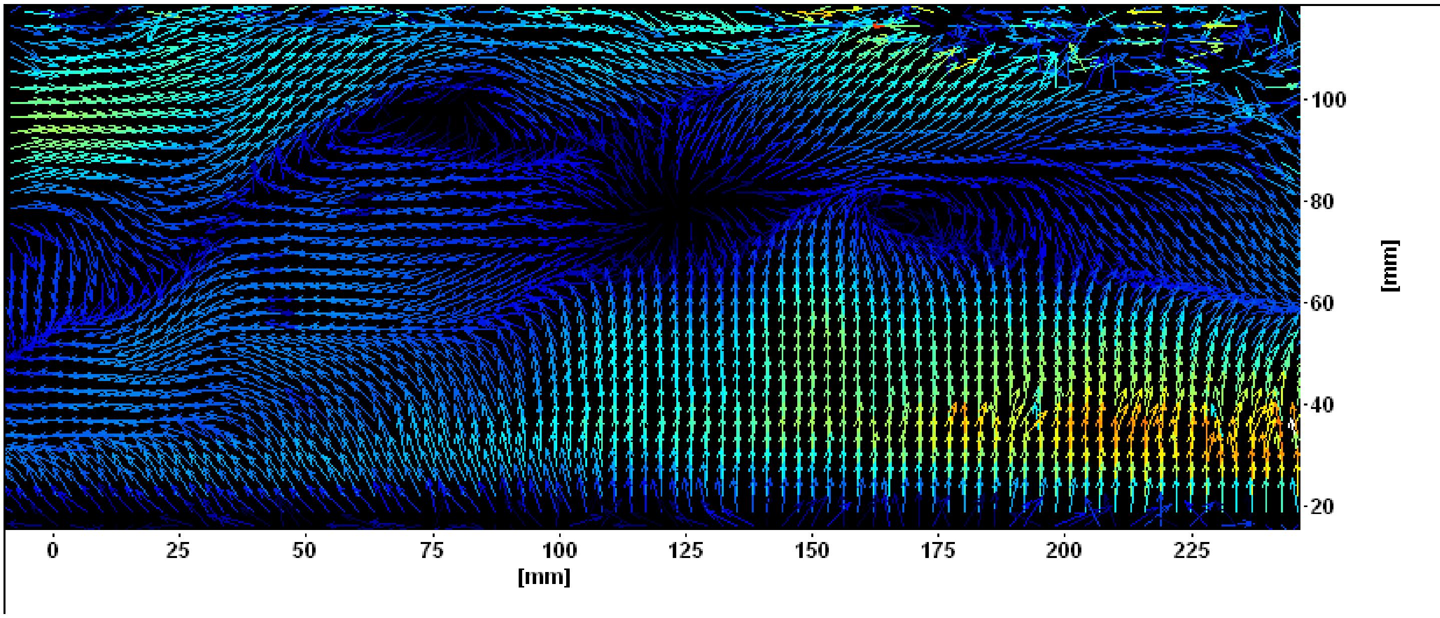

References

[1] Forstrom, R. J. and Sparrow, E.M., "Experiments on the Buoyant Plume Above a Heated Horizontal Wire," *International Journal of Heat and Mass Transfer*, Vol. 10, 1967, pp. 321-331.

[2] Schorr, A. W. and Gerbhart, B., "An Experimental Investigation of Natural Convection Wakes Above a Line Heat Source," *International Journal of Heat and Mass Transfer*, Vol. 13, 1970, pp.557-571.

[3] Fujii, T., Morioka, I., and Uehara, H., "Buoyant Plume Above A Horizontal Line Heat Source," *International Journal of Heat and Mass Transfer*, Vol. 16, No.4, 1973, pp.755-768.

[4] Akiyama, M., "Experimental Study of Natural Convection Heat Transfer from a Horizontal Line Heat Source," *Proceedings of the 11th National Heat Transfer Symposium of Japan*, Nagoya, Japan, 1974, pp.397-400.

[5] Igarashi, T. and Kada, S., "Natural Convective Oscillatory Flow in an Enclosed Space: Part 1, Natural Convection from a Heated Wire Placed Along the Axis of a Horizontal Cylinder," *Transactions of the Japan Society of Mechanical Engineers*, Vol. 41, No. 345, 1975, pp. 1500-1507.

[6] Igarashi, T., "Natural Convective Oscillatory Flow in an Enclosed Space: Part 2, Natural Convection from a Heated Wire in a Horizontal Rectangle Cylinder," *Transactions of the Japan Society of Mechanical Engineers*, Vol. 43, No. 347, 1977, pp. 3839-3847.

[7] Eichhorn, R. and Vedhanayagam, M., "The Swaying Frequency of Line Source Plumes," *Proceedings of the 7th International Heat Transfer Conference*, München, FRG, Vol. 2, 1982, pp. 407-412.

[8] Urakawa, K., Morioka, I., and Kiyota, M., "Swaying Motion of the Buoyant Plume Above a Horizontal Line Heat Source," *Proceedings of the 1st ASME-JSME Thermal Engineering Conference*, Honolulu, HI, Vol. 3, 1983, pp. 215-220.

[9] Yoshinobu, H., Onishi, Y., Amano, S., Enyo, S., and Wakitani, S., "Experimental Study on Instability of a Natural Convection Flow Above a Horizontal Line Heat Source," *Journal of the Physical Society of Japan*, Vol. 47, No.1, 1979, pp. 312-319.

[10] Bill, R. G. and Gebhart, H., "The Transition of Plane Plumes," *International Journal of Heat and Mass Transfer*, Vol. 18, 1975, pp. 513-526.

[11] Noto, K., Ishida, H., and Matsumoto, R., "Thermal Plume Above a Horizontal Line Heat Source (Spectrum and Several Facorts of the Swaying Motion in Transition and Turbulent States)," *Proceedings of the 21st National Heat Transfer Symposium of Japan*, Kyoto, Japan, 1984, pp. 166-168.

[12] Noto, K., Matsui, S., and Matsumoto, R., "Observation on Vortex Pair of Plane Thermal Plume in Thermally Stratified Fluid," *Flow Visualization*, Vol IV, Springer-Verlag, Berlin, 1982, pp. 697-702.

[13] Noto, K., "Swaying Motion in Thermal Plume Above a Horizontal Line Heat Source" *Journal of Thermophysics and Heat Transfer*, Vol. 3, No. 4, 1989, pp. 428-434.

[14] Carlomagno, G. M., Cenedese, A., and Iannetta, S., "L.D.A Velocity Measurements in the Buoyant Plume Above a Heated Horizontal Cylinder" *Archives of Mechanics*, Vol. 36, No. 4, 1984, pp. 515-521.

[15] Desrayaud, G., and Lauriat, G., "Unsteady confined Buoyant Plumes," *Journal of Fluid Mechanics*, Vol. 252, 1993, pp. 617-646.

[16] Cesini, G., Paroncini, M., Cortella, G., and Manzan, M., "Natural Convection from a Horizontal Cylinder in a Rectangular Cavity," *International Journal of Heat and Mass Transfer*, Vol. 42, No. 10, 1999, pp. 1801-1811.

[17] Kitamura, K., Kami-iwa, F., and Misumi, T., "Heat Transfer and Fluid Flow of Natural Convection Around Large Horizontal Cylinders," *International Journal of Heat and Mass Transfer*, Vol. 42, 1999, pp. 4093-4106.

[18] Gorman, I., Murray, D., Byrne, G., and Persoons, T., "Natural Convection from Isothermal Horizontal Cylinders," *Proceedings of the ASME 2009 International Mechanical Engineering Congress & Exposition*, Lake Buena Vista, Florida, 2009, pp. 1891-1897.

[19] Atmane, M., Chan, V., and Murray, D., "Natural Convection around a Horizontal Heated Cylinder: The Effects of Vertical Confinement," *International Journal of Heat and Mass Transfer*, Vol. 43, 2003, pp. 3661-3672.